Aus der Abteilung Strahlenzytogenetik
des Helmholtz Zentrum München
Leitung: Prof. Dr. rer. nat. Horst Zitzelsberger
Vorsitzende des Aufsichtsrats: Dr. Bärbel Brumme-Bothe

MicroRNAs als Biomarker für Kopf-Hals-Tumore und ihre Bedeutung für eine individualisierte Strahlentherapie

Dissertation

zum Erwerb des Doktorgrades der Naturwissenschaften

an der Medizinischen Fakultät der

Ludwig-Maximilians-Universität zu München

vorgelegt von
Isolde Summerer
aus München
2016

Mit Genehmigung der Medizinischen Fakultät der Ludwig-Maximilians-Universität München

Betreuer:	Prof. Dr. rer. nat. Horst Zitzelsberger
Zweitgutachter:	Prof. Dr. rer. nat. Olivier Gires
Dekan:	Prof. Dr. med. dent. Reinhard Hickel
Tag der mündlichen Prüfung:	25. Mai 2016

EIDESSTATTLICHE VERSICHERUNG

Ich erkläre hiermit an Eides statt, dass ich die vorliegende Dissertation mit dem Thema

„MicroRNAs als Biomarker für Kopf-Hals-Tumore und ihre Bedeutung für eine individualisierte Strahlentherapie“

selbständig verfasst, mich außer der angegebenen keiner weiteren Hilfsmittel bedient und alle Erkenntnisse, die aus dem Schrifttum ganz oder annähernd übernommen sind, als solche kenntlich gemacht und nach ihrer Herkunft unter Bezeichnung der Fundstelle einzeln nachgewiesen habe. Ich erkläre des Weiteren, dass die hier vorgelegte Dissertation nicht in gleicher oder in ähnlicher Form bei einer anderen Stelle zur Erlangung eines akademischen Grades eingereicht wurde.

_____	_____
Ort, Datum	Isolde Summerer

INHALTSVERZEICHNIS

ABKÜRZUNGSVERZEICHNIS

^{137}Cs	^{137}Cäsium
5-FU	5-Fluorouracil
AGO	Argonaute Protein
APC	Allophycocyanin
bp	base pairs
BPE	bovine pituitary extract
CCND1	Cyclin D1
CGH	comparative genomic hybridization
cRNA	copyRNA
CTP	Cytosintriphosphat
DMEM	Dulbecco's modified eagle medium
DMSO	Dimethylsulfoxid
EBA-1	EpCAM Antikörper 1
EBV	Ebstein Barr Virus
EGF	epidermal growth factor
EGFR	epidermal growth factor receptor
F	female
FC	fold change
FCS	fetal calf serum
FDR	false discovery rate
FFPE	formalin fixed paraffin embedded
HDL	high density lipoprotein
HNSCC	head and neck squamous cell carcinoma
HPV	humanes Papillomvirus
HSP70	heat shock protein 70
hTERT	human telomerase reverse transcriptase
IMRT	intensity modulated radiotherapy
KCl	Kaliumchlorid
lncRNA	long non-coding RNA
LRC	locoregional control
M	male

MMC	Mitomycin C
miRNA	microRNA
mRNA	messengerRNA
MRT	Magnetresonanztomographie
NA	not available
NGS	next generation sequencing
NPM1	Nucleophosmin 1
OD	optical density
OS	overall survival
PBMC	peripheral blood mononuclear cells
PBS	phosphate buffered saline
PCR	polymerase chain reaction
PE	Phycoerythrin
PET	Positronen-Emissions-Tomographie
pre-miRNA	precursor microRNA
pri-miRNA	primary microRNA
PFS	progression-free survival
qRT-PCR	quantitative real-time PCR
Rb	Retinoblastom
RIN	RNA integrity number
SD	standard deviation
SF	surviving fraction
SKY	spectral karyotyping
snRNA	small nucleolar RNA
SSC	saline sodium citrate
TCGA	The cancer genome atlas
TD	tetramerization domain
UNG	Uracil N-Glycosylase
XRT	Radiotherapie

PUBLIKATIONEN

Publikationen in referierten Fachzeitschriften

1. **Summerer I**, Hess J, Pitea A, Unger K, Hieber L, Selmansberger M, Lauber K, Zitzelsberger H. Integrative analysis of the microRNA-mRNA response to radiochemotherapy in primary head and neck squamous cell carcinoma cells. **BMC Genomics**. **2015** Sep 2;16**:**654.

2. **Summerer I**, Unger K, Braselmann H, Schuettrumpf L, Maihoefer C, Baumeister P, Kirchner T, Niyazi M, Sage E, Specht HM, Multhoff G, Moertl S, Belka C, Zitzelsberger H. Circulating microRNAs as prognostic therapy biomarkers in head and neck cancer patients. **Br J Cancer**. **2015** Jun 30;113(1):76-82.

3. **Summerer I**, Niyazi M, Unger K, Pitea A, Zangen V, Hess J, Atkinson MJ, Belka C, Moertl S, Zitzelsberger H. Changes in circulating microRNAs after radiochemotherapy in head and neck cancer patients. **Radiat Oncol**. **2013** Dec 28;8:296.

4. Heiliger K, Vitagliano D, Heß J, Salerno P, Braselmann H, Salvatore G, Ugolini C, **Summerer I**, Bogdanova T, Unger K, Thomas G, Santoro M, Zitzelsberger H. Novel candidate genes of thyroid tumourigenesis identified in Trk-T1 transgenic mice. **Endocr Relat Cancer**. **2012** May 24;19(3):409-21.

Präsentationen

1. Circulating MicroRNAs as Biomarkers in Radiation Therapy of Head and Neck Cancer Patients. **2nd International Radiation Proteomics Workshop**. Oktober 2012, München (Posterpräsentation)

2. Circulating MicroRNAs as Biomarkers in Radiotherapy of Head and Neck Cancer Patients. **ERR (European Radiation Research Society) – Jährliche Konferenz**. Oktober 2012, Vietri sul Mare, Italien (Vortrag)

3. Circulating MicroRNAs as Biomarkers in Radiation Therapy of Head and Neck Cancer Patients. **5th International Systems Radiation Biology Workshop**. September 2012, Oxford, UK (Posterpräsentation)

4. Circulating MicroRNAs as Biomarkers in Radiation Therapy of Head and Neck Cancer Patients. **GBS (Gesellschaft für Biologische Strahlenforschung) – Jährliche Konferenz**. September 2012, München (Posterpräsentation, Posterpreis)

5. Molecular Biomarkers for Radiation Sensitivity in Human Peripheral Blood Mononuclear Cells. **ICRR (International Congress of Radiation Research) – Jährliche Konferenz**. August 2011, Warschau, Polen (Posterpräsentation)

1 EINLEITUNG

1.1 Kopf-Hals-Tumore

Epidemiologie

Maligne Tumore des Kopf-Hals-Bereiches gehören zu den sechs häufigsten Krebserkrankungen weltweit mit ca. 650 000 Neuerkrankungen und 350 000 Todesfällen pro Jahr [1-3]. Zu den malignen Kopf-Hals-Tumoren zählen Karzinome der Lippen, der Mundhöhle, der Kieferhöhle, der Nasenhöhle und Nasennebenhöhlen, sowie des Kehlkopfes (Larynx) und des Rachens (Pharynx). Mundhöhlenkarzinome werden weiter in Karzinome des harten Gaumens, der Zungenunterseite, des Mundbodens, des Zahnfleisches und der Mundschleimhäute untergliedert. Pharynxkarzinome werden entsprechend ihrer Lokalisation in Karzinome des Oropharynx, Nasopharynx und Hypopharynx unterteilt. In 90% aller Fälle handelt es sich um Plattenepithelkarzinome der Schleimhäute (HNSCC = *head and neck squamous cell carcinoma*). Die Inzidenz zeigt deutliche geografische Unterschiede, die je nach Tumorlokalisation variieren. Mundhöhlenkarzinome treten am häufigsten in Melanesien, im südlichen Zentralasien, sowie in Mittel- und Osteuropa auf. Nasopharynxkarzinome sind hingegen wesentlich häufiger in Entwicklungsländern und zeigen die höchste Inzidenz in Südostasien. Allgemein sind Männer wesentlich häufiger von malignen Kopf-Hals-Tumoren betroffen als Frauen, was insbesondere bei Larynxkarzinomen deutlich wird [4].
In den letzten zwei Jahrzehnten ging die Inzidenz für Kopf-Hals-Tumore insgesamt leicht zurück und es konnte eine deutlich verbesserte durchschnittliche 5-Jahres Überlebensrate von ca. 65% beobachtet werden [5, 6]. Das durchschnittliche Diagnosealter für HNSCC liegt bei Anfang 60 [7], jedoch ließ sich in den letzten zwei Jahrzehnten ein Trend zur Häufung von Erkrankungen bei jüngeren Patienten (45-54 Jahre) erkennen [5].

Risikofaktoren

Alkohol- und Tabakkonsum werden mit 75% aller HNSCC-Fälle assoziiert und stellen die größten Risikofaktoren für HNSCC in Nordamerika und Europa dar. Die Kombination beider Faktoren hat dabei einen multiplikativen Effekt, jedoch erhöht auch starker Tabak- oder Alkoholmissbrauch allein das Risiko für HNSCC [6, 8]. Kautabak und das Kauen von Betel, was hauptsächlich in asiatischen Ländern eine Rolle spielt, erhöht insbesondere das Risiko für Mundhöhlenkarzinome [9].

Auch die Ernährung beeinflusst das Risiko für HNSCC. Studien ergaben einen protektiven Effekt von regelmäßigem Verzehr von Obst und Gemüse, sowie einen schädlichen Effekt von hohem Fleischkonsum, insbesondere rotem Fleisch [10, 11]. Diese ernährungsbedingten Effekte sind jedoch vorwiegend bei Rauchern und Alkoholkonsumenten zu beobachten. Es ist daher anzunehmen, dass die in Obst und Gemüse enthaltenen Vitamine C, E und Folsäure eine verbesserte Kompensation der karzinogenen Effekte von Alkohol und Tabak, wie oxidative Schädigungen oder Entzündungen, ermöglichen [11]. Des Weiteren wurden chronische Unterernährung sowie schlechte Mundhygiene in Zusammenhang mit einem erhöhten Krebsrisiko im Mundbereich gebracht [12]. Auch berufsbedingte Risikofaktoren sind bekannt, wie z. B. erhöhtes Risiko für Larynx- und Pharynxkarzinome durch Kohlenstaub- [13] oder Asbestexposition [14].

Einige Studien beschreiben eine geringere Kopf-Hals-Tumorinzidenz für Diabetespatienten, die mit dem Medikament Metformin behandelt werden [15], sowie eine bessere Prognose für Larynxkarzinompatienten, die aufgrund einer Diabeteserkrankung Metformin erhalten [16]. Metformin hat eine antineoplastische Wirkung, die auf der Inhibition von Proliferationssignalwegen und Aktivierung von Zelltodsignalwegen beruht und so der Karzinogenese entgegenwirkt. Die wichtigsten Metformin-*Targets* sind dabei Signalwege, die mit mTOR, NFkB, AKT, MAPK und STAT3 assoziiert sind [17, 18].

Darüber hinaus beeinflusst die individuelle genetische Prädisposition die Suszeptibilität für HNSCC. Dabei spielen vor allem Polymorphismen in Enzymen, die Karzinogene wie die in Tabak enthaltenen polyzyklischen Kohlenwasserstoffe und Nitrosamine metabolisieren, eine wichtige Rolle. Beispiele dafür sind die P450 Cytochrome, die an der metabolischen Aktivierung von Nitrosaminen und dem Alkoholmetabolismus beteiligt sind, sowie Acetyltransferasen und Alkoholdehydrogenasen [19, 20]. Auch erbliche Syndrome, wie das Li-Fraumeni Syndrom, das hereditäre non-polypöse Kolonkarzinom, Fanconi-Anämie oder Ataxia teleangiectasia gehen mit einem erhöhten Risiko für Kopf-Hals-Tumore einher [21, 22].

Neben Tabak- und Alkoholkonsum als Hauptrisikofaktoren gewinnt die Infektion mit humanen Papillomviren (HPV) immer mehr an Bedeutung. Etwa 25% aller HNSCC enthalten genomische HPV DNA [23]. Die Virus-DNA kann mit verschiedenen Methoden, z. B. mittels in situ Hybridisierung [24] oder mittels *real-time PCR* [25] nachgewiesen werden. HPV-Infektion wird hauptsächlich mit dem Auftreten von Oropharynxkarzinomen, insbesondere von Tonsillenkarzinomen, in Verbindung gebracht. Epidemiologische Studien zeigten einen erheblichen Anstieg der Inzidenz von HPV-positiven sowie einen Rückgang von HPV-negativen Oropharynxkarzinomen über die letzten Jahrzehnte [26]. HPV-16 und in geringerem Umfang auch

HPV-18 stellen die onkogenen Hochrisikovarianten dar [27]. Die maligne Transformation beruht dabei in erster Linie auf der Aktivität der Virusproteine E6 und E7, die die Zellproliferation fördern und Apoptose unterdrücken [28]. Nach Integration des Virusgenoms in die zelluläre Wirts-DNA bewirkt die Expression des Onkoproteins E6 die Degradation des Tumorsuppressors p53 durch Ubiquitinierung und darauffolgenden proteasomalen Abbau. Die p53-Defizienz führt in der Folge zu zunehmender chromosomaler Instabilität und Akkumulation von Mutationen. Das Virusprotein E7 inaktiviert den Tumorsuppressor Rb und führt so zu einem Verlust der Zellzykluskontrolle [28]. Durch die Inaktivierung von Rb kommt es zudem zu einer Akkumulation von $p16^{INK4A}$, welches immunhistochemisch nachgewiesen werden kann, und somit als Marker für HPV-transformierte Zellen dient. $P16^{INK4A}$ vermittelt in normalen Zellen stressbedingten Zellzyklusarrest, wofür jedoch funktionelles Retinoblastom-Protein (Rb) benötigt wird. Demzufolge kann daraus geschlossen werden, dass Zellen, die eine $p16^{INK4A}$-Akkumulation zeigen und dennoch proliferieren, HPV-transformierte Zellen darstellen [29]. HPV-positive Oropharynxkarzinome unterscheiden sich hinsichtlich ihrer Epidemiologie von HPV-negativen Karzinomen. HPV-positive HNSCC betreffen typischerweise jüngere Menschen, überwiegend Männer, und zeigen eine starke Assoziation mit dem Sexualverhalten. Ein wesentlicher Unterschied besteht in der deutlich besseren Prognose im Vergleich zu HPV-negativen HNSCC Patienten [30, 31].

Molekulare Pathogenese von HNSCC

Die Pathogenese von HPV-negativen HNSCC ist ein komplexer mehrstufiger Prozess und kann auf Mutationen verschiedenster Tumorsuppressor- und Onkogene zurückgeführt werden. Zu den gängigen Veränderungen in prämalignen Läsionen gehören *loss of heterozygosity* Mutationen auf Chromosom 3p, 9p und 17p, während Veränderungen auf Chromosom 4q, 8 und 11q auf ein fortgeschrittenes Stadium der Karzinogenese hinweisen [32]. Die häufigsten Mutationen in HNSCC betreffen Signalwege, die an der Zellzykluskontrolle beteiligt sind. TP53 ist auf Chromosom 17p lokalisiert und zeigt in 60% aller HNSCC inaktivierende somatische Mutationen. Eine kürzlich veröffentlichte Studie, in der miRNA Daten, DNA-Methylierungsmuster, Genexpressionsdaten und Nukleotidsubstitutionen von 279 HNSCC Patienten analysiert wurden, zeigte *loss of function* Mutationen in TP53 und CDKN2A Inaktivierung in nahezu allen HNSCC, die auf Tabakkonsum zurückzuführen sind [33]. CDKN2A, lokalisiert auf Chromosom 9p21, welches für das Protein $p16^{INK4A}$ kodiert, ist häufig inaktiviert durch Mutation oder Methylierung und verliert somit seine Zellzyklus-regulierende Funktion, welche auf Inhibition des Übergangs von der G1- in die S-Phase basiert [32]. Zu den frühen Läsionen in mehr als 80% aller HNSCC zählt auch eine Amplifikation von Cyclin D1 (CCND1) auf Chromosom 11q13. CCND1 vermittelt die Phosphorylierung von Rb,

was den Eintritt in die S-Phase ermöglicht [34]. Ein weiterer Signalweg, der häufig Mutationen in Kopf-Hals-Tumoren aufweist, ist der NOTCH-Signalweg. Dieser Signalweg beeinflusst unter anderem die Regulierung der Selbsterneuerungs-Kapazität einer Zelle, den Austritt aus dem Zellzyklus und das zelluläre Überleben [35]. NOTCH1 Mutationen sind in 10–15% der HNSCC Tumore zu finden und sind meist inaktivierend, was darauf schließen lässt, dass NOTCH1 in HNSCC als Tumorsuppressor fungiert [36].

Neben Veränderungen Zellzyklus-regulierender Komponenten ist auch das Umgehen der Telomerverkürzung von großer Bedeutung für das unlimitierte replikative Potenzial einer Zelle. 90% aller HNSCC sowie prämaligne Läsionen des Kopf-Hals-Bereiches zeigen eine Reaktivierung der Telomerase, welche eine zentrale Rolle bei der zellulären Immortalisierung spielt [37].

Der epidermale Wachstumsfaktorrezeptor (EGFR) gehört zu den ErbB Wachstumsfaktor-Rezeptor-Tyrosinkinasen. Durch Bindung von Wachstumsfaktoren wird eine Signalkaskade ausgelöst, die wiederum zur Aktivierung von Signalwegen führt, die mit der Regulierung von Zellproliferation, Apoptose, Angiogenese oder Metastasierung assoziiert sind [6]. Aktivierende Mutationen, Amplifikationen und Überexpression von EGFR sind in vielen HNSCC zu beobachten [32]. Dadurch kommt es zu einer übermäßigen Aktivierung der *downstream* Signalwege Ras-MAPK und PI3K-PTEN-AKT. Auch der STAT Signalweg und Cyclin D1 werden von EGFR positiv reguliert, was zu erhöhter mitogener Aktivität führt. Darüber hinaus sind Komponenten des PI3K-PTEN-AKT Signalwegs selbst häufig von Signalwegs-aktivierenden Mutationen betroffen [38]. HPV-positive HNSCC weisen vorwiegend Mutationen in dem Onkogen PIK3CA, sowie Amplifikationen des Zellzyklusregulators E2F1 auf [33].

Therapie

Als Grundlage für Therapieentscheidungen dient primär das *Staging* des Tumors, welches jedoch je nach Lokalisation des Primärtumors unterschiedlichen Richtlinien folgt [39]. Das *Staging* basiert auf der TNM-Klassifikation, welche die Tumorgröße (T), Lymphknotenmetastasierung (N) und Fernmetastasierung (M) beschreibt [40]. Dazu wird meist ein CT (Computertomographie) Scan und/oder eine MRT (Magnetresonanztomographie) durchgeführt. Zur Detektion von Metastasen, die bei HNSCC neben den regionären Lymphknoten häufig in der Lunge und weniger häufig in den mediastinalen Lymphknoten, der Leber und den Knochen zu finden sind, wird meist ein PET (Positronen-Emissions-Tomographie) Scan mit ^{18}F-2-Fluordesoxyglucose herangezogen [41]. In der Regel werden PET und CT kombiniert angewendet in einem sogenannten PET-CT Scan, wodurch eine höhere Genauigkeit der Ergebnisse erlangt werden kann.

Als Therapie für HNSCC wird nach Möglichkeit die operative Entfernung des Tumors eingesetzt. Dabei gibt es jedoch Limitierungen, wie die anatomische Ausbreitung des Tumors und die notwendige Erhaltung essentieller Organe im Kopf-Hals-Bereich, wie z. B. die Carotis-Arterie oder Speicheldrüsen. Im Laufe der letzten Jahrzehnte konnten bedeutende technische Fortschritte bei der Chirurgie von HNSCC erreicht werden, vor allem durch die Entwicklung minimalinvasiver Methoden. Dazu gehören die Laser-Mikrochirurgie und die Roboterchirurgie, die für transoral zugängliche Tumore der Mundhöhle, des Pharynx und des Larynx eingesetzt werden und sowohl bessere onkologische Ergebnisse als auch bessere Funktionserhaltung der Organe ermöglichen [42].

Eine weitere Behandlungsmethode für HNSCC ist die Radiotherapie, die entweder als primäre Therapieform oder adjuvant eingesetzt wird. Der Wirkmechanismus der Radiotherapie beruht auf der Induktion von DNA-Schäden, die durch die ionisierende Strahlung erzeugt werden, und anschließend zum Tod der Zelle führen sollen. Da die Strahlung jedoch nicht nur Tumorzellen, sondern auch Normalgewebe schädigt, muss die Therapie so konzipiert werden, dass die maximale Dosis im Tumorvolumen appliziert wird, während die Dosis für angrenzendes Normalgewebe minimal ist. Eine Radiotherapie bei HNSCC besteht in der Regel aus fraktionierter Bestrahlung des Tumors (üblicherweise in täglichen Dosen von 2 Gy an 5 Tagen der Woche) bis zu einer Gesamtdosis von 70 Gy [6]. Neue Technologien, wie die Intensitäts-modulierte Radiotherapie (IMRT), erlauben eine räumlich optimierte Bestrahlung des Zielvolumens bei gleichzeitiger Reduktion der Dosis für angrenzendes Normalgewebe [43]. Weitere Neuerungen auf dem Gebiet der Strahlentherapie von HNSCC sind Protonentherapie, Neutronentherapie, Schwerionentherapie, Brachytherapie, stereotaktische Radiochirurgie und die Integration von bildgebenden Verfahren (CT oder PET-CT) in Linearbeschleuniger [6]. Zudem konnten in einigen Studien durch Hyper- oder Hypofraktionierung der Bestrahlung zum Teil bessere Therapieerfolge erzielt werden [44, 45]. Um eine verbesserte Tumorkontrolle zu erreichen, wird die Radiotherapie häufig in Verbindung mit Chemotherapie angewendet. Radio(chemo)therapie wird vor allem bei Patienten mit lokal fortgeschrittenen und/oder inoperablen Tumoren eingesetzt, kommt jedoch auch oftmals postoperativ zum Einsatz, um die lokale und lokoregionäre Tumorkontrolle zu erhöhen [46]. In Form einer neoadjuvanten Behandlung dient die Radio(chemo)therapie zur Reduktion des Tumorvolumens, um eine anschließende Operation zu ermöglichen.

Die Chemotherapie war lange Zeit vorwiegend für palliative Behandlungen von Bedeutung, wird jedoch heutzutage für lokal fortgeschrittene HNSCC meist in Kombination mit Radiotherapie kurativ eingesetzt [47]. Auch die Induktionschemotherapie bei fortgeschrittenen HNSCC wurde in Studien getestet. Dabei wird neoadjuvant oder in Kombination mit einer Radiotherapie eine

Chemotherapie durchgeführt, um das Risiko für spätere Fernmetastasen oder Tumorrezidive zu reduzieren. Es konnte jedoch bislang keine signifikante Verbesserung der Überlebensraten oder Tumorkontrollraten gezeigt werden [48]. Die gängigsten Chemotherapeutika in der Therapie von HNSCC sind der Replikationshemmer Cisplatin [49] und der Antimetabolit 5-Fluorouracil (5-FU) [50], welche als zusätzliche Therapie zur Bestrahlung einen positiven Effekt auf das Überleben und die lokoregionäre Tumorkontrolle haben. Taxane (Paclitaxel, Docetaxel), die die Funktion des Spindelapparates und somit die Zellteilung hemmen, werden meist in neoadjuvanten Behandlungsschemata und in Kombination mit Cisplatin und 5-FU eingesetzt [51].

Die Radio(chemo)therapie stellt neben der operativen Behandlung die Standardtherapie für lokal fortgeschrittene HNSCC dar, obwohl sie häufig mit Akuttoxizitäten, wie Dysphagie, Mukositis und Dermatitis verbunden ist sowie mit einem Risiko für langfristige Folgen in Form von Sekundärtumoren. Eine Limitation der Radiotherapie ist eine mögliche intrinsische Radioresistenz der Tumorzellen, die häufig bei lokal fortgeschrittenen HNSCC zu beobachten ist. Diese basiert in vielen Fällen auf hypoxischen schlecht vaskularisierten Bereichen innerhalb des Tumors, welche radioresistente Tumorstammzellen enthalten [52]. Eine geringe Strahlenempfindlichkeit kann zudem auf entartete Proliferations-Signalwege, insbesondere das EGFR-Signaling, den PI3K-AKT-mTOR Signalweg und die P53 Signalkaskade zurückgeführt werden [53]. Neue Strategien die Antitumor-Wirkung der Therapien zu intensivieren und gleichzeitig die oft schwerwiegenden Nebenwirkungen systemischer Behandlungen zu vermeiden zielen daher auf molekulare therapeutische *Targets* in deregulierten Signalwegen ab. EGFR-Inhibitoren, wie der monoklonale Antikörper Cetuximab, sind die ersten klinisch angewendeten molekularen Tumortherapeutika für HNSCC [54]. Ein weiteres molekulares Therapeutikum für HNSCC ist Bevacizumab, ein monoklonaler Antikörper gegen VEGF, der anti-angiogenetisch wirkt und somit durch verminderte Nährstoff- und Sauerstoffversorgung zur Hemmung der Proliferation des Tumors beiträgt [55]. Der Antikörper Trastuzumab hemmt den epidermalen Wachstumsfaktorrezeptor HER2, der die Zellproliferation über den MAPK-Weg stimuliert und die Apoptose über den mTOR-Signalweg unterdrückt [56]. Der duale Antikörper Lapatinib ermöglicht die gleichzeitige Inhibition von EGFR und HER2 [57]. Darüber hinaus wird der mTOR-Inibitor Rapamycin in der Therapie von HNSCC eingesetzt [58]. Sorafenib steigert den antiproliferativen Effekt von Radiochemotherapie durch Inhibition der DNA-Reparaturproteine ERCC1 und XRCC1 [59].

Nicht jede Therapie ist für jeden HNSCC Patienten geeignet, nicht zuletzt aufgrund der Heterogenität der Kopf-Hals-Tumore. Spezifische Marker, die Vorhersagen über das individuelle Ansprechen auf eine Behandlungsform zulassen, würden die Möglichkeit bieten, vermeidbare Belastungen durch wenig erfolgversprechende Therapien zu umgehen. Daher fokussieren sich

aktuelle Studien auf die Identifikation von Biomarkern, die Aussagen über den individuellen Krankheitsverlauf, sowie über potentielle Therapieerfolge erlauben. Darüber hinaus werden neue molekulare *Targets* untersucht, die der gezielten Therapie dienen und zu einem verbesserten Überleben bei HNSCC Patienten beitragen könnten.

1.2 Biomarker

Ein Biomarker ist ein messbarer Indikator, der präzise, objektiv und reproduzierbar zwischen normalem und pathologischem Zustand unterscheiden, oder die Reaktion auf eine spezifische therapeutische Intervention vorhersagen kann [60]. Tumorbiomarker reflektieren den Status der zugrunde liegenden Erkrankung und ermöglichen die Stratifizierung von Patienten. Sie dienen der Identifikation von Patienten, die keine weitere Therapie benötigen, oder von Patienten, die voraussichtlich nicht von einer bestimmten Behandlung profitieren. Dadurch können effektivere und kostengünstigere Therapien gewählt und für jeden Patienten individuell angepasst werden. Solche Marker stellen prädiktive Marker dar, da sie Vorhersagen über die Wirksamkeit einer Therapieform erlauben. Biomarker, die Aussagen über das Überleben und damit auch die Aggressivität des Tumors zulassen, werden als prognostische Marker bezeichnet. Diagnostische Tumormarker hingegen dienen der Detektion von Krebserkrankungen. Darüber hinaus können Tumormarker zur Überwachung einer Therapie oder zur Abschätzung des Risikos für ein Rezidiv herangezogen werden. Tumorbiomarker können zudem molekulare *Targets* für neue gezielte Therapien darstellen [61].

Von der Entdeckung eines Biomarkers bis zu seiner klinischen Implementierung ist es jedoch ein langer Weg. Ein verlässlicher Biomarker muss eine hohe Spezifität und Sensitivität aufweisen. An großen Patientenkohorten müssen standardisierte Nachweisverfahren entwickelt werden, um einen Biomarker zu etablieren. Zudem ist es von Vorteil, wenn ein Biomarker leicht, idealerweise minimalinvasiv, zugänglich ist. Molekulare Biomarker können auf DNA-Ebene in Form von Kopienzahlveränderungen, Polymorphismen, Punktmutationen, Translokationen oder Insertionen zu finden sein. Auf RNA-Ebene können erhöhte oder verminderte Transkription sowie posttranskriptionelle Modifikationen als Biomarker dienen. Ebenso können Expressionsänderungen von Proteinen oder posttranslationale Effekte Marker darstellen [62]. Auch epigenetische Faktoren, wie z. B. Methylierungsmuster können als Biomarker genutzt werden [63]. Ein bereits in der Klinik etablierter prognostischer Marker für Kopf-Hals-Tumore ist der HPV-Status [31]. Des Weiteren stellt die Oxygenierung eines HNSCC Tumors einen prädiktiven Marker für den Erfolg von Radiotherapie dar [64]. Auch EGFR-Überexpression wird mit einem schlechten Therapie-Ansprechen und geringerem Überleben in Verbindung gebracht [65]. EGFR-

Inhibitoren werden daher therapeutisch eingesetzt, haben jedoch nur für bestimmte Patientengruppen einen positiven Effekt. Dies beruht auf der komplexen Regulation des EGFR-Signalwegs durch *feedback-loops* und die Interaktion mit dem MAPK-Signalweg [66]. Daher werden weitere molekulare Marker benötigt, um Patienten zu identifizieren, die von einer Anti-EGFR Therapie profitieren können [67]. Weitere molekulare Marker in HNSCC, für die bereits gezielte Therapiestrategien entwickelt wurden, sind in 1.1.4 aufgeführt. Eine Vielzahl aktueller Studien beschreibt neue Biomarker und potenzielle therapeutische *Targets* für HNSCC, wie z. B. CD44, ein Oberflächenmarker für Krebsstammzellen, der mit einer schlechten Prognose und Therapieresistenz in Larynx- und Pharynxkarzinomen korreliert [68]. Auf RNA-Ebene sind insbesondere nicht-kodierende regulatorische RNAs, *long non-coding* RNAs (lncRNAs) [69] und microRNAs (miRNAs) [70], im Fokus der Tumormarkerforschung.

1.3 MicroRNAs

Weniger als 2% des Genoms werden in *messenger* RNAs (mRNAs) übersetzt und kodieren für Proteine [71]. Kleine regulatorische nicht-kodierende RNAs rücken immer mehr in den Fokus der Wissenschaft. Die größte Gruppe darunter repräsentieren die *long non-coding RNAs* (lncRNAs). LncRNAs weisen eine Länge von ca. 200 Nukleotiden auf und stellen epigenetische Regulatoren der Genexpression dar, die mittels Chromatinmodifizierung die Transkription ihrer Zielgene beeinflussen [72]. Sie sind involviert in Differenzierung, Entwicklung und Karzinogenese [73]. Eine weitere Klasse nicht-kodierender RNAs sind microRNAs (miRNAs), evolutiv hoch konservierte RNAs mit einer Länge von ca. 22 Nukleotiden. Sie agieren als posttranskriptionelle Regulatoren der Genexpression, indem sie durch Basenpaarung an ihre Ziel-mRNA binden und entweder die Translation blockieren oder die mRNA degradieren [74]. Die erste miRNA, *lin-4*, wurde 1993 in *Caenorhabditis elegans* entdeckt. *Lin-4* reguliert das Protein LIN-14, welches für den Entwicklungsprozess essentiell ist [75]. In den darauffolgenden Jahrzehnten wurden zahlreiche miRNAs in Pflanzen, Tieren und Viren identifiziert. Bislang sind über 2500 verschiedene humane miRNAs in der Datenbank *human genome miRBase* (Release 21.0) bekannt [76], die auf die Expression von über 60% der humanen Gene Einfluss nehmen [77]. Dabei kann eine miRNA mehrere Ziel-mRNAs regulieren und umgekehrt eine mRNA Erkennungssequenzen für mehrere miRNAs besitzen.

Die für miRNAs kodierenden Sequenzen stellen entweder eigene Gene in Form von polycistronischen *Clustern* dar oder liegen in Introns, manchmal auch in Exons anderer Gene. Sie werden zunächst von der Polymerase II, seltener auch von der Polymerase III, zu sogenannten

primary precursor miRNAs (pri-miRNAs) transkribiert [78, 79]. Diese sind zu einer Haarnadelstruktur gefaltet und werden von dem RNase III Enzym Drosha endonukleolytisch gespalten, wodurch etwa 70 Nukleotide lange *precursor* miRNAs (pre-miRNAs) entstehen. Einige miRNAs werden jedoch Drosha-unabhängig mittels *Splicing* aus Introns generiert [79]. Nach dem Exportin-5 vermittelten Export der pre-miRNA ins Zytoplasma wird die Haarnadelstruktur durch das RNase III Enzym Dicer entfernt. Dadurch entsteht ein ca. 22 Nukleotide langer RNA-Duplex, wobei ein RNA-Strang die reife miRNA darstellt. Dieser wird bevorzugt in den *miRNA induced silencing complex* (miRISC) integriert, während der Gegenstrang meist degradiert wird [79]. Die Hauptkomponenten des miRISC sind Argonaute (AGO) Proteine. MRNAs, die von miRNAs reguliert werden, befinden sich zusammen mit Argonaute Proteinen in zytoplasmatischen Foci, den sogenannten *Processing bodies* [78].

Die Erkennung der Ziel-mRNA beruht auf der Komplementarität von miRNA und mRNA. Dabei kann eine Interaktion nur stattfinden, wenn die sogenannte *seed*-Region, die durch die Nukleotide 2-7 der miRNA repräsentiert wird, Komplementarität zu einer Erkennungssequenz der mRNA aufweist. Die Erkennungssequenz befindet sich meist in der 3‘-untranslatierten Region der mRNA, kann jedoch auch in der 5‘-untranslatierten Region oder im kodierenden Bereich liegen [80]. Während in Pflanzen eine perfekte Basenpaarung von miRNA und Ziel-mRNA üblich ist, ist in tierischen Zellen eine Komplementarität der *seed*-Region ausreichend. Für die Interaktion zwischen der *seed*-Region und der Erkennungssequenz sind vier konservierte Strukturen bekannt. Bei der 6mer-Struktur stimmt die Erkennungssequenz lediglich mit den sechs Nukleotiden der *seed*-Region überein. Bei der 7mer-m8-Struktur hybridisiert die Erkennungssequenz ebenfalls mit der gesamten *seed*-Region und wird erweitert durch eine Basenpaarung mit dem achten Nukleotid der miRNA. Bei der 7mer-A1-Struktur wird die Erkennungssequenz durch ein Adenosin gegenüber dem ersten Nukleotid der miRNA verlängert. Die 8mer-Struktur stellt eine Kombination aus der 7mer-m8- und 7mer-A1-Struktur dar [77]. Die Expression des Zielgens wird am effizientesten reguliert, wenn eine 8mer-Struktur vorliegt, gefolgt von der 7mer-m8- und der 7mer-1A-Struktur. Die 6mer-Struktur hat den geringsten Einfluss auf die Expression [80]. Auch die Position der Erkennungssequenz und die Zusammensetzung der benachbarten Sequenzen wirken sich auf die Effizienz der Regulation aus [81].

Die miRNA vermittelte Regulation einer mRNA beruht entweder auf einer Inhibition der Translation oder auf Destabilisierung und Degradation der mRNA [82]. Die in Pflanzen übliche perfekte Basenpaarung von miRNA und mRNA induziert die endonukleolytische Spaltung der mRNA durch AGO, was zu einer schnellen Degradation der mRNA führt. In tierischen Zellen, in denen miRNA und mRNA eine meist unvollständige Paarung aufweisen, wird die Ziel-mRNA

vorwiegend durch miRISC induzierte Deadenylierung destabilisiert, was eine Degradation der mRNA zur Folge hat. Eine miRISC vermittelte Inhibition der Translation hingegen beruht auf Ribosomen *drop-off* oder Proteolyse des entstehenden Peptids [82].

MiRNAs als Biomarker

MiRNAs spielen in nahezu allen zellulären Signalwegen eine regulatorische Rolle. Somit beeinflussen sie wichtige zelluläre Prozesse wie Entwicklung, Differenzierung, Proliferation und Zelltod. Infolgedessen kommt ihnen auch eine wichtige Bedeutung in der Stressantwort zu. Die miRNA Expression wird durch Stressoren wie Nährstoffmangel, Hypoxie, DNA-Schädigung, z. B. durch ionisierende Strahlung, sowie durch Krankheiten beeinflusst [83, 84]. Dadurch ist die Zelle in der Lage auf Stresssituationen zu reagieren und die Genexpression entsprechend zu adaptieren. Als Folge von DNA-Schäden wird beispielsweise TP53 induziert, ein Transkriptionsfaktor, der die Zellzykluskontrollpunkte aktiviert und entweder die DNA-Reparatur einleitet oder bei einer zu starken Schädigung der DNA den programmierten Zelltod induziert. TP53 reguliert im Kontext der Schadensantwort die Expression mehrerer miRNAs und umgekehrt wird auch TP53 von miRNAs reguliert [85]. Aufgrund der Beteiligung der miRNAs an der DNA-Schadensantwort kommt ihnen auch eine wichtige Bedeutung in der Karzinogenese zu. Es ist bekannt, dass miRNAs neben Krebserkrankungen auch eine Rolle bei kardiovaskulären, neurologischen und inflammatorischen Erkrankungen spielen [84]. Sie zeigen oft klare Signaturen, die spezifisch für eine Krankheit sind und eine Abgrenzung zu gesunden Individuen erlauben. Aufgrund ihrer Gewebsspezifität und ihrer vielfältigen *Targets* können miRNAs nicht eindeutig als Onkogen oder Tumorsuppressor klassifiziert werden. Somit kann eine miRNA in unterschiedlichen Tumorentitäten unterschiedliche Effekte haben [86]. Diese Spezifität und die Tatsache, dass miRNA-Signaturen nicht nur den malignen Charakter von Tumoren reflektieren, sondern auch nach Parametern, wie Geschlecht und Alter des Patienten oder Stadium und Invasivität des Tumors unterscheiden können, qualifiziert miRNAs als vielversprechende Biomarker in der Krebsdiagnostik [87]. Darüber hinaus verändert Strahlentherapie oder Chemotherapie die Expression bestimmter miRNAs [88, 89], was diese zu geeigneten Biomarkern für die Therapieüberwachung und Prognose macht. Umgekehrt beeinflussen miRNAs die Empfindlichkeit von Tumoren gegenüber strahlentherapeutischer oder chemotherapeutischer Behandlung [90] und stellen somit potenzielle therapeutische *Targets* dar. Auch für HNSCC konnten bereits einige miRNAs als vielversprechende diagnostische und prognostische Marker identifiziert werden [91, 92]. Die Anwendung von miRNAs in der Klinik birgt jedoch einige Herausforderungen. MiRNAs weisen eine hohe Sensitivität auf und können durch zahlreiche Faktoren und Umwelteinflüsse, wie physische

Betätigung [93] oder Ernährung [94], beeinflusst werden. Darüber hinaus reguliert eine miRNA zahlreiche Ziel-mRNAs, weshalb einer therapeutischen Anwendung eine eingehende Analyse des funktionalen Netzwerks einer miRNA vorangehen muss. Die erste Phase 1 klinische Studie zu miRNAs untersucht derzeit den therapeutischen Einsatz der *miR-34* Familie bei nicht operablen primären Leberkarzinomen und fortgeschrittenen oder metastasierenden Karzinomen mit Beteiligung der Leber [95].

Zellfreie zirkulierende miRNAs

MiRNAs existieren nicht nur intrazellulär, sondern sind auch in extrazellulärer Form in Körperflüssigkeiten, wie Blut, Tränenflüssigkeit, Urin, Liquor oder Speichel, detektierbar. Zellfreie miRNAs in Blutplasma und Serum sind resistent gegen Ribonukleasen und weisen eine hohe Stabilität gegenüber wiederholter Einfrier- und Auftauvorgänge oder pH-Veränderungen auf [96]. Dies beruht darauf, dass einige miRNAs in Nukleoproteinkomplexen an Ago2 oder Nukleophosmin 1 (NPM1) gebunden sind oder wenn sie als freie miRNAs, z. B. aus nekrotischen Zellen, in die Körperflüssigkeit gelangen mit dem *high-density lipoprotein* (HDL) assoziieren.

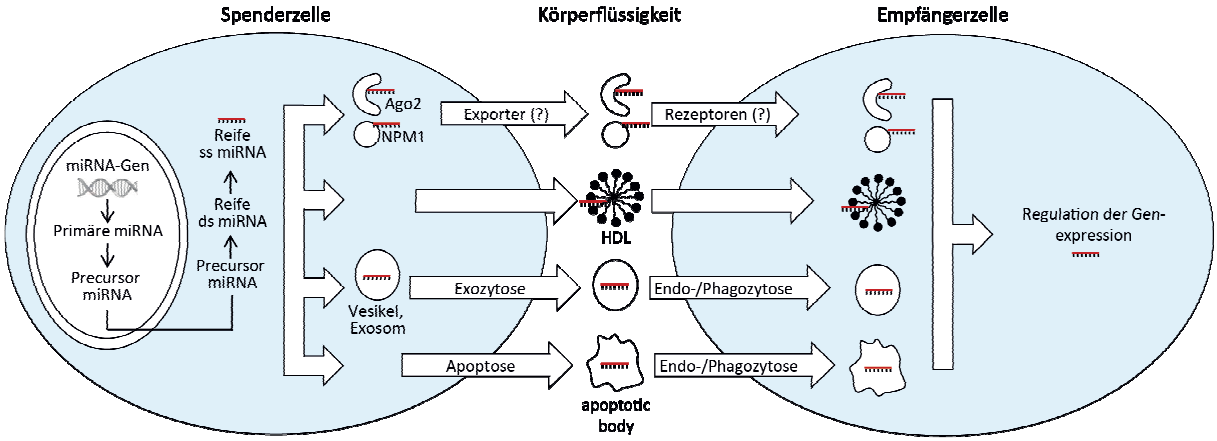

Abbildung 1 Mögliche Zell-Zell-Übertragungsmechanismen von miRNAs über Körperflüssigkeiten (modifiziert nach Selth et al., 2012 [97]). Die miRNAs werden in der Spenderzelle transkribiert und prozessiert. Die reifen miRNAs werden anschließend entweder in Nukleoproteinkomplexen mit Ago2 oder NPM1 oder in Lipidvesikeln (Exosomen) aus der Zelle exportiert. Freie miRNAs können mit HDL assozieren, wodurch sie vor dem Abbau durch Ribonukleasen geschützt sind. Auch als Produkt apoptotischer Zellen können miRNAs extrazellulär vorkommen in Form von *apoptotic bodies*. Die miRNAs können dann von Empfängerzellen durch verschiedene mögliche Mechanismen (z. B. Endozytose) aufgenommen werden, wo sie die Genexpression regulieren können.
ds: *double stranded*, ss: *single stranded,* Ago2: Argonaute2, NPM1: Nukleophosmin1, HDL: *high-density lipoprotein*

Andere zellfreie miRNAs liegen eingeschlossen in Lipidvesikel, den sogenannten Exosomen, oder in *apoptotic bodies* vor (Abb. 1) [97].

MiRNAs können entweder durch zielgerichtete Exkretion (z. B. Exosomen) oder aber durch ungerichtete Freisetzung (z. B. durch Nekrose) in die Körperflüssigkeiten gelangen. Durch die Verbreitung über Körperflüssigkeiten könnten die miRNAs einen hormonartigen Effekt zeigen und so weitreichende Auswirkungen haben [98]. Der Ursprung der miRNAs ist dabei meist unklar, da die „Spenderzellen" oft nicht eindeutig identifiziert werden können. Es konnte jedoch gezeigt werden, dass diese miRNAs ebenso wie zelluläre miRNAs als Biomarker dienen können. *MiR-21* wurde beispielsweise als Tumormarker in der Zirkulation von HNSCC Patienten identifiziert und zeigte eine deutliche Reduktion nach operativer Entfernung des Tumors [99], ebenso wie *miR-195* und *miR-let-7a* im Blut von Brustkrebspatienten [100]. Diese Resultate deuten darauf hin, dass miRNAs in der Zirkulation den Tumorstatus reflektieren und somit als Marker für Prognose und Therapieentscheidungen dienen können. Zudem zeigen Plasma-miRNAs Veränderungen durch ionisierende Strahlung [101] und chemotherapeutische Behandlung [89]. In Exosomen Transfer Experimenten konnten Effekte exosomaler miRNAs auf die Chemoresistenz oder das Metastasierungspotenzial der Zielzellen beobachtet werden [102]. Diese Eigenschaften verbunden mit der Möglichkeit eines minimalinvasiven Nachweises machen zellfreie zirkulierende miRNAs zu äußerst attraktiven Biomarkern für den Therapieverlauf.

1.4 Ziele der Arbeit

Da die Überlebensrate von HNSCC Patienten in fortgeschrittenen Stadien trotz beträchtlicher Weiterentwicklung der Therapiemethoden immer noch gering ist [5], stellt die Erforschung gut zugänglicher Biomarker einen vielversprechenden Ansatz für individuell abgestimmte und effektive Therapieentscheidungen dar.

Ziel der vorliegenden Arbeit war die Identifikation von Plasma-miRNAs, die als Biomarker zur Therapieüberwachung und Prognose von HNSCC Patienten dienen können. Zudem sollten Untersuchungen durchgeführt werden, die Aussagen über den Ursprung der Marker-miRNAs im Plasma zulassen. Des Weiteren sollten die funktionellen Netzwerke der durch die therapeutische Intervention veränderten miRNAs analysiert werden, um einen Überblick über die zellulären Prozesse, die durch die Radio(chemo)therapie beeinflusst werden, zu erhalten und molekulare *Targets* zu identifizieren, die potenziell für gezielte Therapien verwendet werden können.

Um diese Aspekte zu adressieren, sollten sowohl Analysen an Patientenmaterial als auch im Zellkulturmodell durchgeführt werden. Dazu sollte ein Untersuchungskollektiv (*discovery cohort*) von HNSCC Patienten, die entweder mit definitiver Radiotherapie oder einer

Kombinationstherapie aus Radiotherapie und Chemotherapie bzw. Immuntherapie behandelt wurden, analysiert werden. Dabei sollten nur Patienten eingeschlossen werden, die keiner operativen Tumortherapie unterzogen wurden, um die Hypothese zu prüfen, dass Veränderungen der Plasma-miRNAs während der Therapie den Tumorstatus reflektieren, und Aussagen über den Erfolg der Therapie ermöglichen. Mittels quantitativer *real-time PCR (qRT-PCR) arrays* sollten Veränderungen der Plasma-miRNAs nach zwei Fraktionen therapeutischer Bestrahlung im Vergleich zu dem Plasma-miRNA Status vor Beginn der Therapie ermittelt werden. Die dadurch identifizierten Marker-Kandidaten sollten anschließend mit *single qRT-PCR assays* technisch validiert werden. Ein Vergleich der miRNA-Profile im Plasma vor und nach Radio(chemo)therapie mit den Profilen der peripheren mononukleären Zellen (PBMNC) derselben Patienten sollte die Überprüfung einer möglichen Herkunft der Kandidaten-miRNAs aus Blutzellen ermöglichen. Des Weiteren sollten die Plasma-miRNA Profile der HNSCC Patienten mit denen eines nach Alter und Geschlecht angepassten Kollektivs gesunder Spender verglichen werden, um Hinweise auf einen möglichen Tumorursprung der Plasma-miRNAs zu erhalten.

Alle Plasma-miRNAs, die eine Differenzierung zwischen gesunden Individuen und HNSCC Patienten erlaubten sowie alle Plasma-miRNAs, die eine Veränderung nach Radiochemotherapie zeigten, sollten in einem unabhängigen HNSCC Patientenkollektiv validiert werden.

Die so ermittelten Marker-miRNAs sollten sowohl im Untersuchungskollektiv als auch im Validierungskollektiv auf ihre prognostische Aussagekraft bezüglich lokoregionärer Tumorkontrolle, Progress-freien Überlebens und des Gesamtüberlebens getestet werden. Um weitere Informationen über die Herkunft dieser miRNAs zu gewinnen, sollte die Expression der Marker-miRNAs zudem in Tumorbiopsien von Patienten aus beiden Kohorten bestimmt werden.

Zu demselben Zweck und für funktionelle Studien sollte im Rahmen der vorliegenden Arbeit ein Zellkulturmodell entwickelt werden, welches die Radiochemotherapie in der Klinik simuliert. Dafür sollten primäre HNSCC Zellen entsprechend des in den verwendeten Patientenkollektiven üblichen Schemas behandelt werden. Nach globaler miRNA- und mRNA-Analyse der HNSCC Zellen sollten mögliche funktionelle Netzwerke der durch die Behandlung veränderten miRNAs erstellt werden, die auf einer negativen Korrelation der jeweiligen miRNA-Expression mit der Expression bereits bekannter validierter Ziel-mRNAs mit einer ebenfalls signifikanten Veränderung nach der Behandlung, basieren. Anhand der veränderten mRNAs sollten zudem Signalwege identifiziert werden, die von der simulierten Radiochemotherapie betroffen waren, um so mögliche therapeutische Targets zu identifizieren. Darüber hinaus sollten im Zellkulturmodell potenzielle Zielgene und Signalwege der im Plasma von HNSCC Patienten identifizierten Marker-miRNAs ermittelt werden, um einen Einblick in deren Funktion zu erhalten.

2 PUBLIZIERTE ERGEBNISSE

2.1 Zusammenfassung

Maligne Tumore des Kopf-Hals-Bereiches, meist Plattenepithelkarzinome (HNSCC), stellen die sechsthäufigste Krebserkrankung weltweit dar. Da Kopf-Hals-Tumore, besonders in fortgeschrittenen Stadien, aufgrund ihrer Lokalisation in direkter Nähe zu essentiellen Strukturen häufig nicht operabel sind, werden alternative Therapieformen benötigt. Spezifische Marker, die Vorhersagen über das individuelle Ansprechen auf eine Behandlungsform, wie z. B. eine Radiotherapie, zulassen, können zur Stratifizierung von Patienten herangezogen werden, um individuell angepasste Therapieentscheidungen zu treffen. Zudem kann eine Therapie gegen molekulare Zielstrukturen den Effekt einer Radio(chemo)therapie intensivieren und somit zu einer verbesserten Tumorkontrolle und einer höheren Überlebensrate bei HNSCC Patienten beitragen.

In der vorliegenden Arbeit sollten microRNAs (miRNAs) identifiziert werden, die als Biomarker für Prognose und den Therapieverlauf in der Radio(chemo)therapie von HNSCC Patienten genutzt werden können. Dazu wurde die miRNA-Expression mittels quantitativer *real-time PCR* im Blutplasma von 18 HNSCC Patienten (Untersuchungskollektiv) vor Beginn der Therapie und nach zwei Fraktionen therapeutischer Bestrahlung verglichen. Die Plasma-miRNAs *miR-21-5p*, *miR-28-3p*, *miR-93-5p*, *miR-142-3p*, *miR-191-5p*, *miR-195-5p*, *miR-425-5p* und *miR-574-3p* wurden als die vielversprechendsten Marker für die lokoregionäre Tumorkontrolle bzw. das Überleben der HNSCC Patienten identifiziert. MiRNA-Analysen der mononukleären Blutzellen wiesen darauf hin, dass die Expressionsänderungen der zirkulierenden miRNAs nach radio(chemo)therapeutischer Behandlung nicht von peripheren mononukleären Blutzellen verursacht werden. Es wurden hingegen starke Indizien für einen Zusammenhang zwischen Plasma-miRNAs und dem Tumorstatus gefunden. So repräsentierte die Mehrheit der nach Radio(chemo)therapie veränderten Plasma-miRNAs bereits bekannte Tumormarker. Darüber hinaus konnten miRNAs identifiziert werden (z. B. *miR-93-5p*, *miR-425-5p*), die sowohl im Plasma der HNSCC Patienten eine Therapieantwort zeigten, als auch in einem Zellkulturmodell primärer HNSCC Zellen nach simulierter Radiochemotherapie. Weiterhin zeigten Analysen der Plasma-miRNAs einer nach Alter und Geschlecht angepassten Gruppe gesunder Individuen signifikant geringere Expressionswerte für nahezu alle detektierbaren miRNAs im Vergleich zu den HNSCC Patienten. Die Beobachtung, dass diese Plasma-miRNAs, die gesunde Individuen von HNSCC Patienten unterscheiden, auch eine Therapieantwort im Plasma von HNSCC Patienten zeigen, weist darauf hin, dass diese miRNAs die Antwort des Tumors auf die Therapie reflektieren, was auf einen Tumorursprung

dieser miRNAs schließen lässt. Zudem konnte mittels miRNA-Expressionsanalysen an Tumorbiopsien der HNSCC Patienten gezeigt werden, dass alle Therapie-sensitiven Plasma-miRNAs auch im Tumorgewebe exprimiert werden.

In einer unabhängigen HNSCC Patientengruppe konnten alle zuvor identifizierten Therapie-sensitiven Plasma-miRNAs, sowie alle Plasma-miRNAs, die eine Differenzierung zwischen HNSCC Patienten und gesunden Individuen erlaubten, validiert werden. Um das prognostische Potenzial dieser Marker-miRNAs zu bestimmen, wurde eine mögliche Assoziation ihrer Expressionslevels im Plasma der HNSCC Patienten mit lokoregionärer Tumorkontrolle, Progress-freiem Überleben und Gesamtüberleben getestet. Die Analyse ergab jeweils einen signifikanten Zusammenhang hoher Plasma-Levels der miRNAs *miR-142-3p*, *miR-186-5p*, *miR-374b-5p*, *miR-195-5p* und *miR-574-3p* mit einer schlechteren Prognose.

Ein weiteres Ziel dieser Arbeit war die Identifikation der funktionellen Netzwerke von miRNAs, deren Expression nach radiochemotherapeutischer Behandlung verändert ist, sowie der davon betroffenen molekularen Prozesse. Dadurch sollte einerseits ein besseres Verständnis der Funktion der potenziellen Marker-miRNAs erlangt werden, andererseits sollten exemplarisch potenzielle therapeutische Zielstrukturen identifiziert werden, die einen Einfluss auf die Therapiesensitivität des Tumors besitzen. Dazu wurden in einem integrativen Ansatz globale miRNA- und mRNA-Arraydaten und die daraus resultierenden Signalwege aus einem zuvor etablierten Radiochemotherapie-Zellkulturmodell zweier primärer HNSCC Zelllinien kombiniert. Die zentralen zellulären Prozesse, die in beiden Primärzelllinien von der simulierten Radiochemotherapie betroffen waren, waren Zellzyklus und Proliferation, Zelltod und Stressantwort. TGF-beta-, TNF- und IL6- assoziierte Signalwege traten hingegen nur in einer der beiden Primärzelllinien als wesentlicher Teil der Therapieantwort auf. Da diese Zytokine eine wichtige Rolle in Entzündungsreaktionen spielen, ist dieses Resultat ein erster Hinweis darauf, dass inflammatorische Prozesse in der Therapieantwort potenziell für eine Stratifizierung von HNSCC Patienten genutzt werden können. Eine weitere Analyse fokussierte sich auf die funktionellen Netzwerke von miRNAs, die zuvor im Plasma der HNSCC Patienten als Therapiemarker identifiziert worden waren und gleichzeitig im Zellkulturmodell eine veränderte Expression nach simulierter Radiochemotherapie zeigten (*miR-21-5p*, *miR-93-5p*, *miR-106b-5p*, *miR-425-5p*). Die Analyse ergab, dass diese miRNAs hauptsächlich eine Rolle im E2F Transkriptionsfaktor Netzwerk und im PTEN/AKT Signalweg spielen. Diese Signalwege enthalten zahlreiche Tumorsuppressor- und Onkogene, was darauf schließen lässt, dass eine gezielte Deregulation dieser Signalwege einen vielversprechenden Ansatz zur Optimierung der

Tumortherapie darstellt. Um jedoch allgemeingültige Aussagen treffen zu können, werden umfangreichere Modelle mit zusätzlichen HNSCC Kulturen benötigt.

Die hier präsentierten Daten zeigen, dass miRNAs im Blutplasma von HNSCC Patienten die Antwort des Tumors auf die kombinierte Radiochemotherapie wiederspiegeln. Dies eröffnet die Möglichkeit die hier identifizierten Marker-miRNAs als minimalinvasiv verfügbare Biomarker zur Abschätzungsprognose und Therapieüberwachung zu nutzen. Die Analyse der funktionellen Netzwerke der Marker-miRNAs und der von Radiochemotherapie betroffenen zellulären Signalwege ermöglicht weiterhin die Identifikation neuer potenzieller therapeutischer Zielstrukturen.

2.2 Summary

Head and neck cancer represents the sixth most common cancer world-wide. Most of the malignancies in the head and neck region are squamous cell carcinomas (HNSCC), which are often not detected until they have developed advanced stages. Many advanced HNSCC are not resectable due to their close vicinity to essential anatomical structures, such as salivary glands and major blood vessels. Specific markers for a prediction of the individual therapy success, e.g. of radiotherapy, are needed for patient stratification and individualized treatment decisions. Another approach for a more effective treatment is the identification of novel therapeutic targets in order to enhance the therapy success and survival rate of HNSCC patients.

The presented work aimed to identify microRNAs (miRNAs) that can serve as biomarkers for prognosis and therapy monitoring during radio(chemo)therapy of HNSCC patients. For this purpose, the miRNA expression levels in the blood plasma of 18 HNSCC patients (discovery cohort) were determined by quantitative real-time PCR before therapy and after the second therapeutic irradiation. The plasma miRNAs *miR-21-5p*, *miR-28-3p*, *miR-93-5p*, *miR-142-3p*, *miR-191-5p*, *miR-195-5p*, *miR-425-5p* and *miR-574-3p* were identified as the most promising biomarkers for locoregional tumor control and survival of the HNSCC patients. MiRNA analyses of the peripheral blood mononuclear cells suggested that the expression changes of the circulating miRNAs following radio(chemo)therapy are not related to the peripheral blood mononuclear cells. However, strong evidence was found that the plasma miRNAs are related to the tumor status. To begin with, the majority of deregulated plasma miRNAs following radio(chemo)therapy represented known tumor markers. Moreover, miRNAs were identified that showed a response to therapy in the plasma of the HNSCC patients and that were also deregulated in a cell culture model of primary HNSCC cell lines after simulated radiochemotherapy (e.g. *miR-93-5p*, *miR-425-*

5p). Furthermore, plasma miRNA analysis of a group of age- and sex-matched healthy donors showed significantly lower expression levels for almost all detectable miRNAs compared to the HNSCC patients. The observation that plasma miRNAs differentiating patients and healthy individuals also represented therapy-responsive plasma miRNAs in HNSCC patients, hints to a tumor origin of these miRNAs. Moreover, miRNA expression analysis of tumor biopsies from the HNSCC patients demonstrated that all therapy-responsive plasma miRNAs are also expressed in the tumor tissues, which further supports the hypothesis of a tumor origin of these miRNAs.

All plasma miRNAs identified as differentially expressed between HNSCC patients and healthy individuals, as well as the therapy-responsive miRNAs identified in this study, were confirmed in an independent cohort of HNSCC patients. In order to determine the prognostic potential of these miRNAs their ability to predict locoregional tumor control, progression-free survival and overall survival was tested. The analysis revealed a significant association of high plasma levels of *miR-142-3p*, *miR-186-5p*, *miR-374b-5p*, *miR-195-5p* and *miR-574-3p* with an unfavorable prognosis.

A further aim of the presented work was the identification of the functional networks of miRNAs showing changed expression after radiochemotherapy and the related cellular pathways. This analysis intended to provide a deeper understanding of the function of the potential marker miRNAs and to identify potential therapeutic targets, which influence the sensitivity of the tumor towards therapy. For this purpose, a cell culture model of two primary HNSCC cell lines with simulated radiochemotherapy was established. In an integrative approach, global miRNA and mRNA array data as well as the resulting cellular pathways of the radiochemotherapy cell culture model from two primary cell lines were combined. The main pathways affected in both primary cell lines were related to cell cycle and proliferation, cell death and stress response. However, TGF-beta, TNF and IL6 related signaling pathways were affected only in one of the two cell lines after treatment. Since these cytokines play an important role in inflammatory processes, this finding represents a first hint to the potential use of inflammatory processes in the therapy response for stratification of HNSCC patients. A further analysis focused on the functional networks of miRNAs that were identified as therapy markers in the blood plasma of HNSCC patients and also showed altered expression following simulated radiochemotherapy in the cell culture model (*miR-21-5p*, *miR-93-5p*, *miR-106b-5p*, *miR-425-5p*). The analysis revealed a major role of these miRNAs in the E2F transcription factor network and the PTEN/AKT signaling. Since these pathways contain several tumor suppressor genes and oncogenes, there is an indication that a deregulation of these pathways might enhance the curative effect of a radiochemotherapy. However, extended models including additional HNSCC cultures are required for general assumptions.

The presented work demonstrates that miRNAs in the blood plasma of HNSCC patients reflect the response of the tumor to the radiochemotherapy treatment. This opens up the possibility to utilize the marker miRNAs identified in this study as minimally invasive biomarkers for prognosis and therapy monitoring. The analysis of the functional networks of the marker miRNAs and the cellular pathways affected by radiochemotherapy further enables the identification of new potential therapeutic targets.

2.3 Beschreibung des Journals Radiation Oncology

Radiation Oncology (ISI Abkürzung: Radiat Oncol) publiziert Forschungsergebnisse aus den Bereichen der Strahlenbiologie, Strahlenphysik, Strahlentechnologie und klinischen Onkologie. Der Fokus des Journals liegt auf Aspekten, die die Behandlung von Krebs durch Bestrahlung beeinflussen.

Das Journal wird von Thomson Reuters in den Kategorien *Oncology* und *Radiology, nuclear medicine & medical imaging* geführt. Mit einem *Impact factor* von 2,546 und einem 5-Jahres *Impact factor* von 2,75 liegt es nach den *Journal Citation Reports* 2014 auf Rang 119 von 211 in der Kategorie *Oncology* und auf Rang 40 von 125 in der Kategorie *Radiology, nuclear medicine & medical imaging*.

Summerer et al. Radiation Oncology 2013, 8:296
http://www.ro-journal.com/content/8/1/296

RADIATION ONCOLOGY

RESEARCH Open Access

Changes in circulating microRNAs after radiochemotherapy in head and neck cancer patients

Isolde Summerer[1], Maximilian Niyazi[2], Kristian Unger[1,4], Adriana Pitea[1], Verena Zangen[1,4], Julia Hess[1,4], Michael J Atkinson[3], Claus Belka[2,1], Simone Moertl[3] and Horst Zitzelsberger[1,4*]

Abstract

Introduction: Circulating microRNAs (miRNAs) are easily accessible and have already proven to be useful as prognostic markers in cancer patients. However, their origin and function in the circulation is still under discussion. In the present study we analyzed changes in the miRNAs in blood plasma of head and neck squamous cell carcinoma (HNSCC) patients in response to radiochemotherapy and compared them to the changes in a cell culture model of primary HNSCC cells undergoing simulated anti-cancer therapy.

Materials and methods: MiRNA-profiles were analyzed by qRT-PCR arrays in paired blood plasma samples of HNSCC patients before therapy and after two days of treatment. Candidate miRNAs were validated by single qRT-PCR assays. An *in vitro* radiochemotherapy model using primary HNSCC cell cultures was established to test the possible tumor origin of the circulating miRNAs. Microarray analysis was performed on primary HNSCC cell cultures followed by validation of deregulated miRNAs via qRT-PCR.

Results: Unsupervised clustering of the expression profiles using the six most regulated miRNAs (*miR-425-5p*, *miR-21-5p*, *miR-106b-5p*, *miR-590-5p*, *miR-574-3p*, *miR-885-3p*) significantly ($p = 0.012$) separated plasma samples collected prior to treatment from plasma samples collected after two days of radiochemotherapy. MiRNA profiling of primary HNSCC cell cultures treated *in vitro* with radiochemotherapy revealed differentially expressed miRNAs that were also observed to be therapy-responsive in blood plasma of the patients (*miR-425-5p*, *miR-21-5p*, *miR-106b-5p*, *miR-93-5p*) and are therefore likely to stem from the tumor. Of these candidate marker miRNAs we were able to validate by qRT-PCR a deregulation of eight plasma miRNAs as well as *miR-425-5p* and *miR-93-5p* in primary HNSCC cultures after radiochemotherapy.

Conclusion: Changes in the abundance of circulating miRNAs during radiochemotherapy reflect the therapy response of primary HNSCC cells after an *in vitro* treatment. Therefore, the responsive miRNAs (*miR-425-5p*, *miR-93-5p*) may represent novel biomarkers for therapy monitoring. The prognostic value of this exciting observation requires confirmation using an independent patient cohort that includes clinical follow-up data.

Keywords: Head and neck cancer, Circulating non-coding RNA, Biomarker, Radiotherapy outcome, HNSCC cell culture model

* Correspondence: zitzelsberger@helmholtz-muenchen.de
[1]Research Unit Radiation Cytogenetics, Helmholtz Center Munich, Ingolstaedter Landstr 1, 85764, Neuherberg, Germany
[4]Clinical Cooperation Group 'Personalized Radiotherapy of Head and Neck Cancer', Helmholtz Center Munich, Ingolstaedter Landstr 1, 85764, Neuherberg, Germany
Full list of author information is available at the end of the article

Introduction

Surgical treatment of head and neck squamous cell carcinoma (HNSCC) is limited by the complex anatomy of the tumors and the associated risk of morbidity. Hence, for many patients an alternative treatment strategy of definitive radiotherapy alone or in conjunction with chemotherapy or immunotherapy is required [1]. Despite considerable progress in treatment options, disease recurrence and metastasis with a very strong impact on long-term survival are still the major challenges [2].

MicroRNAs (miRNAs) are evolutionarily conserved small RNAs, representing a class of regulators of post-transcriptional gene expression. There are more than 2000 mature miRNAs currently annotated in the human genome miRBase (release 19.0) [3] potentially targeting over 60% of all proteins [4]. Fundamental cellular processes including development, apoptosis [5], cell cycle control, proliferation [6] and DNA-damage repair [7] are influenced by miRNAs. During the last decade alterations in miRNA expression have been associated with a number of human diseases, including cancer (reviewed in [8]). The recent discovery of miRNAs in body fluids such as cerebrospinal fluid [9] and blood plasma [10] opens up the possibility of using miRNAs as minimally invasive biomarkers for the prediction of clinical endpoints such as overall survival [11,12]. The well described 'onco-miR' *miR-21* has already been identified as a valuable plasma biomarker with high prognostic power in esophageal squamous cell carcinoma [13] and gastric cancer [14].

Since the expression of miRNAs is known to be altered by ionizing radiation at both the cellular level [15] and plasma levels of mice [16], they might serve as easily accessible predictors of the individual response to radiation therapy. Additionally, miRNAs regulate drug sensitivity [17] and influence radioresistance [18-20]. This offers the possibility of using specific plasma miRNAs as biomarkers for optimized treatment decisions.

The present study aimed to identify blood plasma miRNAs showing a response to radiochemotherapy and further to clarify the origin of these miRNAs in order to use them as minimally invasive tools for therapy monitoring.

For this purpose we compared miRNA levels in samples of blood plasma from HNSCC patients prior to treatment and after the completion of the first two fractions of therapeutic irradiation. MiRNAs displaying altered concentration levels after treatment were further analyzed in peripheral blood mononuclear cells (PBMC) of the same patients to test the hypothesis of PBMC-derived alterations of the plasma miRNAs. Moreover, we established an *in vitro* radiochemotherapy model using primary HNSCC cells in order to investigate a potential tumor origin of the therapy-responsive miRNAs in blood plasma.

Materials and methods

Patient samples

Plasma miRNA analysis was performed on 18 patients (17 HNSCC, 1 esophageal adenocarcinoma) treated with local X-ray-irradiation using a linear accelerator (6 MV, Siemens Mevatron M or ELEKTA Synergy®). After a planning (PET-) CT scan 70 Gy were applied to the macroscopic tumor and involved lymph nodes in daily dose fractions of 2 Gy five days per week. The adjuvant lymphatics were irradiated with up to 50 Gy and the high-risk lymphatics (adjacent to the involved lymph node levels) with up to 60 Gy.

16 out of 18 patients received concurrent chemotherapy (12 patients received 5-fluorouracil (5-FU) plus mitomycin C (MMC) [21], 3 patients MMC and 1 patient cisplatin weekly). None of the patients underwent surgical treatment. 5-FU treatment was usually applied on each of the first 5 days of therapeutic irradiation whereas MMC was applied only on day 5 and day 36 during radiotherapy. Patient characteristics are listed in Table 1.

After obtaining ethical approval and informed consent, 15 ml of EDTA-peripheral blood were collected from each patient prior to the first fraction of therapy and within one hour after the second fraction of therapeutic irradiation. EDTA-blood samples were centrifuged at 350 × g for 10 min within two hours after collection to obtain plasma. To avoid cellular contamination the plasma samples were re-centrifuged at 1,200 × g for 3 min and subsequently at 14,000 × g for 10 min to remove cell debris.

PBMC were isolated using Ficoll gradient centrifugation.

Samples were stored at −20°C until further analysis or at −80°C for long term storage.

The study was approved by the ethics committee of the University of Munich (Germany).

Primary HNSCC cells

Primary tumor cells were obtained from the fresh tumor biopsies of two HNSCC cases, HN1957 (left maxilla/left nasal floor) and HN2092 (right floor of mouth) received from the Wales Cancer Bank, UK [22]. The tumor tissues were rinsed with PBS, minced and cultivated in keratinocyte media supplemented with L-glutamine, penicillin/streptomycin, EGF, BPE, $CaCl_2$, F-12, DMEM (all components: Life Technologies) and 10% FBS at 37°C and 5% CO_2. To ensure the exclusive cultivation of epithelial cells from tissue particles, fibroblast cells were identified via frequent microscopy and removed by scraping. The FBS-content of the media was continuously reduced down to serum-free cultivation. The epithelial origin of both cultures was assessed by positive cytokeratin staining via immunohistochemistry (Additional file 1). Characteristics of the two primary HNSCC cultures are listed in Table 2.

Summerer et al. Radiation Oncology 2013, 8:296
http://www.ro-journal.com/content/8/1/296

Table 1 Patient characteristics

Characteristic		Number of patients
Gender		
	male	14
	female	4
Median age, years		57.9
Age range, years		45.1–80.6
Tumor site		
	Larynx	5
	Oropharynx	3
	Mouth floor	2
	Tongue	2
	Esophagus	1
	Hypopharynx	1
	Maxilla	1
	Nasopharynx	1
	Sinuses	1
	Soft palate	1
T-Stage		
	I	4
	II	2
	III	6
	IV	6
N-Stage		
	N0	4
	N1	4
	N2	10
M-Stage		
	M0	16
	M1	2
Concomitant therapy (in addition to radiotherapy)		
	5-FU + MMC	12 (patient 3, 5–7, 9–13, 15–17)
	MMC	3 (patient 1, 14, 18)
	Cisplatin	1 (patient 8)
	Cetuximab	1 (patient 4)
	none	1 (patient 2)
Acute Toxicity		
	severe	11
	moderate	5
	n.a.	2

5-FU = 5-fluorouracil; MMC = mitomycin C;
n.a. = not available.

Table 2 Characteristics of primary HNSCC cell cultures

Characteristic	HN1957	HN2092
Gender of patient	female	male
Age at diagnosis, years	85	73
Tumor site	left maxilla/left nasal floor	right floor of mouth
TNM	n.a.	pT4pN0
Cell type	epithelial	epithelial

n.a. = not available.

Treatment of HNSCC cells

To model as closely as possible the most frequent chemotherapy treatment we tested different 5-FU treatment options using the primary HNSCC cultures. Cell viability was measured using the XTT cell proliferation kit II (Roche) for both cell cultures after applying a wide range of 5-FU doses (Figure 1a, b). The 5-FU concentrations were selected to be relatively high, however lying within the linear region of the dose–response curve. Thus, HN1957 cells were treated with 50 μM 5-FU and HN2092 cells, as they showed less sensitivity towards the agent, were treated with 100 μM 5-FU.

Cells were seeded in 60 mm-dishes and 24-well plates for RNA assays and cell viability assays, respectively. On the following day, cells were irradiated with 2 Gy using a ^{137}Cs source and treated with 5-FU (Sigma; solved in DMSO). Controls were treated with the corresponding volumes of DMSO and sham-irradiated. 24 h after the first irradiation a second fraction of 2 Gy was applied to the 5-FU-treated cells followed by incubation for 1 h at 37°C. Cells were harvested by trypsinization and stored at −20°C until further processing.

Cell viability assay (XTT)

In order to determine cell viability of cells treated with *in vitro* radiochemotherapy or 5-FU treatment alone, 24-well plates were used for three biological and two technical replicates of each condition. XTT-assay was conducted using 350 μl of Medium and 150 μl of XTT-labeling mixture. Measurement was performed 24 h after 5-FU treatment.

Colony forming assay

In order to determine the radiation sensitivity of the primary HNSCC cells, the colony forming assay was performed in 6-well plates (Figure 1c, d). To ensure stable growth of the primary cells, a feeder layer consisting of the same HNSCC cells was used. Feeder cells were irradiated with 50 Gy in a ^{60}Co source before seeding in the 6-well plates (10,000 cells/well). The following day, fresh cells for colony formation were plated on the feeder layer. On the following day the cells were irradiated using a ^{137}Cs source with 0, 0.5, 1, 2, 3, 5 or 7.5 Gy. HN1957 colonies were stained with Giemsa six days and HN2092 colonies 12 days after irradiation. Colonies consisting of at least 50 cells were scored. Each colony

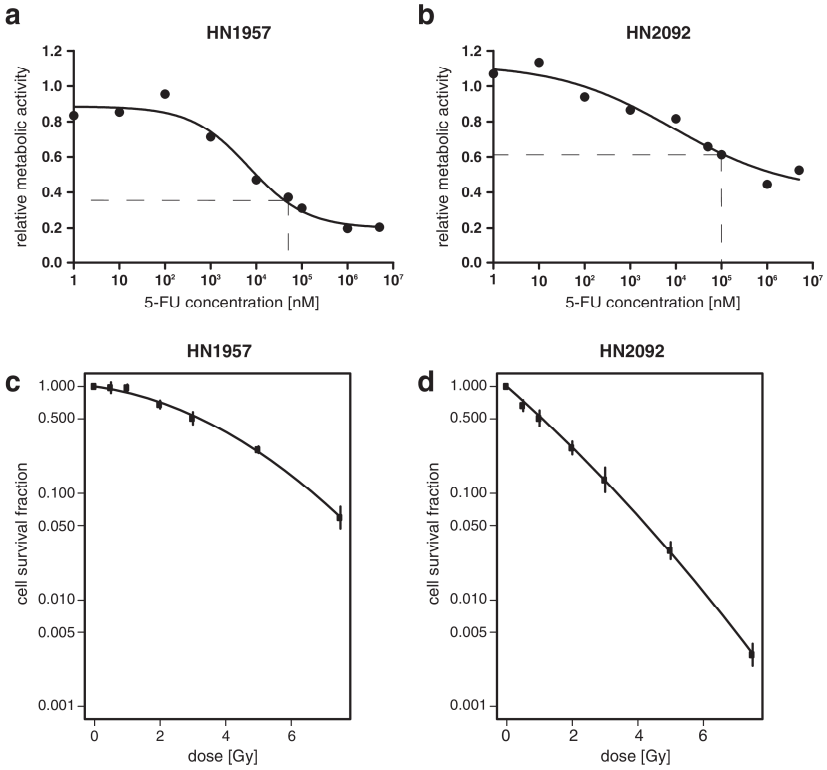

Figure 1 Sensitivity of primary HNSCC cell cultures to 5-FU treatment and ionizing radiation. Cell viability (XTT-assay) of HN1957 **(a)** and HN2092 **(b)** 48 h after 5-FU treatment relative to DMSO-controls. Each data point represents the mean of three biological replicates. Dashed lines mark the 5-FU concentrations selected for *in vitro* radiochemotherapy modeling. Survival curves were generated by colony forming assay for HN1957 **(c)** 6 days after irradiation and HN2092 **(d)** 12 days after irradiation. Error bars represent the standard deviation of three biological replicates.

formation assay was carried out in triplicate and repeated three times.

RNA extraction

Total RNA was extracted from 300 μl plasma using the mirVana miRNA Isolation Kit (Ambion) according to the manufacturer's protocol with the following modification: 1,000 μl of lysis buffer was added to 300 μl of plasma. 1.04 fmol of synthetic *cel-miR-39 (C. elegans)* was added to each plasma sample (300 μl) after the protein denaturation step to normalize sample-to-sample variation in RNA recovery. RNA was finally eluted into 50 μl of pre-heated (95°C) nuclease-free water.

RNA from PBMC was extracted with the mirVana miRNA Isolation Kit (Ambion) according to the manufacturer's protocol. RNA purity was measured by spectrophotometry (OD 260/280 ratio) using a Nanodrop ND-1000 (Thermo Scientific). Ratios were in the range of 1.89 to 2.09.

Extraction of total RNA from primary HNSCC cells was performed using the miRNeasy mini kit (Qiagen) according to the manufacturer's protocol without DNase digest or small RNA enrichment. OD 260/280 ratios, measured on a Nanodrop ND-1000 (Thermo Scientific), were in the range of 1.92 to 2.04. Additionally, RNA quality was assessed prior to the Agilent microarray experiments using an Agilent 2100 Bioanalyzer (Agilent Technologies). The computed RNA integrity numbers (RINs) ranged from 9.3 to 10.0.

MiRNA profiling in patient plasma

TaqMan Array Human MicroRNA A Cards v2.0 (Applied Biosystems) representing 377 mature human miRNAs were used to obtain miRNA profiles of the blood plasma samples. Reverse transcription was performed using the TaqMan miRNA reverse transcription kit (Applied Biosystems) in combination with the stem-loop megaplex primer pool set A v2.1. Because of the low abundance of circulating miRNA in the starting material we used a fourfold volume of the reaction mix, prepared according to the manufacturer's protocol adding 12 μl of total plasma RNA.

For the subsequent quantitative real-time PCR 30 μl of cDNA was used for each array and PCR was carried out on an Applied Biosystems 7900HT. The reaction mixtures were incubated at 50°C for 2 min and 95°C for 10 min, followed by 45 cycles of 95°C for 30 s and 60°C for 1 min. All Ct values were normalized using the median Ct value of all detectable miRNAs on the array.

MicroRNA profiling in HNSCC cells

To analyze the effects of *in vitro* radiochemotherapy on the cellular miRNA expression levels Sure Print G3 human 8x60k miRNA microarrays (Agilent Technologies) were used covering 1205 human miRNAs (Sanger miRBase release 16). 100 ng of total RNA was dephosphorylated and labeled with cyanine 3-cytidine biphosphate including a labeling spike-in solution (Agilent Technologies) to assess the labeling efficiency. After purification of the labeled RNA, the samples were hybridized on the arrays including a hybridization spike-in solution (Agilent Technologies) to monitor hybridization efficiency. Arrays were scanned with a G2505C Sure Scan Microarray Scanner (Agilent Technologies) using Scan Control software. For data processing the following software was used: Feature extraction 10.7 (Agilent Technologies) and GeneSpring 11.5. MiRNA analysis was conducted with three biological and two technical replicates for each data point. All steps were performed according to the manufacturer's protocol. The raw data were imported into the R statistical platform [23]. The total microRNA gene signal (TGS) was computed by the Agilent Extraction feature. The resulting signal was normalized to the mean signal of all arrays for compensation of systematic technical slide-to-slide variations. A differential expression analysis was performed using the linear model components implemented in *limma* [24] and empirical Bayes methods were applied in order to attain moderated statistics [25].

Real-time PCR quantification of individual miRNAs

Reverse transcription was performed using the TaqMan miRNA reverse transcription kit and miRNA-specific stem-loop primers (Applied Biosystems). Reverse transcription was performed on a Cyclone PCR system (Peqlab) according to the manufacturer's protocol. For miRNA assays in plasma samples 3 μl of cDNA was used for reverse transcription because of the low RNA content. Real-time PCR was performed in duplicates and included non-template negative controls. PCR was performed on a ViiA 7 real-time PCR System (Applied Biosystems) following the manufacturer's protocol. For plasma samples the miRNA concentration levels were normalized to the spiked-in *cel-miR-39*, for cellular samples the U6 snRNA was used for normalization. Fold changes were calculated using the $2^{-\Delta\Delta Ct}$ method [26].

Statistical analysis

To identify differentially expressed miRNAs in plasma samples of patients prior to radiotherapy and after the second fraction of therapeutic irradiation Wilcoxon test was performed. All miRNAs that were detected in less than 30% of either control samples or irradiated samples were excluded from further analysis. Unsupervised hierarchical clustering was performed using the top distinctive miRNAs applying the parameters maximum distance and Ward's method. Fisher's exact test was applied to check for significant clustering of samples from patients prior to treatment and those collected after treatment. P values < 0.05 were considered statistically significant.

Correlation coefficients for miRNA changes in PBMC and plasma as well as in arrays and single assays were calculated using Pearson correlation. All statistical analyses were performed using The R Project for Statistical Computing [23].

Results

MiRNA profiling of the plasma samples from 18 head and neck cancer patients revealed 54 miRNAs with altered expression levels after treatment (Additional file 2). Unsupervised hierarchical clustering using the expression levels of the top six significantly deregulated miRNAs revealed two main clusters. Cluster 1 represents ten samples collected prior to treatment and two samples collected after treatment, whereas cluster 2 consists of eight pre-treatment samples and 16 post-treatment samples. Consequently, the miRNA profiles of these six miRNAs differentiated significantly ($p = 0.012$) between samples collected before therapy and those collected after two days of treatment (Figure 2). For technical validation of the array data eight miRNAs (*miR-590-5p, miR-574-3p, miR-425-5p, miR-885-3p, miR-21-5p, miR-28-3p, miR-195-5p, miR-191-5p*) were selected from the top list of deregulated miRNAs. Additionally, *miR-150-5p* and *miR-142-3p*, both known to play a role in esophageal carcinoma [27,28], were used for validation. For these ten miRNAs the differences between the two groups were validated using single qRT-PCR assays. The correlation coefficients of the normalized Ct values demonstrated a good correlation between the results of the TaqMan low density array and the TaqMan single assays for most of the tested miRNAs (Additional file 3). The single assays of *miR-590-5p* and *miR-885-3p* were below the detection level in almost all plasma samples and were consequently excluded from further analyses.

Many plasma miRNAs are known to originate from peripheral blood mononuclear cells (PBMC) [29]. Therefore, we measured the expression levels of the candidate therapy biomarker miRNAs (*miR-574-3p, miR-425-5p, miR-21-5p, miR-28-3p, miR-195-5p, miR-191-5p, miR-150-5p, miR-142-3p*) in PBMC samples obtained from

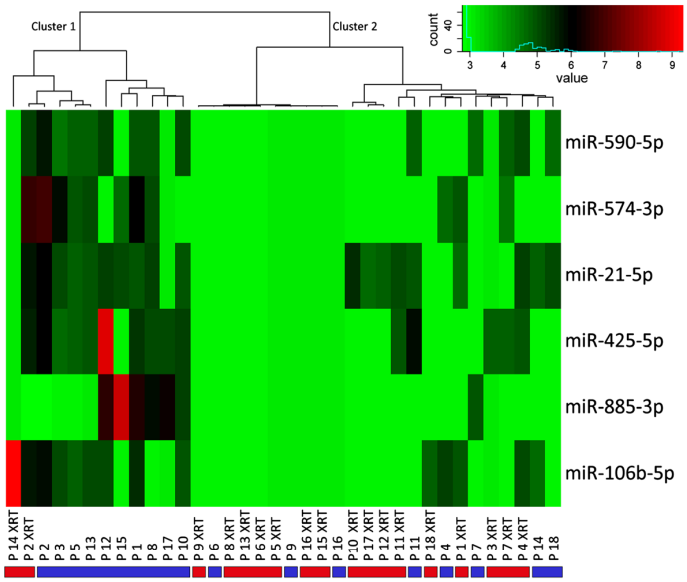

Figure 2 Unsupervised hierarchical cluster analysis of samples collected before therapy and after two days of treatment. Samples collected prior to treatment are marked with blue bars, samples collected after two days of treatment (XRT = radiotherapy) are marked with red bars. *Cluster 1* and *Cluster 2* indicate the two main clusters emerging from unsupervised cluster analysis using blood plasma concentration levels of the top six distinctive miRNAs.

the same patients. Correlation coefficients of the normalized Ct values indicated that the changed miRNA levels after treatment do not originate from PBMC (Additional file 4).

In order to further investigate whether the plasma miRNA changes following tumor therapy originate from the tumor cells we established an *in vitro* radiochemotherapy model using primary HNSCC from two different patients, HN1957 and HN2092 (Table 2).

For assessment of the sensitivity of the primary tumor cells to 5-FU and to ionizing radiation dose-response curves (Figure 1a, b) and survival curves (Figure 1c, d) were generated, respectively. HN2092 cells showed higher sensitivity to ionizing radiation but lower sensitivity to 5-FU treatment compared to HN1957 cells. In order to simulate the treatment of the patient samples in the present study cells were irradiated with 2 Gy followed by treatment with 5-FU and on the following day irradiation with a second 2 Gy fraction. Subsequent measurement of the cell viability (24 h after 5-FU treatment) showed no significant effect of 5-FU or irradiation on HN2092 cell cultures, whereas cell viability of HN1957 cell cultures was already reduced by 5-FU treatment alone with a significant additive effect of irradiation on the cell viability (Figure 3).

MiRNA profiling using Agilent microarrays in the sham-irradiated and DMSO-treated control cells compared to cells treated with *in vitro* radiochemotherapy revealed several miRNAs that differentiate control cells and treated cells for HN1957 and HN2092 (Additional files 5 and 6). We selected three miRNAs (*miR-425-5p, miR-21-5p, miR-106b-5p*) that were altered after *in vitro* treatment and were also in the top list of therapy-responsive miRNAs in patient plasma samples after *in vivo* tumor therapy. Additionally, *miR-93-5p* was included as it shows deregulation after *in vitro* treatment and *in vivo* treatment in most of the patients, although it is not among the top significant therapy-responsive miRNAs due to the different directions of regulation (Additional file 7). For these miRNAs we conducted TaqMan single assays in control and treated cells to validate the array results. The qRT-PCR assays confirmed an up-regulation of *miR-425-5p* with a *p* value close to the significance level ($p = 0.552$) in HN1957 cell cultures, while for *miR-93-5p* a significant down-regulation ($p < 0.001$) in HN2092 cell cultures became apparent (Table 3). Thus, at least two of the four treatment-regulated plasma miRNAs are likely to be associated with the direct response of tumor cells to treatment.

Discussion

The present study aimed to identify circulating miRNA markers in the plasma of HNSCC patients that are indicative of the efficacy of radiochemotherapy. Our finding that a limited panel of deregulated plasma miRNAs discriminates between pre- and post-radiochemotherapy samples (Figure 2) supports previous evidence [16] for

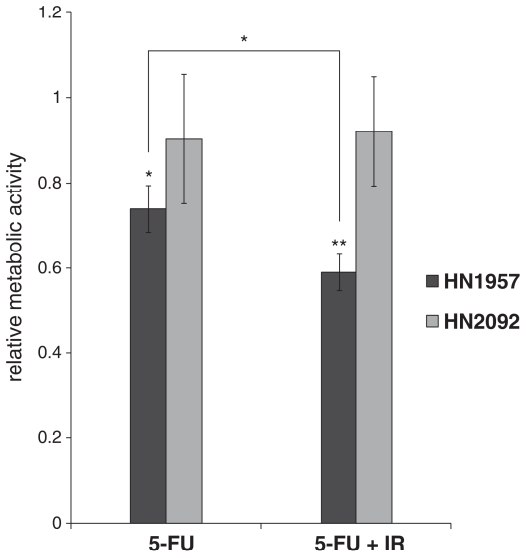

Figure 3 Cell viability (XTT-assay) of primary HNSCC cell cultures. Absorption was measured 24 h after exclusive 5-FU treatment and 5-FU treatment in combination with 2 x 2 Gy *in vitro* irradiation relative to DMSO-controls. Error bars represent the standard deviation of three biological replicates (*p < 0.05, **p < 0.01).

the potential use of plasma miRNAs as radiation-responsive biomarkers. Moreover, several candidates altered after the second fraction of therapeutic irradiation, such as *miR-93-5p*, *miR-142-3p*, *miR-106b-5p*, *miR-191-5p* and *miR-21-5p* (Additional file 2) have been previously described to be induced by ionizing radiation [30].

Although it is known that circulating miRNAs are present in stable forms, there is still uncertainty about their transport and cellular origin (reviewed in [31]). Since circulating miRNAs may originate from blood cells [29] we tested the hypothesis that the observed therapy-responsive plasma miRNAs originate from peripheral blood mononuclear cells (PBMC) of the same patients. Our analyses of the miRNA profiles of PBMC revealed no significant correlation between the miRNA expression in PBMC and plasma in patients before or after treatment (Additional file 4). We conclude that the plasma miRNA changes detected in response to anti-cancer therapy are most likely not originating from circulating PBMC.

It has frequently been hypothesized that plasma miRNAs originate from tumor cells, either based on active secretion [32] or in apoptotic bodies released from dead tumor cells [33]. This is supported by the present study as several candidates among the top significant plasma miRNAs that were altered after radiochemotherapy (Additional file 2) have already been reported to be tumor markers before. *MiR-195-5p, miR-574-3p* and *miR-28-3p* have been described as being differentially expressed in esophageal squamous cell carcinoma [34,35]. *MiR-191-5p* and *miR-21-5p* play a role in lung cancer diagnosis and prognosis [36], while *miR-21-5p* in plasma also is known to serve as prognostic marker in esophageal cancer patients [13]. Taken together, these reports indicate that the observed changes in plasma miRNAs in our study might be related to therapy effects on tumor cells.

To further strengthen this hypothesis we investigated the miRNA expression of primary HNSCC cell cultures under simulated radiochemotherapeutic treatment *in vitro*. The results of the miRNA expression analysis of this *in vitro* model further supported the assumption that the observed plasma miRNA changes are likely to originate from the tumor cells. We were able to show a significant deregulation of four plasma miRNAs in HN1957 cell cultures (*miR-425-5p*, *miR-21-5p*, *miR-106b-5p*, *miR-93-5p*) and one plasma miRNA in HN2092 cell cultures (*miR-93-5p*) by microarray profiling. The observation that the same miRNAs were altered in both tumor cells and plasma leads us to conclude that plasma miRNA changes following radiochemotherapeutic treatment are the result of miRNA release from damaged tumor cells. The observed differences in deregulated miRNAs between the two cell cultures, however, were not comparable. The two primary HNSCC cell cultures had different responses to radiochemotherapeutic treatment. This may be due to differences in the responsiveness of the cell cultures. Indeed, the cell viability assay (XTT) exhibited a significant effect 24 h after irradiation and 5-FU

Table 3 MicroRNAs significantly deregulated after radiochemotherapeutic treatment in primary HNSCC cell cultures and in plasma of HNSCC patients

miRNA	Agilent microarray		TaqMan single qRT-PCR assay	
	HN1957	HN2092	HN1957	HN2092
	FC (*p* value)	FC (*p* value)	FC (*p* value)	FC (*p* value)
rniR-425-5p	1.27 (0.004)	-	1.28 (0.052)	-
miR-21-5p	1.11 (0.031)	-	1.11 (0.543)	-
miR-106b-5p	0.95 (0.042)	-	1.04 (0.830)	-
miR-93-5p	0.92 (0.023)	0.96 (0.001)	1.03 (0.552)	0.84 (0.000)

FC = fold change.

treatment on HN1957 cells, but not on HN2092 cells (Figure 3). This reflects a higher short-term toxicity of the treatment on HN1957 cell cultures compared to HN2092 cell cultures, whereas the long-term effect of irradiation is stronger on HN2092 cell cultures as shown in the colony forming assay (Figure 1c, d). The common deregulation of 43 miRNAs in both primary HNSCC cell cultures (Additional files 5 and 6) suggests a similar miRNA response to therapeutic treatment independent from the individual tumor. We also observed differences in the miRNA response of both HNSCC cell cultures, which might reflect variations in the individual sensitivity to radiation and chemotherapeutic treatment (Figure 1).

The major finding of this study, i.e. therapy-related miRNA expression in the blood plasma is similar to miRNA changes reported for treated tumor cells, is not only based on global miRNA array screens but was also technically validated by qRT-PCR studies of the most distinctive miRNAs (Table 3). We identified *miR-425-5p* (HN1957) and *miR-93-5p* (HN2092) as top candidates of commonly deregulated miRNAs in primary HNSCC cell cultures and blood plasma of HNSCC patients.

In conclusion, the present study compared miRNA data from blood plasma of radiochemotherapy-treated HNSCC patients and from an *in vitro* model of primary tumor cell radiochemotherapy. This comparison sheds light on the origin and potential use of circulating miRNAs in the blood plasma of HNSCC patients as therapy-responsive biomarkers. We will further integrate these therapy-responsive plasma miRNAs with clinical data of the patients (e.g. overall survival) and seek for independent validation in another patient cohort in order to evaluate their potential for prognostic use. The established HNSCC cell culture model further allows us to investigate the molecular interactome of the deregulated miRNA candidates by adding mRNA expression data and subsequent integrative data analysis.

The current study strongly suggests that alterations of miRNAs following radiochemotherapy in the blood plasma are associated with the tumor response to therapy and therefore might represent novel biomarkers for therapy monitoring.

Additional files

Additional file 1: Immunohistochemical cytokeratin-staining of primary HNSCC cultures.

Additional file 2: Therapy-responsive microRNAs in plasma samples of 18 head and neck cancer patients.

Additional file 3: Correlation coefficients of normalized Ct values (ΔCt) of plasma miRNAs analyzed with arrays and single assays.

Additional file 4: Correlation coefficients of normalized Ct values (ΔCt) of miRNAs analyzed with TaqMan single assays in PBMC and plasma.

Additional file 5: Significantly deregulated microRNAs in HN1957 primary cell cultures after *in vitro* radiochemotherapy.

Additional file 6: Significantly deregulated microRNAs in HN2092 primary cell cultures after *in vitro* radiochemotherapy.

Additional file 7: Expression levels of *miR-93-5p* in plasma of 18 head and neck cancer patients prior and post treatment.

Competing interests
The authors declare that they have no competing interests.

Authors' contributions
IS: Experiments, manuscript, MN: Patient recruitment, ethics approval, AP: Biostatistics analysis, KU: Bioinformatics and biostatistics analysis, Support for experimental design/concept, VZ: Establishment of primary HNSCC cell cultures, JH: Support for microarray experiments, MJA: Support for planning of experiments, CB: Review of clinical data of patients, SM: Conceived the project, designed the *in vivo* study, HZ: Study design and critical revision of the manuscript. All authors read and approved the final manuscript.

Acknowledgements
We thank Klaudia Winkler, Aaron Selmeier and Claire Innerlohinger for their excellent technical assistance. We further thank Herbert Braselmann for the graphical design of survival curves as well as Maya Flieger for the collection of clinical data of the patients and the support for patient recruitment. Tissue samples were obtained from the Wales Cancer Bank, which is funded by the Wales Assembly Government and Cancer Research Wales. Other investigators may have received specimens from the same subjects.

Author details
[1]Research Unit Radiation Cytogenetics, Helmholtz Center Munich, Ingolstaedter Landstr 1, 85764, Neuherberg, Germany. [2]Department of Radiation Oncology, University of Munich, Marchioninistr 15, 81377, Munich, Germany. [3]Institute of Radiation Biology, Helmholtz Center Munich, Ingolstaedter Landstr 1, 85764, Neuherberg, Germany. [4]Clinical Cooperation Group 'Personalized Radiotherapy of Head and Neck Cancer', Helmholtz Center Munich, Ingolstaedter Landstr 1, 85764, Neuherberg, Germany.

Received: 13 November 2013 Accepted: 23 December 2013
Published: 28 December 2013

References
1. May JT, Rao N, Sabater RD, Boutrid H, Caudell JJ, Merchant F, Han G, Padhya TA, Mccaffrey JC, Tanvetyanon T, Deconti R, Kish J, Mccaffrey TV, Trotti A: **Intensity-modulated radiation therapy as primary treatment for oropharyngeal squamous cell carcinoma.** *Head & neck* 2013, **35:**1796–1800.
2. Ho AS, Kraus DH, Ganly I, Lee NY, Shah JP, Morris LG: **Decision making in the management of recurrent head and neck cancer.** *Head & neck* 2013, **36:**144–151.
3. **miRBase: the microRNA database.** www.miRbase.org.
4. Friedman RC, Farh KK-H, Burge CB, Bartel DP: **Most mammalian mRNAs are conserved targets of microRNAs.** *Genome Res* 2009, **19:**92–105.
5. Liu X, Jiang L, Wang A, Yu J, Shi F, Zhou X: **MicroRNA-138 suppresses invasion and promotes apoptosis in head and neck squamous cell carcinoma cell lines.** *Cancer Lett* 2009, **286:**217–222.
6. Novello C, Pazzaglia L, Cingolani C, Conti A, Quattrini I, Manara MC, Tognon M, Picci P, Benassi MS: **miRNA expression profile in human osteosarcoma: role of miR-1 and miR-133b in proliferation and cell cycle control.** *Int j of oncol* 2013, **42:**667–675.
7. Wu CW, Dong YJ, Liang QY, He XQ, Ng SS, Chan FK, Sung JJ, Yu J: **MicroRNA-18a attenuates DNA damage repair through suppressing the expression of ataxia telangiectasia mutated in Colorectal cancer.** *PloS one* 2013, **8:**e57036.
8. Calin GA, Croce CM: **MicroRNA signatures in human cancers.** *Nat Rev Cancer* 2006, **6:**857–866.
9. Gallego J, Gordon M, Claycomb K, Bhatt M, Lencz T, Malhotra A: **In vivo microRNA detection and quantitation in cerebrospinal fluid.** *J Mol Neurosci* 2012, **47:**243–248.
10. Mitchell PS, Parkin RK, Kroh EM, Fritz BR, Wyman SK, Pogosova-Agadjanyan EL, Peterson A, Noteboom J, O'briant KC, Allen A, Lin DW, Urban N, Drescher

CW, Knudsen BS, Stirewalt DL, Gentleman R, Vessella RL, Nelson PS, Martin DB, Tewari M: **Circulating microRNAs as stable blood-based markers for cancer detection.** *Proc Natl Acad Sci* 2008, **105:**10513–10518.
11. Liu R, Chen X, Du Y, Yao W, Shen L, Wang C, Hu Z, Zhuang R, Ning G, Zhang C, Yuan Y, Li Z, Zen K, Ba Y, Zhang C-Y: **Serum microRNA expression profile as a biomarker in the diagnosis and prognosis of pancreatic cancer.** *Clin Chem* 2012, **58:**610–618.
12. Niyazi M, Zehentmayr F, Niemoller O, Eigenbrod S, Kretzschmar H, Schulze-Osthoff K, Tonn J-C, Atkinson M, Mortl S, Belka C: **MiRNA expression patterns predict survival in glioblastoma.** *Radiat oncol* 2011, **6:**153.
13. Komatsu S, Ichikawa D, Takeshita H, Konishi H, Nagata H, Hirajima S, Kawaguchi T, Arita T, Shiozaki A, Fujiwara H, Okamoto K, Otsuji E: **Prognostic impact of circulating miR-21 and miR-375 in plasma of patients with esophageal squamous cell carcinoma.** *Expert Opin on Biol Ther* 2012, **12**(1):S53–59.
14. Komatsu S, Ichikawa D, Tsujiura M, Konishi H, Takeshita H, Nagata H, Kawaguchi T, Hirajima S, Arita T, Shiozaki A, Kubota T, Fujiwara H, Okamoto K, Otsuji E: **Prognostic impact of circulating miR-21 in the plasma of patients with gastric carcinoma.** *Anticancer Res* 2013, **33:**271–276.
15. Simone NL, Soule BP, Ly D, Saleh AD, Savage JE, Degraff W, Cook J, Harris CC, Gius D, Mitchell JB: **Ionizing radiation-induced oxidative stress alters miRNA expression.** *PloS one* 2009, **4:**e6377.
16. Cui W, Ma J, Wang Y, Biswal S: **Plasma miRNA as biomarkers for assessment of total-body radiation exposure dosimetry.** *PloS one* 2011, **6:**e22988.
17. Du L, Pertsemlidis A: **microRNA regulation of cell viability and drug sensitivity in lung cancer.** *Expert Opin on biol Ther* 2012, **12:**1221–1239.
18. Xiao-Chun W, Wei W, Zhu-Bo Z, Jing Z, Xiao-Gang T, Jian-Chao L: **Overexpression of miRNA-21 promotes radiation-resistance of non-small cell lung cancer.** *Radiat Oncol* 2013, **8:**146.
19. Anastasov N, Hofig I, Vasconcellos IG, Rappl K, Braselmann H, Ludyga N, Auer G, Aubele M, Atkinson M: **Radiation resistance due to high expression of miR-21 and G2/M checkpoint arrest in breast cancer cells.** *Radiat Oncol* 2012, **7:**206.
20. Svoboda M, Sana J, Fabian P, Kocakova I, Gombosova J, Nekvindova J, Radova L, Vyzula R, Slaby O: **MicroRNA expression profile associated with response to neoadjuvant chemoradiotherapy in locally advanced rectal cancer patients.** *Radiat Oncol* 2012, **7:**195.
21. Budach V, Stuschke M, Budach W, Baumann M, Geismar D, Grabenbauer G, Lammert I, Jahnke K, Stueben G, Herrmann T, Bamberg M, Wust P, Hinkelbein W, Wernecke KD: **Hyperfractionated accelerated chemoradiation with concurrent fluorouracil-mitomycin is more effective than dose-escalated hyperfractionated accelerated radiation therapy alone in locally advanced head and neck cancer: final results of the radiotherapy cooperative clinical trials group of the German cancer society 95–06 prospective randomized trial.** *J of Clin Oncol: official j of the AmSocof ClinOncol* 2005, **23:**1125–1135.
22. **Wales cancer bank.** www.walescancerbank.com.
23. **The R project for statistical computing.** www.r-project.org.
24. Smyth GK: **Limma: linear models for microarray data.** In *Bioinformatics and computational biology solutions using R and bioconductor.* Edited by Gentleman R, Carey V, Huber W, Irizarry R, Dudoit S. New York: Springer; 2005:397–420. Statistics for Biology and Health.
25. Smyth GK: **Linear models and empirical bayes methods for assessing differential expression in microarray experiments.** *Stat Appl in Genet and Mol Biol* 2004, **3:**Article3.
26. Livak KJ, Schmittgen TD: **Analysis of relative gene expression data using real-time quantitative PCR and the 2(−delta delta C(T)) method.** *Methods (San Diego, Calif)* 2001, **25:**402–408.
27. Yokobori T, Suzuki S, Tanaka N, Inose T, Sohda M, Sano A, Sakai M, Nakajima M, Miyazaki T, Kato H, Kuwano H: **MiR-150 is associated with poor prognosis in esophageal squamous cell carcinoma via targeting the EMT inducer ZEB1.** *Cancer Sci* 2013, **104:**48–54.
28. Lin R-J, Xiao D-W, Liao L-D, Chen T, Xie Z-F, Huang W-Z, Wang W-S, Jiang T-F, Wu B-L, Li E-M, Xu L-Y: **MiR-142-3p as a potential prognostic biomarker for esophageal squamous cell carcinoma.** *J Surg Oncol* 2012, **105:**175–182.
29. Hunter MP, Ismail N, Zhang X, Aguda BD, Lee EJ, Yu L, Xiao T, Schafer J, Lee M-LT, Schmittgen TD, Nana-Sinkam SP, Jarjoura D, Marsh CB: **Detection of microRNA expression in human peripheral blood microvesicles.** *PloS one* 2008, **3:**e3694.
30. Chaudhry MA, Omaruddin RA, Brumbaugh CD, Tariq MA, Pourmand N: **Identification of radiation-induced microRNA transcriptome by next-generation massively parallel sequencing.** *J Radiat Res* 2013, **54:**808–822.
31. Selth LA, Tilley WD, Butler LM: **Circulating microRNAs: macro-utility as markers of prostate cancer?** *Endocr Relat Cancer* 2012, **19:**R99–R113.
32. Hannafon B, Ding W-Q: **Intercellular communication by exosome-derived microRNAs in cancer.** *Int J Mol Sci* 2013, **14:**14240–14269.
33. Zernecke A, Bidzhekov K, Noels H, Shagdarsuren E, Gan L, Denecke B, Hristov M, Koppel T, Jahantigh MN, Lutgens E, Wang S, Olson EN, Schober A, Weber C: **Delivery of microRNA-126 by apoptotic bodies induces CXCL12-dependent vascular protection.** *Sci Signal* 2009, **2:**ra81.
34. Liu SG, Qin XG, Zhao BS, Qi B, Yao WJ, Wang TY, Li HC, Wu XN: **Differential expression of miRNAs in esophageal cancer tissue.** *Oncology letters* 2013, **5:**1639–1642.
35. Fu M-G, Li S, Yu T-T, Qian L-J, Cao R-S, Zhu H, Xiao B, Jiao C-H, Tang N-N, Ma J-J, Hua J, Zhang W-F, Zhang H-J, Shi R-H: **Differential expression of miR-195 in esophageal squamous cell carcinoma and miR-195 expression inhibits tumor cell proliferation and invasion by targeting of Cdc42.** *FEBS Lett* 2013, **587:**3471–3479.
36. Yanaihara N, Caplen N, Bowman E, Seike M, Kumamoto K, Yi M, Stephens RM, Okamoto A, Yokota J, Tanaka T, Calin GA, Liu C-G, Croce CM, Harris CC: **Unique microRNA molecular profiles in lung cancer diagnosis and prognosis.** *Cancer Cell* 2006, **9:**189–198.

doi:10.1186/1748-717X-8-296
Cite this article as: Summerer *et al.*: Changes in circulating microRNAs after radiochemotherapy in head and neck cancer patients. *Radiation Oncology* 2013 **8**:296.

Alle Additional files sind auf beiliegender CD verfügbar.

Summerer et al. Radiation Oncology (2015) 10:102
DOI 10.1186/s13014-015-0394-8

RADIATION ONCOLOGY

ERRATUM Open Access

Erratum: Changes in circulating microRNAs after radiochemotherapy in head and neck cancer patients

Isolde Summerer[1], Maximilian Niyazi[2], Kristian Unger[1,4], Adriana Pitea[1], Verena Zangen[1,4], Julia Hess[1,4], Michael J Atkinson[3], Claus Belka[2,4], Simone Moertl[3] and Horst Zitzelsberger[1,4*]

Erratum

After the publication of this work [1], a few points were brought to our attention:

The clinical data of patient 2 are incorrect. A revised version of Table 1 [1] showing the corrected patient characteristics is presented here. Consequently, the description of the patient cohort in the Materials and Methods section is incorrect. The correct description is: "*Plasma miRNA analysis was performed on 18 HNSCC patients treated with local X-ray-irradiation using a linear accelerator [...].*

17 out of 18 patients received concurrent chemotherapy (13 patients received 5-fluorouracil (5-FU) plus mitomycin C (MMC) [21], 3 patients MMC and 1 patient cisplatin weekly)".

There is a typing error in the Results section [1] concerning the p value of the up-regulation of *miR-425-5p*. The correct sentence is:

"The qRTPCR assays confirmed an up-regulation of miR-425-5p with a p value close to the significance level ($p = 0.052$) [...]".

The corrections do not affect any results or conclusions of the published work.

* Correspondence: zitzelsberger@helmholtz-muenchen.de
[1]Research Unit Radiation Cytogenetics, Helmholtz Center Munich, Ingolstaedter Landstr 1, 85764 Neuherberg, Germany
[4]Clinical Cooperation Group 'Personalized Radiotherapy of Head and Neck Cancer', Helmholtz Center Munich, Ingolstaedter Landstr 1, 85764 Neuherberg, Germany
Full list of author information is available at the end of the article

Table 1 Patient characteristics

Characteristic	Number of patients
Gender	
Male	14
Female	4
Median age, years	57.5
Age range, years	45.1–80.6
Tumor site	
Larynx	5
Oropharynx	3
Mouth floor	2
Tongue	2
Hypopharynx	1
Maxilla	1
Nasopharynx	1
Sinuses	1
Soft palate	2
T-Stage	
I	4
II	3
III	5
IV	6
N-Stage	
N0	3
N1	4
N2	11
M-Stage	
M0	17
M1	1
Concomitant therapy (in addition to radiotherapy)	
5-FU + MMC	13 (patient 2, 3, 5–7, 9–13, 15–17)
MMC	3 (patient 1, 14, 18)
Cisplatin	1 (patient 8)
Cetuximab	1 (patient 4)
Acute toxicity	
Severe	12
Moderate	5
n.a.	1

5-FU = 5-fluorouracil; MMC = mitomycin C; n.a. = not available.

Author details
[1]Research Unit Radiation Cytogenetics, Helmholtz Center Munich, Ingolstaedter Landstr 1, 85764 Neuherberg, Germany. [2]Department of Radiation Oncology, University of Munich, Marchioninistr 15, 81377 Munich, Germany. [3]Institute of Radiation Biology, Helmholtz Center Munich, Ingolstaedter Landstr 1, 85764 Neuherberg, Germany. [4]Clinical Cooperation Group 'Personalized Radiotherapy of Head and Neck Cancer', Helmholtz Center Munich, Ingolstaedter Landstr 1, 85764 Neuherberg, Germany.

Received: 25 March 2015 Accepted: 25 March 2015
Published online: 24 April 2015

Reference

1. Summerer I, Niyazi M, Unger K, Pitea A, Zangen V, Hess J, et al. Changes in circulating microRNAs after radiochemotherapy in head and neck cancer patients. Radiat Oncol. 2013;8:296.

2.6 Beschreibung des Journals British Journal of Cancer

Das British Journal of Cancer (ISI Abkürzung: Br J Cancer) publiziert Forschungsergebnisse aus den Bereichen der Genetik, Epidemiologie, molekularen Diagnostik und translationalen Therapie sowie klinische Studien in Verbindung mit Krebserkrankungen.

Ziel des Journals ist es ein Forum zu schaffen für die Kommunikation innovativer Forschungsergebnisse, die für das Verständnis der Ätiologie von Krebserkrankungen und die Verbesserung der Behandlungsmethoden sowie des Überlebens der Patienten relevant sind.

Das Journal wird von Thomson Reuters in der Kategorie *Oncology* geführt. Mit einem *Impact factor* von 4,836 und einem 5-Jahres *Impact factor* von 5,31 liegt es nach den *Journal Citation Reports* 2014 auf Rang 34 von 211 in der Kategorie *Oncology*.

FULL PAPER

BJC

British Journal of Cancer (2015), 1–7 | doi: 10.1038/bjc.2015.111

Keywords: head and neck cancer; radiochemotherapy; circulating non-coding RNA; biomarker; prognosis; radiotherapy outcome

Circulating microRNAs as prognostic therapy biomarkers in head and neck cancer patients

I Summerer[1], K Unger[1,2], H Braselmann[1], L Schuettrumpf[2,3], C Maihoefer[2,3], P Baumeister[2,4], T Kirchner[5], M Niyazi[2,3], E Sage[6], H M Specht[6], G Multhoff[6,7], S Moertl[8], C Belka[2,3] and H Zitzelsberger*[,1,2]

[1]*Research Unit Radiation Cytogenetics, Helmholtz Center Munich, Ingolstaedter Landstrasse 1, 85764 Neuherberg, Germany;* [2]*Clinical Cooperation Group 'Personalized Radiotherapy of Head and Neck Cancer', Helmholtz Center Munich, Ingolstaedter Landstrasse 1, 85764 Neuherberg, Germany;* [3]*Department of Radiation Oncology, Ludwig-Maximilians-Universitaet Muenchen, Marchioninistrasse 15, 81377 Munich, Germany;* [4]*Department of Otorhinolaryngology, Head and Neck Surgery, Ludwig-Maximilians-Universitaet Muenchen, Marchioninistrasse 15, 81377 Munich, Germany;* [5]*Institute of Pathology, Ludwig-Maximilians-Universitaet Muenchen, Thalkirchner Strasse 36, 80337 Munich, Germany;* [6]*Department of Radiation Oncology, Technische Universitaet Muenchen, Ismaninger Strasse 22, 81675 Munich, Germany;* [7]*Clinical Cooperation Group 'Innate Immunity', Helmholtz Center Munich, Ingolstaedter Landstrasse 1, 85764 Neuherberg, Germany and* [8]*Institute of Radiation Biology, Helmholtz Center Munich, Ingolstaedter Landstrasse 1, 85764 Neuherberg, Germany*

Background: The prediction of therapy response in head and neck squamous cell cancer (HNSCC) requires biomarkers, which are also a prerequisite for personalised therapy concepts. The current study aimed to identify therapy-responsive microRNAs (miRNAs) in the circulation that can serve as minimally invasive prognostic markers for HNSCC patients undergoing radiotherapy.

Methods: We screened plasma miRNAs in a discovery cohort of HNSCC patients before therapy and after treatment. We further compared the plasma miRNAs of the patients to age- and sex-matched healthy controls. All miRNAs identified as biomarker candidates were then confirmed in an independent validation cohort of HNSCC patients and tested for correlation with the clinical outcome.

Results: We identified a signature of eight plasma miRNAs that differentiated significantly ($P = 0.003$) between HNSCC patients and healthy donors. *MiR-186-5p* demonstrated the highest sensitivity and specificity to classify HNSCC patients and healthy individuals. All therapy-responsive and patient-specific miRNAs in plasma were also detectable in tumour tissues derived from the same patients. High expression of *miR-142-3p*, *miR-186-5p*, *miR-195-5p*, *miR-374b-5p* and *miR-574-3p* in the plasma correlated with worse prognosis.

Conclusions: Circulating *miR-142-3p*, *miR-186-5p*, *miR-195-5p*, *miR-374b-5p* and *miR-574-3p* represent the most promising markers for prognosis and therapy monitoring in the plasma of HNSCC patients. We found strong evidence that the circulating therapy-responsive miRNAs are tumour related and were able to validate them in an independent cohort of HNSCC patients.

Squamous cell carcinomas represent the most common malignancies of the head and neck region. About two-thirds of patients with head and neck squamous cell carcinoma (HNSCC) exhibit advanced stage disease, usually involving regional lymph nodes (Argiris *et al*, 2008). Advanced HNSCC have often a poor prognosis despite intensive local treatment due to tumour recurrences and distant metastases. About 50–60% of patients with advanced disease develop local or regional recurrences after treatment (Hoffmann, 2012).

Known risk factors for the development of HNSCC are tobacco use and alcohol consumption (Blot *et al*, 1988; Tuyns *et al*, 1988), as well as human papillomavirus (HPV) infection, mainly type 16,

*Correspondence: Professor H Zitzelsberger; E-mail: zitzelsberger@helmholtz-muenchen.de

Received 9 December 2014; revised 19 February 2015; accepted 27 February 2015

which particularly increases the risk for tonsillar and oropharyngeal cancers (D'souza *et al*, 2007). Human papillomavirus-positive HNSCC tumours have a favourable prognosis (Licitra *et al*, 2006; Bledsoe *et al*, 2013) and show a better therapy response (Argiris *et al*, 2008). Thus, HPV status represents a valuable predictive biomarker that should be taken into consideration for treatment planning to prevent excessive therapy.

To date no biomarker for therapy monitoring or patient surveillance is established. Predictive biomarkers in the peripheral blood, such as the newly identified marker HSP70 in HNSCC patients (Gehrmann *et al*, 2014), provide a minimally invasive way to predict therapy outcome. Recently, it was shown that microRNAs (miRNAs) in plasma samples exhibit high stability and are resistant to RNase activity (Mitchell *et al*, 2008). This stability combined with the good accessibility make circulating miRNAs attractive biomarker candidates. MiRNAs represent a class of promising biomarkers in cancer research since they are highly specific and are associated with pathoclinical parameters of the disease (Sethi *et al*, 2013). They can have protective or carcinogenic effects by post-transcriptional regulation of either tumour suppressor genes (Zheng *et al*, 2011) or oncogenes (Nohata *et al*, 2011). Since miRNAs are part of the cellular stress response they bear a high potential for diagnostic and prognostic use in cancer patients (Li *et al*, 2009).

The aim of the present study was to evaluate blood plasma miRNAs as minimally invasive biomarkers for radiotherapy monitoring and prognosis. For this purpose, we used a cohort of HNSCC patients with locally advanced and unresectable tumours undergoing radiochemotherapy or radiotherapy alone, which is the common treatment for these cases (Adelstein *et al*, 2003). We previously analysed the therapy effect on the plasma miRNAs by comparing the miRNA profiles in plasma of HNSCC patients before therapy and after the completion of the first two fractions of therapeutic irradiation (Summerer *et al*, 2013). MiRNAs showing changed levels were tested in the present study to determine their prognostic value and their potential for predicting the individual tumour response to radio(chemo)therapy. For this purpose, we tested the expression levels of the miRNAs for their correlation with locoregional tumour control (LRC), progression-free survival (PFS) and overall survival (OS). To check for a possible tumour origin of the therapy-regulated plasma miRNAs, we compared miRNA levels in plasma samples from HNSCC patients prior to treatment with an age- and sex-matched group of healthy donors. MiRNAs that were identified as patient-specific markers or as therapy-responsive miRNAs were validated in an independent HNSCC patient cohort. To further support the hypothesis that the detected alterations in plasma miRNAs are tumour related, we analysed tumour biopsies from the same patient cohorts.

MATERIALS AND METHODS

Patients and samples

Discovery cohort. The discovery cohort comprising 18 HNSCC patients treated with radio(chemo)therapy was described earlier in the study by Summerer *et al* (2013). All patients were treated with local X-ray-irradiation using a linear accelerator (6 MV, Siemens Mevatron M, Siemens Medical Solutions, Malvern, PA, USA or ELEKTA Synergy, ELEKTA, Stockholm, Sweden). After a planning (PET-)CT scan, 70 Gy of radiation was applied to the macroscopic tumour and involved lymph nodes in daily dose fractions of 2 Gy, 5 days per week. The adjuvant lymphatics were irradiated with up to 50 Gy and the high-risk lymphatics (adjacent to the involved lymph node levels) with up to 60 Gy. Seventeen out of 18 patients received concurrent chemotherapy (13 patients received 5-fluorouracil (5-FU) plus mitomycin C (MMC), 3 patients MMC and 1 patient cisplatin weekly). None of the patients underwent surgical treatment. 5-fluorouracil treatment was usually applied on each of the first 5 days of therapeutic irradiation, whereas MMC was applied only on day 5 and day 36 during radiotherapy. Patient characteristics, therapy conditions and pathoclinical parameters are listed in Table 1. After obtaining informed consent, 15 ml EDTA peripheral blood was collected prior to therapy and after the second fraction of therapeutic irradiation to detect therapy-responsive plasma miRNAs. About 10 μm formalin-fixed paraffin-embedded (FFPE) slides from tumour biopsies of 10 out of the 18 patients, which were retrieved prior to therapy, were provided by the Institute of Pathology at the Ludwig-Maximilians-University Munich.

Validation cohort. For validation of candidate biomarker miRNAs a set of 11 HNSCC patients treated with radiotherapy was selected. Radiotherapy was applied in the same manner as in the discovery cohort. None of the patients underwent surgical treatment. Eight patients received concurrent chemotherapy (five patients cisplatin, two patients MMC and one patient 5-FU plus MMC). For patient 1, cisplatin was applied once per week. For patients 6, 8, 10 and 11 cisplatin was applied in the first and the fifth week of radiotherapy for a period of 5 days in each week. 5-fluorouracil treatment was applied on each of the first 5 days of therapeutic irradiation, whereas MMC was applied only on day 5 and day 36 during radiotherapy. Characteristics, therapy conditions and pathoclinical parameters of the validation cohort are listed in Table 2. Blood samples were obtained prior to therapy and after the second fraction of therapeutic irradiation in the same manner as in the discovery cohort. About 10 μm FFPE slides from tumour biopsies of 4 out of the 11 patients retrieved prior to therapy were provided by the Institute of Pathology at the Ludwig-Maximilians-University Munich.

The study was approved by the ethics committee of the University of Munich (Germany).

Healthy donors. Twelve age- and sex-matched controls were selected to elucidate the origin of the plasma miRNA signatures in HNSCC patients. The cohort comprised nine male and three female individuals with a median age of 57.2 years (age range 37–68 years). After obtaining informed consent, EDTA-samples of 8 ml of peripheral blood were collected from healthy volunteers.

RNA extraction from plasma and FFPE tissue. Total RNA was extracted from plasma according to the study by Summerer *et al* (2013).

Formalin-fixed paraffin-embedded-slides were deparaffinised in xylene, washed in isopropanol and rehydrated in ethanol (100 and 70%). After microdissection for removal of normal tissue, RNA was isolated using the RNeasy FFPE Kit (Qiagen, Venlo, Netherlands) following the manufacturer's protocol. RNA was eluted in RNAse-free water (Life Technologies, Carlsbad, CA, USA) with a final volume of 25 μl. Quality assessment using a Nanodrop ND-1000 (Thermo Scientific, Waltham, MA, USA) exhibited OD 260/280 ratios in the range of 1.7 to 2.0.

MicroRNA profiling. MicroRNA profiling in blood plasma samples generated with TaqMan Array Human MicroRNA A Cards v2.0 (Applied Biosystems, Waltham, MA, USA) was previously specified in the study by Summerer *et al* (2013).

Individual miRNA quantification by qRT–PCR. Quantification of individual miRNAs via qRT–PCR was performed as described before (Summerer *et al*, 2013). MiRNAs were considered deregulated when showing a fold change (FC) of $0.75 \leqslant FC \geqslant 1.33$ since single qRT–PCR assays usually show smaller FCs than arrays.

Locoregional control and survival analysis. The locoregional control of the tumour was defined as the time from the date of

Table 1. Characteristics and clinical parameters of patients in the discovery set

Patient	Gender	Age (years)[a]	Tumour site	Histology	TNM[b]	HPV	Cumulative dose (Gy)	Concomitant therapy	Acute toxicity[c]	Progress/ death (event = 1)	Locoregional control[d]/overall survival[e] (weeks)
1	M	80	Larynx	SCC	T3 N1a M0	NA	70	MMC	Severe	0/0	81.9/90.0
2	M	70	Oropharynx	SCC	T2 N2c M0	NA	70	5-FU/MMC	Severe	0/1	38.3/40.9
3	M	49	Maxillary sinus	SCC	T4 N2c M0	–	70	5-FU/MMC	Mild	1/1	15.0/18.9
4	M	63	Larynx	SCC	T4 N2c M1	+	60	Cetuximab	Severe	0/1	48.0/52.3
5	Г	63	Oropharynx	SCC	T3 N1 M0	+	70	5-FU/MMC	Severe	0/1	57.1/61.1
6	M	77	Oropharynx	SCC	T2 N2c M0	+	70	5-FU/MMC	Mild	0/0	144.1/147.1
7	M	52	Oral cavity	SCC	T4 N2b M0	+	70	5-FU/MMC	Severe	1/1	16.9/39.4
8	F	45	Nasopharynx	SCC	T2b N1 M0	–	70	Cisplatin	Severe	1/0	117.4/127.9
9	M	54	Paranasal sinuses	SCC	T4b N0 M0	–	70	5-FU/MMC	Severe	0/0	8.3/21.3
10	M	47	Hypopharynx	SCC	T4 N2c M0	–	70	5-FU/MMC	Mild	0/0	111.3/115.4
11	F	79	Oro/ nasopharynx	SCC	T3 N2b M0	–	70	5-FU/MMC	Severe	0/1	6.0/13.3
12	M	50	Larynx	SCC	T4 N2c M0	–	70	5-FU/MMC	Severe	0/0	106.3/113.3
13	M	46	Larynx	SCC	T1 N2c M0	–	70	5-FU/MMC	Mild	0/0	33.7/43.6
14	F	78	Oropharynx	SCC	T1 N2b M0	+	70	MMC	NA	0/0	103.3/108.9
15	M	70	Larynx	SCC	T3 N2b M0	NA	70	5-FU/MMC	Severe	0/0	101.0/106.0
16	M	57	Oropharynx	SCC	T3 N0 M0	+	70	5-FU/MMC	Mild	0/0	103.3/93.0
17	M	58	Oral cavity	SCC	T1 N1 M0	–	70	5-FU/MMC	Severe	1/1	4.1/43.7
18	M	50	Oral cavity	SCC	T1 N0 M0	–	70	MMC	Severe	0/1	52.1/62.7

Abbreviations: F = female; HPV = human papillomavirus; M = male; MMC = mitomycin C; NA = not available; SCC = squamous cell carcinoma; 5-FU = 5-fluorouracil.
[a]age at diagnosis, median age: 57.5 years, age range (45.1–80.6 years).
[b]T: primary tumour stage; N: regional lymph node stage; M: distant metastasis.
[c]Mild: I°-II°; severe: III° according to CTCAE v4.0 (2009).
[d]Time from start of therapy until last follow-up/death or event.
[e]Time from diagnosis until last follow-up or event.

therapy start until last follow-up/death or event. A progress of the primary tumour or metastases in the locoregional lymphatics were considered as an event, whereas distant metastases were not considered as an event. End of follow-up or tumour-independent death was censored. Locoregional control was assessed by CT scan or sonography. Progression-free survival was determined as the time from the date of therapy start until event (death or progress) or last follow-up (censored). Progress was assessed in accordance with the LRC analysis. Overall survival was defined as the time from diagnosis until event (death) or last follow-up (censored). The correlation analysis of miRNA expression with LRC, PFS and OS was based on the results of the single qRT–PCR assays. Patients were split into two groups, displaying either a ΔCt value $\geq$median ΔCt or $<$median ΔCt for the miRNA of interest, referring to low

Table 2. Characteristics and clinical parameters of patients in the validation set

Patient	Gender	Age (years)[a]	Tumour site	Histology	TNM[b]	HPV	Cumulative dose (Gy)	Concomitant therapy	Acute toxicity[c]	Progress/ death (event = 1)	Locoregional control[d]/overall survival[e] (weeks)
1	M	58	Oropharynx	SCC	T3 N2c Mx	–	70	Cisplatin	Mild	0/0	13.3/20.9
2	M	66	Larynx	SCC	T2 N0 M0	+	70	MMC	Mild	0/0	46.1/55.4
3	M	77	Oropharynx	SCC	T4 N2a M0	+	70	MMC	Severe	0/0	47.0/55.1
4	M	75	Hypopharynx	SCC	T4 N2c M0	–	70	None	Mild	0/1	23.1/26.9
5	F	69	Oropharynx	SCC	T3 N2c M0	NA	70	5-FU/MMC	Mild	0/0	19.0/24.6
6	M	55	Hypopharynx	SCC	T4a N2b M0	NA	70	Cisplatin	Mild	1/0	32.4/36.3
7	M	79	Oropharynx	SCC	T2c N2c Mx	NA	70	None	Mild	1/0	31.3/36.3
8	M	55	Larynx	SCC	T3 N0 M0	NA	70	Cisplatin	Mild	0/0	13.6/20.1
9	M	75	Oropharynx	SCC	T3 N2 Mx	NA	70	None	Mild	0/0	19.0/25.3
10	F	65	Oropharynx	SCC	T4 N2b Mx	NA	70	Cisplatin	Mild	1/0	30.3/33.1
11	M	65	Oropharynx	SCC	T2 N0 M0	NA	70.4	Cisplatin	Mild	0/0	49.1/55.1

Abbreviations: F = female; HPV = human papillomavirus; M = male; MMC = mitomycin C; NA = not available; SCC = squamous cell carcinoma; 5-FU = 5-fluorouracil.
[a]Age at diagnosis, median age: 66.1 years, age range (55.0–79.8 years).
[b]T: primary tumour stage; N: regional lymph node stage; M: distant metastasis.
[c]Mild: I°-II°; Severe: III° according to CTCAE v4.0 (2009).
[d]Time from start of therapy until last follow-up/death or event.
[e]Time from diagnosis until last follow-up or event.

and high expression levels, respectively. Expression levels prior to therapy or after therapy were tested for correlation with LRC, PFS and OS. *P*-values were generated by log-rank testing.

Statistical analysis. The Mann–Whitney *U*-test was used to compare the plasma miRNA profiles of head and neck cancer patients before radiotherapy and healthy donors. To identify differential miRNA levels in plasma samples of patients prior to radiotherapy and after the second fraction of therapeutic irradiation the Wilcoxon test was performed. Unsupervised hierarchical clustering was performed using the top distinctive miRNAs applying the parameters maximum distance and Ward's method. *P*-values <0.05 were considered statistically significant. All statistical analyses were performed using the R Project for Statistical Computing, 2014.

RESULTS

Plasma miRNAs differentiate between healthy individuals and HNSCC patients. To test the hypothesis of tumour-related miRNA profiles in the plasma of HNSCC patients (discovery cohort), miRNA profiles prior to treatment were compared with miRNA profiles of healthy donors. The median number of detectable miRNAs in patients' plasma was 42.5, whereas the median number of detectable miRNAs in plasma samples of healthy donors was 33.0, which demonstrated a significantly ($P = 0.017$) elevated number of plasma miRNAs in HNSCC patients compared with healthy subjects. About 56 plasma miRNAs displayed differential expression levels between healthy donors and patients (Supplementary Table 1). The majority of miRNAs revealed lower expression levels in the healthy controls, only four miRNAs showed higher expression compared with patients. Unsupervised hierarchical clustering based on the expression levels of the top 8 differentially expressed miRNAs (*miR-21-5p*, *miR-28-3p*, *miR-142-3p*, *miR-186-5p*, *miR-191-5p*, *miR-197-3p*, *miR-425-5p* and *miR-590-5p*) resulted in two main clusters (Supplementary Figure 1). Cluster 1 included 7 healthy donors and 1 patient, while cluster 2 represented 17 patients and 5 healthy donors, which demonstrated a significant ($P = 0.003$) differentiation of patient and healthy donor samples.

Technical validation of the array data for healthy donors and HNSCC patients prior to therapy was done with single qRT–PCR assays for selected miRNAs. Due to limited plasma samples, 3 out of 18 patients from the discovery cohort had to be excluded for technical validation. For validation of the patient-specific miRNAs, 11 out of the top 12 distinctive miRNAs were selected. The normalised Ct values resulting from single qRT–PCR assays demonstrated high consensus with the normalised Ct values resulting from the TaqMan array profilling for all of the 11 miRNAs (Supplementary Table 2).

Plasma miRNAs that were detectable in ⩽1 healthy donor were tested for their ability to identify HNSCC patients (Table 3). *MiR-186-5p* demonstrated the highest sensitivity and specificity.

Validation of therapy-responsive and patient-specific plasma miRNAs in an independent cohort of HNSCC patients. For an independent validation of the patient-specific and therapy-responsive miRNAs identified in the discovery cohort, expression levels in the plasma of a validation cohort comprising 11 HNSCC patients were determined before therapy and after two fractions of radiotherapy. Each of the 9 candidate therapy-responsive miRNAs that were previously identified in the discovery cohort (Summerer *et al*, 2013) showed a deregulation in at least 7 out of the 11 patients in the validation cohort after 2 days of radiotherapy (Supplementary Table 3). Similarly, all of the 10 patient-specific candidate miRNAs identified in the discovery cohort in the present study displayed significantly higher expression levels in the patients of the validation cohort compared with the healthy donors (Supplementary Table 4). *MiR-590-5p* was not included in the analysis of the patient-specific miRNAs since it was detectable only in 30% of the patients in the discovery cohort.

Expression of plasma miRNAs in tumour tissue of HNSCC patients. To further clarify the origin of the miRNAs in the circulation, we investigated the expression of therapy-responsive and patient-specific plasma miRNAs in tumour biopsies from the same patients. Formalin-fixed paraffin-embedded-tumour biopsies of 10 patients from the discovery cohort and 4 patients from the validation cohort were enriched for tumour material via micro-dissection and analysed with single qRT–PCR assays for the patient-specific and therapy-responsive miRNAs. All candidate miRNAs identified in plasma were also detectable in each of the 14 available FFPE tumour samples. The expression levels in plasma did not show significant correlation with the expression levels in the corresponding tumour tissues (Supplementary Table 5).

Plasma miRNAs as prognostic markers. Plasma miRNAs that were identified previously as therapy-responsive candidates in HNSCC patients (Summerer *et al*, 2013) as well as tumour-specific miRNAs from the present study were tested for their ability to predict LRC, PFS and OS. We investigated if the expression level of a candidate miRNA prior to therapy or after the second day of treatment correlated with LRC, PFS or OS. We identified candidate miRNAs showing a significant correlation ($P<0.05$) or a trend for correlation ($P<0.2$) with LRC, PFS or OS in the discovery cohort (Table 4). High expression levels of *miR-186-5p*, *miR-374b-5p* and *miR-574-3p* prior to treatment correlated with reduced PFS and/or OS, and high expression of *miR-28-3p*, *miR-142-3p*, *miR-191-5p*, *miR-195-5p*, *miR-425-5p* and *miR-574-3p* after treatment showed correlation with worse prognosis. These candidate miRNAs were tested for correlation with LRC, PFS and OS in the validation cohort (Table 5). High expression of *miR-186-5p* and *miR-374b-5p* prior to treatment significantly correlated with reduced LRC. *MiR-195-5p* and *miR-574-3p* correlated with reduced LRC, when highly expressed after treatment. High expression of *miR-142-3p* after treatment was validated as a marker for reduced LRC and PFS. We also tested the HPV status as a predictor of LRC, which resulted in a trend ($P=0.118$) towards better LRC for HPV-positive cases in the discovery cohort (data not shown). Moreover, we tested the therapy-responsive and tumour-specific miRNAs for correlation with the HPV status. None of the candidate miRNAs showed a trend or a significant correlation with the HPV status (data not shown).

Table 3. Sensitivity and specificity of patient-specific plasma miRNAs expressed in ⩽1 healthy donor

miRNA	Sensitivity	Specificity
miR-186-5p	0.938	0.917
miR-374b-5p	0.312	1.000
miR-28-3p	0.625	1.000
miR-195-5p	0.562	1.000
miR-590-5p	0.312	1.000

Abbreviation: miRNA = microRNA.

DISCUSSION

In this study we aimed to establish blood plasma miRNAs as minimally invasive biomarkers from the peripheral blood for therapy monitoring and prognosis in HNSCC patients. Further, we intended to shed light on the origin of these miRNAs. The significantly elevated number of detectable miRNAs in the plasma of HNSCC patients compared with healthy individuals is in accordance with previous findings showing that circulating miRNAs are frequently upregulated in cancer (Lawrie *et al*, 2008; Heneghan *et al*, 2010; Tsujiura *et al*, 2010). In our study we found that not only the total number of detectable miRNAs is higher in patients' plasma compared with healthy individuals but also that the majority of miRNAs showed higher expression levels in patients compared with healthy donors. In the discovery cohort of HNSCC patients, a signature of *miR-21-5p*, *miR-28-3p*, *miR-142-3p*, *miR-191-5p*, *miR-186-5p*, *miR-197-3p*, *miR-425-5p* and *miR-590-5p* was identified to differentiate between HNSCC patients and healthy individuals. The fact that *miR-21-5p*, *miR-28-3p*, *miR-142-3p*, *miR-191-5p* and *miR-425-5p* also represented therapy-responsive miRNAs indicates that these miRNAs are indeed tumour

Table 4. Correlation of expression of plasma miRNAs with LRC, PFS and OS in 15 HNSCC patients (discovery cohort)

miRNA	*P*-value LRC	*P*-value PFS	*P*-value OS
miR-28-3p (after treatment)	0.069	0.027	0.092
miR-142-3p (after treatment)	0.129	—	—
miR-186-5p (prior to treatment)	—	0.165	—
miR-191-5p (after treatment)	0.129	0.002	0.004
miR-195-5p (after treatment)	—	0.029	0.130
miR-374b-5p (prior to treatment)	—	0.039	0.036
miR-425-5p (after treatment)	0.129	0.002	0.004
miR-574-3p (prior to treatment)	—	0.165	—
miR-574-3p (after treatment)	0.069	0.027	0.092

Abbreviations: HNSCC = head and neck squamous cell carcinoma; LRC = locoregional control; miRNA = microRNA; OS = overall survival; PFS = progression-free survival.

Table 5. Correlation of expression of plasma miRNAs with LRC, PFS and OS in 11 HNSCC patients (validation cohort)

miRNA	*P*-value LRC	*P*-value PFS	*P*-value OS
miR-142-3p (after treatment)	0.025	0.018	—
miR-186-5p (prior to treatment)	0.025	—	—
miR-195-5p (after treatment)	0.025	—	—
miR-374b-5p (prior to treatment)	0.025	—	—
miR-574-3p (after treatment)	0.025	—	

Abbreviations: HNSCC = head and neck squamous cell carcinoma; LRC = locoregional control; miRNA = microRNA; OS = overall survival; PFS = progression-free survival.

related. Moreover, *miR-21-5p* is a well-known tumour marker (Xiao-Chun *et al*, 2013; Zhu and Xu, 2014) and upregulated *miR-28-3p* was suggested as a marker for oesophageal carcinoma (Liu *et al*, 2013). *MiR-142-3p* was previously reported to serve as prognostic marker in oesophageal carcinoma (Lin *et al*, 2012) and to predict the response to radiochemotherapy in rectal cancer (Hotchi *et al*, 2013). Similarly, *miR-191-5p* was already described as an important biomarker in cancer (Nagpal and Kulshreshtha, 2014) and *miR-425-5p* was shown to predict survival and disease-free survival in skin cancer patients (Fleming *et al*, 2014). We were able to further support the hypothesis that the therapy-responsive plasma miRNAs are most likely tumour related by demonstrating expression of all candidate miRNAs in all available tumour tissues from our patient cohorts. The lack of significant correlation of expression levels in the tumour tissues with the expression levels of the corresponding plasma samples is not surprising. The various mechanisms of tumour miRNAs entering the blood stream, e.g. apoptotic tumour cells or active secretion (Selth *et al*, 2012), do not allow the conclusion that tumour tissues show the same expression levels as corresponding plasma samples. Furthermore, tumour biopsies as used in this study do not reflect the miRNA expression levels of the whole tumour. Normal tissue would be also necessary for a meaningful comparison.

The therapy-responsive and the tumour-specific miRNAs identified in the discovery cohort were confirmed in an independent patient cohort again suggesting their suitability as predictive markers.

MiR-186-5p represented the best candidate in the plasma to differentiate between healthy individuals and HNSCC patients. It also appeared to be a prognostic marker since the expression level showed a trend for correlation with reduced PFS in the discovery cohort and significantly correlated with LRC in the validation cohort. A prognostic potential of *miR-186-5p* was previously reported for oesophageal and lung carcinoma (Cai *et al*, 2013; Zhao *et al*, 2013). Circulating *miR-374b-5p* represents another promising prognostic marker since it exhibited significant correlation with PFS and OS in the discovery cohort and with LRC in the validation set prior to treatment. This is supported by a study suggesting a prognostic potential of this miRNA in prostate cancer (He *et al*, 2013). The additional miRNA candidates *miR-142-3p, miR-195-5p* and *miR-574-3p* from this study correlated with prognosis after 2 days of treatment indicating that they might be useful tools for therapy monitoring.

MiR-574-3p is known as a stress-responsive miRNA, which was shown previously to serve as a prognostic marker in the serum of glioblastoma patients (Manterola *et al*, 2014). Moreover, it is published that it modulates the therapy response in breast cancer patients (Ujihira *et al*, 2015), which makes it a promising candidate for therapy monitoring in HNSCC. Similarly, *miR-195-5p* is a well-known marker in the circulation of cancer patients (Igglezou *et al*, 2014) and was previously identified as prognostic marker in oesophageal carcinoma (Sun *et al*, 2014). The correlation of the therapy-responsive *miR-142-3p* with LRC suggests *miR-142-3p* as a marker for therapy success. An oncogenic role for *miR-142-3p* was shown in a previous study (Lv *et al*, 2012) supporting the potential use of this miRNA as a prognostic biomarker. The ability to predict the response to therapy might decrease treatment failure and avoid patients' exposure to the side effects of ineffective therapies. The applicability of all five miRNAs as prognostic markers is further supported by the fact that these miRNA markers represent obviously tumour-related miRNAs.

Circulating miRNAs are known to be deregulated in cancer and to predict early disease (Healy *et al*, 2012). Their good availability as well as their stability makes them useful biomarker candidates. In the present study, we discovered *miR-142-3p*, *miR-186-5p*, *miR-374b-5p*, *miR-195-5p* and *miR-574-3p* as the most promising HPV-independent markers for prognosis in the plasma of HNSCC patients treated with combined radiochemotherapy. Studies including a higher number of patients are needed to further validate the prognostic value of these marker miRNAs. We further showed that the same miRNAs were significantly overexpressed in plasma of HNSCC patients compared to healthy individuals, which supports the hypothesis that they originate from the tumour. Our findings represent an important contribution towards a clinical use of plasma miRNAs for therapy monitoring and a potential use in personalised treatment strategies.

ACKNOWLEDGEMENTS

We thank Laura Dajka and Klaudia Winkler for their excellent technical assistance, as well as Maya Flieger for the collection of clinical data of the patients and the support for patient recruitment. We also thank Ulrike Pflugradt for the management of patient data and tumour FFPE samples.

CONFLICT OF INTEREST

The authors declare no conflict of interest.

REFERENCES

The R Project for Statistical Computing (2014). Available at www.r-project.org.

Adelstein DJ, Li Y, Adams GL, Wagner Jr H, Kish JA, Ensley JF, Schuller DE, Forastiere AA (2003) An intergroup phase III comparison of standard radiation therapy and two schedules of concurrent chemoradiotherapy in patients with unresectable squamous cell head and neck cancer. *J Clin Oncol* **21**: 92–98.

Argiris A, Karamouzis MV, Raben D, Ferris RL (2008) Head and neck cancer. *Lancet* **371**: 1695–1709.

Bledsoe T, Noble A, Hunter G, Rybicki L, Hoschar A, Chute D, Saxton J, Greskovich J, Adelstein D, Koyfman S (2013) Oropharyngeal squamous cell carcinoma with known human papillomavirus status treated with definitive chemoradiotherapy: patterns of failure and toxicity outcomes. *Radiat Oncol* **8**: 174.

Blot WJ, Mclaughlin JK, Winn DM, Austin DF, Greenberg RS, Preston-Martin S, Bernstein L, Schoenberg JB, Stemhagen A, Fraumeni Jr JF (1988) Smoking and drinking in relation to oral and pharyngeal cancer. *Cancer Res* **48**: 3282–3287.

Cai J, Wu J, Zhang H, Fang L, Huang Y, Yang Y, Zhu X, Li R, Li M (2013) miR-186 downregulation correlates with poor survival in lung adenocarcinoma, where it interferes with cell-cycle regulation. *Cancer Res* **73**: 756–766.

D'souza G, Kreimer AR, Viscidi R, Pawlita M, Fakhry C, Koch WM, Westra WH, Gillison ML (2007) Case-control study of human papillomavirus and oropharyngeal cancer. *N Engl J Med* **356**: 1944–1956.

Fleming NH, Zhong J, Da Silva IP, Vega-Saenz De Miera E, Brady B, Han SW, Hanniford D, Wang J, Shapiro RL, Hernando E, Osman I (2014) Serum-based miRNAs in the prediction and detection of recurrence in melanoma patients. *Cancer* **121**(1): 51–59.

Gehrmann M, Specht HM, Bayer C, Brandstetter M, Chizzali B, Duma M, Breuninger S, Hube K, Lehnerer S, Van Phi V, Sage E, Schmid TE, Sedelmayr M, Schilling D, Sievert W, Stangl S, Multhoff G (2014) Hsp70–a biomarker for tumor detection and monitoring of outcome of radiation therapy in patients with squamous cell carcinoma of the head and neck. *Radiat Oncol* **9**: 131.

He HC, Han ZD, Dai QS, Ling XH, Fu X, Lin ZY, Deng YH, Qin GQ, Cai C, Chen JH, Jiang FN, Liu X, Zhong WD (2013) Global analysis of the differentially expressed miRNAs of prostate cancer in Chinese patients. *BMC Genomics* **14**: 757.

Healy NA, Heneghan HM, Miller N, Osborne CK, Schiff R, Kerin MJ (2012) Systemic mirnas as potential biomarkers for malignancy. *Int J Cancer* **131**: 2215–2222.

Heneghan HM, Miller N, Lowery AJ, Sweeney KJ, Newell J, Kerin MJ (2010) Circulating microRNAs as novel minimally invasive biomarkers for breast cancer. *Ann Surg* **251**: 499–505.

Hoffmann TK (2012) Systemic therapy strategies for head-neck carcinomas: current status. *GMS Curr Top Otorhinolaryngol Head Neck Surg* **11**: Doc03.

Hotchi M, Shimada M, Kurita N, Iwata T, Sato H, Morimoto S, Yoshikawa K, Higashijima J, Miyatani T (2013) microRNA expression is able to predict response to chemoradiotherapy in rectal cancer. *Mol Clin Oncol* **1**: 137–142.

Igglezou M, Vareli K, Georgiou GK, Sainis I, Briasoulis E (2014) Kinetics of circulating levels of miR-195, miR-155 and miR-21 in patients with breast cancer undergoing mastectomy. *Anticancer Res* **34**: 7443–7447.

Lawrie CH, Gal S, Dunlop HM, Pushkaran B, Liggins AP, Pulford K, Banham AH, Pezzella F, Boultwood J, Wainscoat JS, Hatton CS, Harris AL (2008) Detection of elevated levels of tumour-associated microRNAs in serum of patients with diffuse large B-cell lymphoma. *Br J Haematol* **141**: 672–675.

Li J, Huang H, Sun L, Yang M, Pan C, Chen W, Wu D, Lin Z, Zeng C, Yao Y, Zhang P, Song E (2009) MiR-21 indicates poor prognosis in tongue squamous cell carcinomas as an apoptosis inhibitor. *Clin Cancer Res* **15**: 3998–4008.

Licitra L, Perrone F, Bossi P, Suardi S, Mariani L, Artusi R, Oggionni M, Rossini C, Cantù G, Squadrelli M, Quattrone P, Locati LD, Bergamini C, Olmi P, Pierotti MA, Pilotti S (2006) High-risk human papillomavirus affects prognosis in patients with surgically treated oropharyngeal squamous cell carcinoma. *J Clin Oncol* **24**: 5630–5636.

Lin R-J, Xiao D-W, Liao L-D, Chen T, Xie Z-F, Huang W-Z, Wang W-S, Jiang T-F, Wu B-I., Li E-M, Xu L-Y (2012) MiR-142-3p as a potential prognostic biomarker for esophageal squamous cell carcinoma. *J Surg Oncol* **105**: 175–182.

Liu SG, Qin XG, Zhao BS, Qi B, Yao WJ, Wang TY, Li HC, Wu XN (2013) Differential expression of miRNAs in esophageal cancer tissue. *Oncol Lett* **5**: 1639–1642.

Lv M, Zhang X, Jia H, Li D, Zhang B, Zhang H, Hong M, Jiang T, Jiang Q, Lu J, Huang X, Huang B (2012) An oncogenic role of miR-142-3p in human T-cell acute lymphoblastic leukemia (T-ALL) by targeting glucocorticoid receptor-alpha and cAMP/PKA pathways. *Leukemia* **26**: 769–777.

Manterola L, Guruceaga E, Pérez-Larraya JG, González-Huarriz M, Jauregui P, Tejada S, Diez-Valle R, Segura V, Samprón N, Barrena C, Ruiz I, Agirre A, Ayuso Á, Rodríguez J, González Á, Xipell E, Matheu A, López De Munain A, Tuñón T, Zazpe I, García-Foncillas J, Paris S, Delattre JY, Alonso MM (2014) A small noncoding RNA signature found in exosomes of GBM patient serum as a diagnostic tool. *Neuro Oncol* **16**: 520–527.

Mitchell PS, Parkin RK, Kroh EM, Fritz BR, Wyman SK, Pogosova-Agadjanyan EL, Peterson A, Noteboom J, O'briant KC, Allen A, Lin DW, Urban N, Drescher CW, Knudsen BS, Stirewalt DL, Gentleman R, Vessella RL, Nelson PS, Martin DB, Tewari M (2008) Circulating microRNAs as stable blood-based markers for cancer detection. *Proc Natl Acad Sci* **105**: 10513–10518.

Nagpal N, Kulshreshtha R (2014) miR-191: an emerging player in disease biology. *Front Genet* **5**: 99.

Nohata N, Hanazawa T, Kikkawa N, Mutallip M, Sakurai D, Fujimura L, Kawakami K, Chiyomaru T, Yoshino H, Enokida H, Nakagawa M, Okamoto Y, Seki N (2011) Tumor suppressive microRNA-375 regulates oncogene AEG-1/MTDH in head and neck squamous cell carcinoma (HNSCC). *J Hum Genet* **56**: 595–601.

Selth LA, Tilley WD, Butler LM (2012) Circulating microRNAs: macro-utility as markers of prostate cancer? *Endocr Relat Cancer* **19**: R99–R113.

Sethi S, Ali S, Philip P, Sarkar F (2013) Clinical advances in molecular biomarkers for cancer diagnosis and therapy. *Int J Mol Sci* **14**: 14771–14784.

Summerer I, Niyazi M, Unger K, Pitea A, Zangen V, Hess J, Atkinson M, Belka C, Moertl S, Zitzelsberger H (2013) Changes in circulating microRNAs after radiochemotherapy in head and neck cancer patients. *Radiat Oncol* **8**: 296.

Sun N, Ye L, Chang T, Li X, Li X (2014) microRNA-195-Cdc42 axis acts as a prognostic factor of esophageal squamous cell carcinoma. *Int J Clin Exp Pathol* **7**: 6871–6879.

Tsujiura M, Ichikawa D, Komatsu S, Shiozaki A, Takeshita H, Kosuga T, Konishi H, Morimura R, Deguchi K, Fujiwara H, Okamoto K, Otsuji E (2010) Circulating microRNAs in plasma of patients with gastric cancers. *Br J Cancer* **102**: 1174–1179.

Tuyns AJ, Esteve J, Raymond L, Berrino F, Benhamou E, Blanchet F, Boffetta P, Crosignani P, Del Moral A, Lehmann W, Merletti F, Pequignot G, Riboli E, Sancho-Garnier H, Terracini B, Zubiri A, Zubiri L (1988) Cancer of the larynx/hypopharynx, tobacco and alcohol: IARC international case-control study in Turin and Varese (Italy), Zaragoza and Navarra (Spain), Geneva (Switzerland) and Calvados (France). *Int J Cancer* **41**: 483–491.

Ujihira T, Ikeda K, Suzuki T, Yamaga R, Sato W, Horie-Inoue K, Shigekawa T, Osaki A, Saeki T, Okamoto K, Takeda S, Inoue S (2015) MicroRNA-574-3p, identified by microRNA library-based functional screening, modulates tamoxifen response in breast cancer. *Sci Rep* **5**: 7641.

Xiao-Chun W, Wei W, Zhu-Bo Z, Jing Z, Xiao-Gang T, Jian-Chao L (2013) Overexpression of miRNA-21 promotes radiation-resistance of non-small cell lung cancer. *Radiat Oncol* **8**: 146.

Zhao BS, Liu SG, Wang TY, Ji YH, Qi B, Tao YP, Li HC, Wu XN (2013) Screening of microRNA in patients with esophageal cancer at same tumor node metastasis stage with different prognoses. *Asian Pac J Cancer Prev* **14**: 139–143.

Zheng J, Xue H, Wang T, Jiang Y, Liu B, Li J, Liu Y, Wang W, Zhang B, Sun M (2011) miR-21 downregulates the tumor suppressor P12CDK2AP1 and stimulates cell proliferation and invasion. *J Cell Biochem* **112**: 872–880.

Zhu W, Xu B (2014) MicroRNA-21 Identified as predictor of cancer outcome: a meta-analysis. *PLoS One* **9**: e103373.

Supplementary Information accompanies this paper on British Journal of Cancer website (http://www.nature.com/bjc)

Supplementary material ist auf beiliegender CD verfügbar.

2.8 Beschreibung des Journals BMC Genomics

BMC Genomics (ISI Abkürzung: BMC Genomics) publiziert Forschungsergebnisse aus Genomanalysen, funktionellen Genomanalysen und Proteomanalysen.

Das Journal wird von Thomson Reuters in den Kategorien *Biotechnology & Microbiology* und *Genetics & Heredity* geführt. Mit einem *Impact factor* von 3,986 und einem 5-Jahres *Impact factor* von 4,36 liegt es nach den *Journal Citation Reports* 2014 auf Rang 26 von 163 in der Kategorie *Biotechnology & Microbiology* und auf Rang 40 von 167 in der Kategorie *Genetics & Heredity*.

Summerer et al. BMC Genomics (2015) 16:654
DOI 10.1186/s12864-015-1865-x

BMC Genomics

RESEARCH ARTICLE Open Access

Integrative analysis of the microRNA-mRNA response to radiochemotherapy in primary head and neck squamous cell carcinoma cells

Isolde Summerer[1], Julia Hess[1,2], Adriana Pitea[1], Kristian Unger[1,2], Ludwig Hieber[1,2], Martin Selmansberger[1], Kirsten Lauber[2,3] and Horst Zitzelsberger[1,2*]

Abstract

Background: Head and neck squamous cell carcinoma (HNSCC) is a very heterogeneous disease resulting in huge differences in the treatment response. New individualized therapy strategies including molecular targeting might help to improve treatment success. In order to identify potential targets, we developed a HNSCC radiochemotherapy cell culture model of primary HNSCC cells derived from two different patients (HN1957 and HN2092) and applied an integrative microRNA (miRNA) and mRNA analysis in order to gain information on the biological networks and processes of the cellular therapy response. We further identified potential target genes of four therapy-responsive miRNAs detected previously in the circulation of HNSCC patients by pathway enrichment analysis.

Results: The two primary cell cultures differ in global copy number alterations and *P53* mutational status, thus reflecting heterogeneity of HNSCC. However, they also share many copy number alterations and chromosomal rearrangements as well as deregulated therapy-responsive miRNAs and mRNAs. Accordingly, six common therapy-responsive pathways (*direct P53 effectors*, *apoptotic execution phase*, *DNA damage/telomere stress induced senescence*, *cholesterol biosynthesis*, *unfolded protein response*, *dissolution of fibrin clot*) were identified in both cell cultures based on deregulated mRNAs. However, inflammatory pathways represented an important part of the treatment response only in HN1957, pointing to differences in the treatment responses of the two primary cultures. Focused analysis of target genes of four therapy-responsive circulating miRNAs, identified in a previous study on HNSCC patients, revealed a major impact on the pathways *direct P53 effectors*, the *E2F transcription factor network* and *pathways in cancer* (mainly represented by the *PTEN/AKT* signaling pathway).

Conclusions: The integrative analysis combining miRNA expression, mRNA expression and the related cellular pathways revealed that the majority of radiochemotherapy-responsive pathways in primary HNSCC cells are related to cell cycle, proliferation, cell death and stress response (including inflammation). Despite the heterogeneity of HNSCC, the two primary cell cultures exhibited strong similarities in the treatment response. The findings of our study suggest potential therapeutic targets in the *E2F transcription factor network* and the *PTEN/AKT* signaling pathway.

Keywords: Pathway enrichment analysis, Interaction network, Head and neck squamous cell carcinoma, Integrative biology, Radiochemotherapy, microRNA, HNSCC cell culture model

* Correspondence: zitzelsberger@helmholtz-muenchen.de
[1]Research Unit Radiation Cytogenetics, Helmholtz Center Munich, Ingolstaedter Landstr.1, 85764 Neuherberg, Germany
[2]Clinical Cooperation Group 'Personalized Radiotherapy of Head and Neck Cancer', Helmholtz Center Munich, Ingolstaedter Landstr. 1, 85764 Neuherberg, Germany
Full list of author information is available at the end of the article

Background

Head and neck squamous cell carcinoma (HNSCC) includes epithelial cancers of the lip, oral cavity, nasal cavity, paranasal sinuses, salivary glands, larynx and pharynx (nasopharynx, oropharynx and hypopharynx) [1] and represents the sixth most common cancer in the world [2] with an average 5-year survival rate of approximately 65 % [3]. Some of the tumors are unresectable because of their complex anatomy [4]. In addition, HNSCC is usually not detected in the early stages of the disease due to the lack of clinical symptoms, which aggravates treatment [5]. The challenges in treating HNSCC tumors are functional preservation of substantial organs, such as salivary glands, and minimization of side effects, such as dysphagia. Moreover, HNSCC tumors show a high degree of heterogeneity and variation in the therapeutic response requiring individualized treatment strategies [6, 7]. In order to address these issues, combined and targeted treatment strategies as well as more effective treatment monitoring is needed to improve therapy outcomes and patients' quality of life.

MicroRNAs (miRNAs) represent a class of non-coding RNAs acting as posttranscriptional gene expression regulators by inhibiting translation or destabilizing mRNAs. They are known to be involved in regulating and coordinating multiple cellular pathways and processes. MiRNAs show a response to various cellular stressors and are key players in many diseases such as cancer [8]. Specific miRNA signatures were discovered for several tumor types [9]. For HNSCC a considerable number of miRNAs were identified as promising molecular biomarkers for diagnosis and prognosis targeting either oncogenic or tumor suppressor transcripts [10–12]. However, there is still uncertainty concerning the functional role of most of the miRNAs since one miRNA may target multiple mRNAs while one mRNA can be regulated by a number of different miRNAs.

Network-based integrative analysis combining molecular data from multiple levels represents a valuable tool for a better understanding of complex signaling networks and related biological processes. Correlation analysis of expression values of potentially interacting molecules enables reconstruction of interaction networks based on experimental data. In this study integrative analysis of miRNA and mRNA profiles based on the identification of correlating expression patterns revealed potential functional relationships and pathways involved in the cellular treatment response [13]. The analysis can be strengthened by integration of data bases on previously validated target interactions. Another tool for the *in silico* investigation of interactions is pathway enrichment analysis, which annotates molecules of interest, e.g. differentially expressed genes, to cellular pathways based on over-representation using the information of pathway databases, such as Reactome [14].

The aim of the current study was to shed light on the cellular functions of therapy-responsive miRNAs and to gain additional information on the treatment effects on cellular processes and pathways in order to enable the identification of potential therapeutic targets. For this purpose we used primary HNSCC cells as a cell culture model for radiochemotherapy [15] and performed integrative analysis of the miRNA and mRNA expression profiles in order to analyze affected pathways for a better understanding of the response of HNSCC cells to radiochemotherapy.

We aimed to validate our *in vitro* data by focusing on a therapy-responsive network of patient-derived data from a previous study [15].

Results

Characterization of the primary HNSCC cell lines

The newly established HNSCC cell lines HN1957 (nasopharynx) and HN2092 (oral cavity) were published in a previous study, where a cell culture model was established to simulate radiochemotherapy of a HNSCC patient cohort *in vitro* [15]. For the cell culture model primary cell cultures were selected instead of established cell lines since the features of primary cells are closer to the conditions in the patient. A further selection criterion for the primary cell lines was that they were derived from tumor sites, that were also represented in the HNSCC patient cohort [15]. Apart from that, we selected one *P53*-mutated (HN1957) and one *P53* wild type (HN2092) primary cell line. A nasopharyngeal carcinoma was included since standard treatment for these tumors is radiotherapy or radiochemotherapy due to their high sensitivity towards this treatment [16]. Characteristics of the primary cells lines are listed in Table 1. In the present study we used the radiochemotherapy cell culture model in order to gain information on the molecular radiochemotherapy response. As it was already shown before, HN1957 demonstrated a higher decrease in cellular viability following treatment with ionizing radiation and 5-fluorouracil (5-FU) compared to HN2092 [15]. To further characterize the two cell lines in this study we conducted array comparative genomic hybridization CGH (array CGH) analysis, spectral karyotyping (SKY), *P53* and *EGFR* sequencing analysis as well as *EGFR* and *EpCAM* surface expression.

Array CGH demonstrated 30 copy number alterations involving 18 chromosomes in HN1957 and 46 copy number alterations involving 19 chromosomes in HN2092 (Additional files 1, 2, 3A and 4A). SKY revealed the following clonal karyotype for HN1957 resulting from evaluation of 16 metaphases: 65-81,XX,+X,+del(X)(p13 → qter),+1,+2,+del(2)(p13 → qter),+3,+der(3)t(3;14)(p11 → qter;qter → q11),+4,+5,+i(5)(p10),+6,+7,+i(7)(p10),+8,+der(8)t(5;8)(?;p10 → qter),+9,+der(9)t(X;9)(?;p13 → qter),+10,+der(10)t(10;17)(p10 → qter;qter →q10),+11,+12,+13,der

Table 1 Characteristics of primary HNSCC cell cultures

Case	HN1957	HN2092
Gender of patient	f	m
Age at diagnosis, years	85	73
Tumor site	left maxilla / left nasal floor	right floor of mouth
TNM	n.a.	pT4pN0
HPV-status	negative	negative
EBV-status	negative	n.a.
P53-status	mutated	wild type
Radiosensitivity		
α (+/-SD)	0.094 (+/− 0.022)*	0.614 (+/− 0.019)*
β (+/-SD)	0.038 (+/− 0.004)**	0.021 (+/− 0.003)**
SF2	0.71	0.27
Cell type	epithelial	epithelial

n.a. Not available, *SD* Standard deviation, *SF2* Surviving fraction at 2 Gy
*ttest of α values results in significant difference between HN1957 and HN2092 ($p < 0.05$)
**ttest of β values results in significant difference between HN1957 and HN2092 ($p < 0.05$)

(14)t(13;14)(qter → q11;p11 → qter),+15,i(15)(q10),+16,+17,+19,+20,+21,+22,i(22)(q10). A representative metaphase is shown in Additional file 3B.

HN2092 exhibited the following clonal karyotype resulting from evaluation of 15 metaphases: 69-77,X,Y,+Y,+i(X)(p10),+i(X)(q10),+der(1)t(1;21)(p11 → qter;qter → q11),+2,+3,+der(4)t(1;4)(pter → q21;?),+der(4)t(1;4)(qter → q10;q10 → qter),+5,+i(5)(p10),+6,+der(7)addv(7)(q31)t(7;11)(?;?),+der(8)t(8;14)(p11 → qter;qter → q11),+der(9)t(9;13)(p11 → qter;qter → q14),+10,+11,+12,der(13)t(12;13)(?;p13 → q22),+14,der(15)t(3;15)(?;p11 → qter),+16,+17,+19,+20,+22. Additional file 4B shows a representative metaphase. The karyotypes reflected many of the copy number alterations that were detected by array CGH in HN1957 (isochromosomes, gains of chromosomes and chromosome arms: 5p, 7p, 8, 9, 11, 13q, 15, 17q, 20) and HN2092 (isochromosomes, gains of chromosomes and chromosome arms: 5p, 8, 9, 11q, 12q, 13q, 14, 16, 20).

Further, sequencing analysis revealed no mutations of *EGFR* in both cell cultures, but two point mutations of the *P53* gene in HN1957 (P72R and Δ331). Both cell cultures strongly overexpressed *EGFR* and *EpCAM* compared to OKF6-hTERT keratinocytes as determined by flow cytometry surface staining (Additional file 5).

MiRNA and mRNA expression following radiochemotherapy treatment

In order to analyze common features and differences in the radiochemotherapy response on the miRNA and mRNA level, expression changes were assessed following treatment in both primary cell lines. Significantly deregulated miRNAs in the primary cells after radiochemotherapy treatment were previously reported by Summerer et al. [15]. A heatmap of the expression profiles of the top 50 deregulated miRNAs revealed distinctive patterns for the two different tumor cell cultures (Fisher's exact test $p = 0.001$) as well as for untreated and treated samples (three biological and two technical replicates each) resulting in significant or close to significant clustering (Fisher's exact test HN1957: $p = 0.015$, HN2092: $p = 0.080$) (Fig. 1). In HN1957 57 significantly deregulated miRNAs were identified while HN2092 showed deregulated expression of 79 miRNAs with an overlap of 27 miRNAs between the two cell cultures.

Global mRNA expression was measured for both cultures after radiochemotherapy or sham-treatment and unsupervised hierarchical clustering of the gene expression patterns using the 50 mRNAs with the highest variance resulted in two main clusters separating samples of the two cell cultures (Fisher's exact test $p = 0$). Further, the cluster analysis revealed significant or border line significant separation of control samples and treated samples (Fisher's Exact test HN1957: $p = 0$, HN2092: $p = 0.061$) (Fig. 2).

For HN1957 612 genes (Additional file 6) and for HN2092 598 genes (Additional file 7) were significantly (adjusted p-value < 0.05) deregulated after radiochemotherapy treatment with an overlap of 190 genes between both primary cultures.

Pathway enrichment analysis

For a comprehensive insight in the cellular pathways, which were affected by the radiochemotherapy treatment, a pathway enrichment analysis was applied based on the significantly deregulated mRNAs. The analysis exhibited *DNA damage/telomere stress induced senescence*, *direct P53 effectors*, *cholesterol biosynthesis*, *dissolution of fibrin clot*, *unfolded protein response* and *apoptotic execution phase* as overlap of significantly (FDR < 0.05) enriched pathways (Additional files 8 and 9). Differences in the treatment response between the two primary cultures are reflected by pathways such as *TGF-beta signaling pathway*, *regulation of nuclear SMAD2/3 signaling*, *TNF signaling pathway* and *IL6-mediated signaling events*, which play a role only in the treatment response in HN1957, but not in HN2092.

MiRNA-mRNA interactions

We further aimed to identify potential miRNA-mRNA interactions that are part of the treatment response in order to gain information on the function of the treatment-responsive miRNAs. Integrative network analysis of significantly deregulated miRNAs and differentially expressed mRNAs including adjustment with validated miRNA-mRNA interactions derived from the miRTarBase

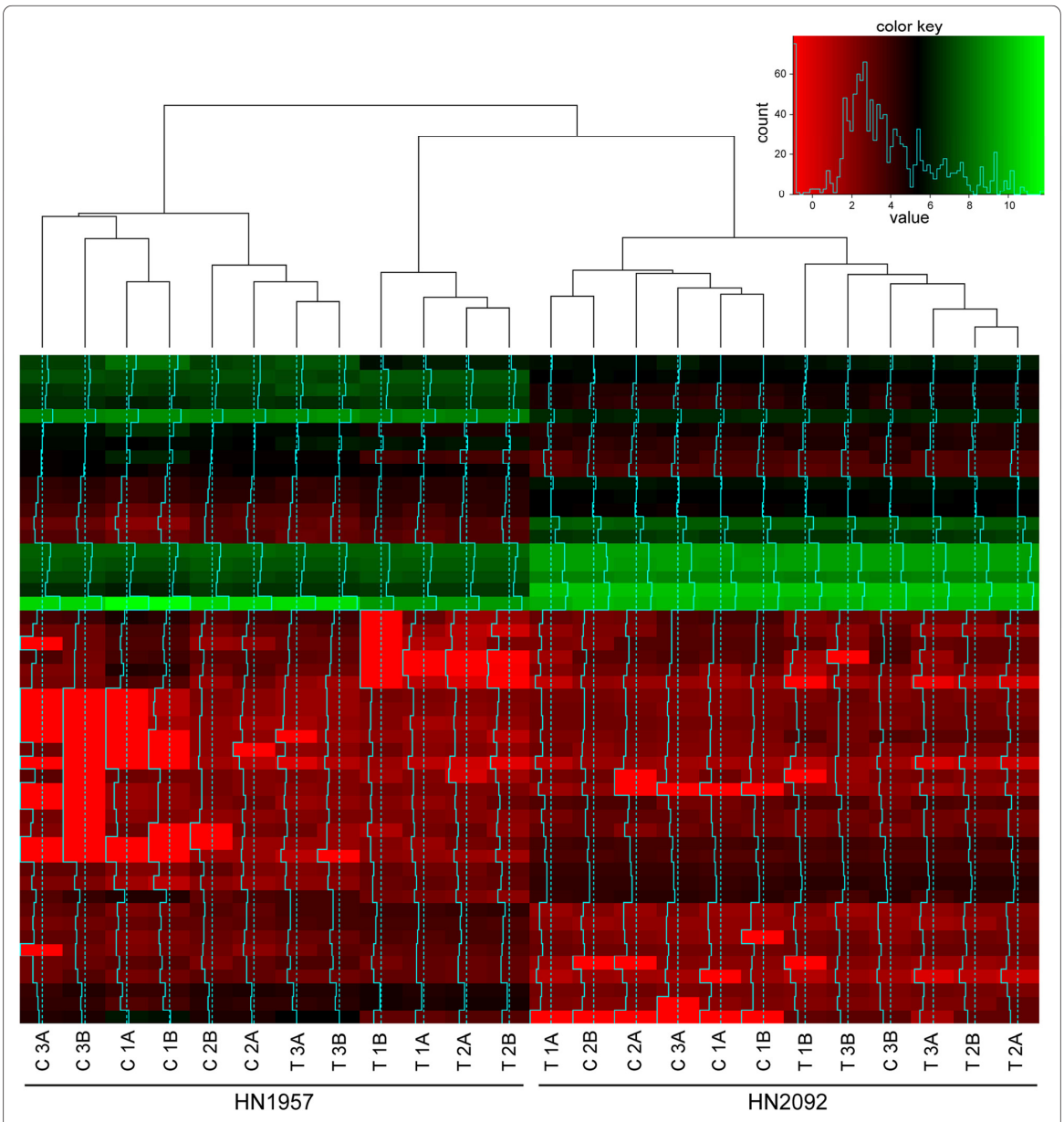

Fig. 1 Unsupervised hierarchical cluster analysis of the expression levels of the top 50 differentially expressed miRNAs in untreated and radiochemotherapy treated HN1957 and HN2092 primary HNSCC cells. Control samples (C) were treated with DMSO and sham-irradiated, treated samples (T) were treated with 5-FU and irradiated with 2 × 2 Gy. A and B represent technical replicates; 1, 2 and 3 represent biological replicates

[17, 18] resulted in functional miRNA-mRNA networks affected by radiochemotherapy treatment in HN1957 (Fig. 3) and HN2092 (Fig. 4). The miRNAs appearing in the interaction networks of both primary cell lines and their corresponding target mRNAs are combined in Fig. 5.

For technical validation by quantitative real-time PCR (qRT-PCR) individual miRNA and mRNA candidates were selected according to the following criteria: miRNA-mRNA correlation values ≤ −0.8, tumor-related genes or deregulated miRNAs in blood plasma of radiochemotherapy-treated HNSCC patients (Tables 2 and 3). In HN1957 upregulation of *miR-181b-5p* (p = 0.008) as well as *miR-425-5p* (with a p-value close to the significance level, p = 0.052) was confirmed. Moreover, for

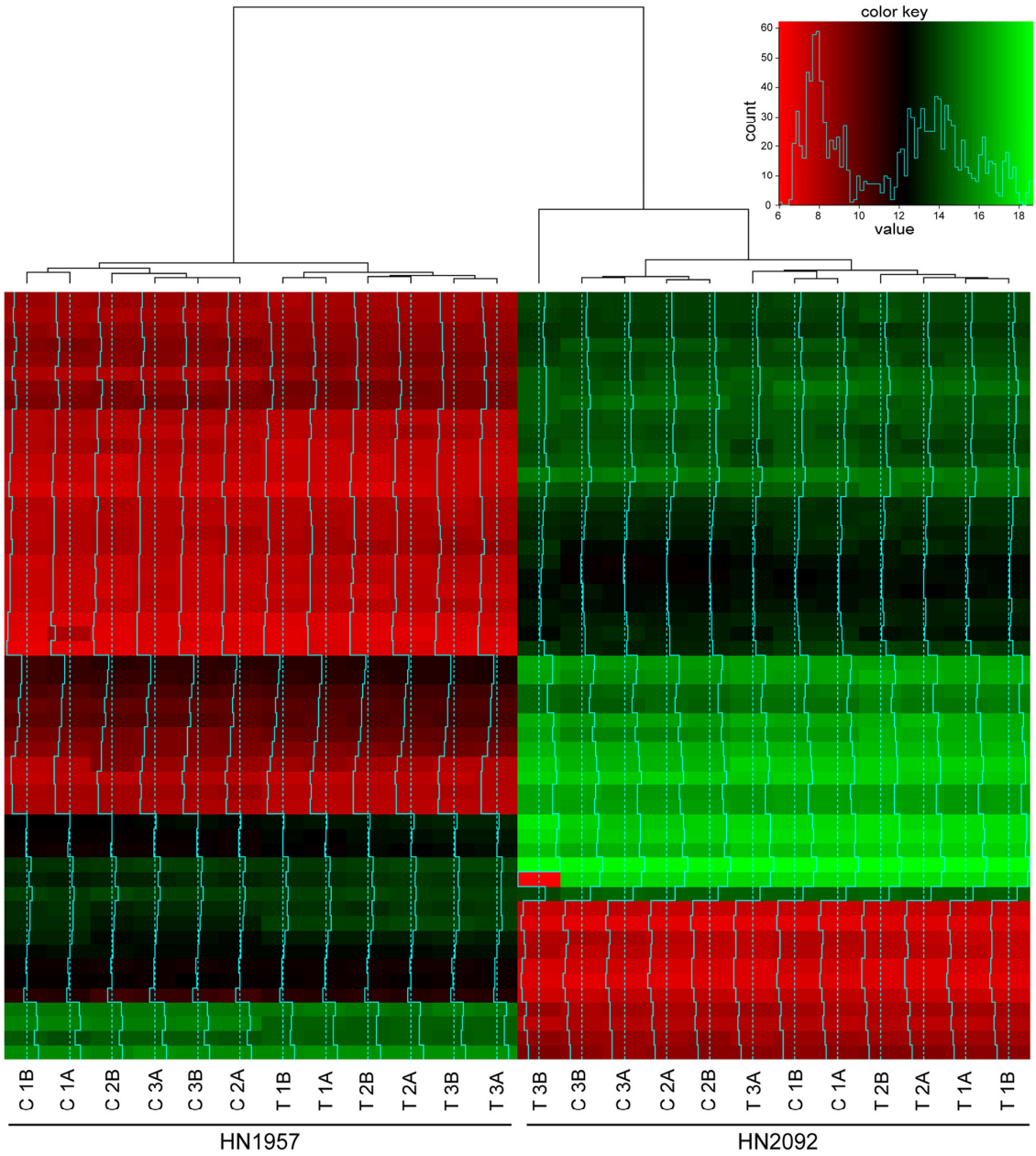

Fig. 2 Unsupervised hierarchical cluster analysis of the expression levels of the top 50 differentially expressed mRNAs in untreated and radiochemotherapy treated HN1957 and HN2092 primary HNSCC cells. Control samples (C) were treated with DMSO and sham-irradiated, treated samples (T) were treated with 5-FU and irradiated with 2 × 2 Gy. A and B represent technical replicates; 1, 2 and 3 represent biological replicates

the target genes of *miR-181b-5p, ASB13* ($p = 0.004$) and *SEC24C* ($p = 0.018$), a significant downregulation was confirmed by qRT-PCR as well as downregulation of *TRAPPC9* ($p = 0.046$). In HN2092 downregulation of *miR-93-5p* ($p < 0.001$) as well as upregulation of *miR-181a-5p* ($p = 0.001$) was validated. *MiR-183-5p* was upregulated (with a *p*-value close to the significance level, $p = 0.071$) while downregulation of its target genes *ASNS* ($p = 0.017$)

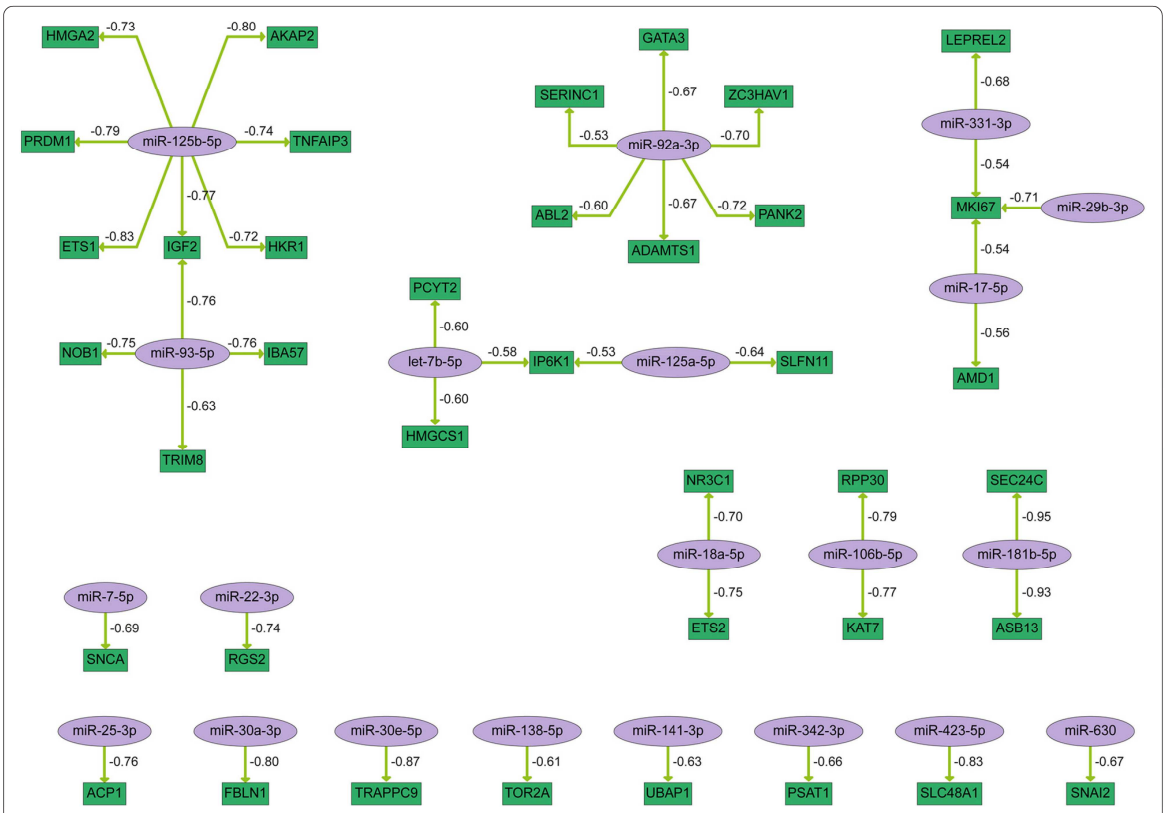

Fig. 3 MiRNA-mRNA interaction network reflecting the response to radiochemotherapy treatment in HN1957. MiRNA-mRNA pairs were generated based on the correlation coefficient (c ≤−0.5) of their expression levels. MiRNAs are shown in purple, potential target genes are shown in green. Arrows indicate the direction of regulation. The numbers refer to the correlation value of the respective miRNA and mRNA expression levels

and *IDH2* ($p = 0.045$) was confirmed by qRT-PCR. Additionally, downregulation of *ACTR1B* ($p = 0.012$) and *FASN* ($p = 0.007$) was verified.

Furthermore, qRT-PCR analyses were performed in order to validate the network showing common interactions of HN1957 and HN2092 in response to radiochemotherapy-treatment (Fig. 5). Upregulation of *miR-7-5p* and *miR-17-5p* was verified for both cell lines as well as downregulation of their target genes *SNCA*, *AMD1*, *MKI67*, *BACE1* and NAGK in HN1957 or HN2092 (Table 4). Additionally, downregulation of *miR-93-5p* in HN2092 and upregulation of its target gene *SLC19A1* were verified (Table 4). Spearman correlation coefficients demonstrated a negative correlation (≤ −0.5) for five out of the eight miRNA-mRNA pairs of the combined network (Table 4).

Characterization of the role of therapy-responsive circulating miRNAs on cellular pathways

As it was already shown by Summerer et al. [15], several miRNAs significantly deregulated in the presented radiochemotherapy cell culture model were also detectable as circulating deregulated miRNAs in HNSCC patients after radiochemotherapy. In order to gain information on the function of these therapy-responsive miRNAs (*miR-21-5p*, *miR-93-5p*, *miR-106b-5p* and *miR-425-5p*) all mRNAs that showed negatively correlating expression values (c ≤ −0.5) in the primary cell cultures and additionally representing validated targets in the miRTarBase were determined (Additional files 10 and 11). Pathway enrichment analysis (FDR < 0.05) of these potential target genes revealed predominantly signaling molecules that represent *direct P53 effectors* and play a role in *pathways in cancer*, *cell cycle* and the *E2F transcription factor network* (Tables 5 and 6). The key players of these pathways were *E2F1*, *PTEN*, *AKT2*, *JUN*, *HSP90AA1*, *KAT2B* in HN1957 and *JUN*, *KAT2B*, *BIRC5*, *CCND2*, *RBL2* in HN2092.

Discussion

In the present study we applied an integrative approach for the delineation of the effects of radiochemotherapy on the molecular processes in a HNSCC cell culture

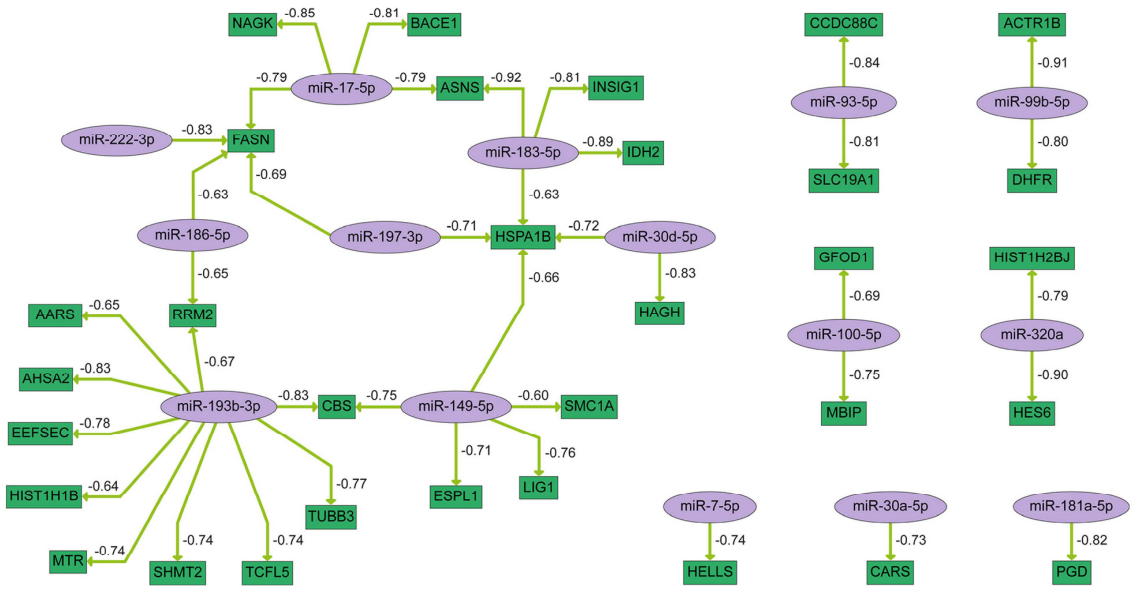

Fig. 4 MiRNA-mRNA interaction network reflecting the response to radiochemotherapy treatment in HN2092. MiRNA-mRNA pairs were generated based on the correlation coefficient (c ≤−0.5) of their expression levels. MiRNAs are shown in purple, potential target genes are shown in green. Arrows indicate the direction of regulation. The numbers refer to the correlation value of the respective miRNA and mRNA expression levels

model. Based on these data, we analyzed the cellular pathways affected by the treatment. The usefulness of this approach for the identification of regulatory networks has already been demonstrated in previous studies [19, 20]. For the first time we used this approach on a cell culture model with primary HNSCC cells mimicking a common therapy regime for HNSCC [4]. In this way we aimed for a better understanding of the treatment response, with respect to a common and individually varying molecular response.

The observed overlap of deregulated miRNAs and mRNAs between HN1957 and HN2092 hints to a partially common response to radiochemotherapy treatment. At the same time, the separation of the two primary HNSCC cell cultures in distinct clusters for both, the top 50 deregulated miRNAs (Fig. 1) and mRNAs (Fig. 2), suggests individual differences in the response to the treatment. This is consistent with differences between HN1957 and HN2092 in the sensitivity towards radiochemotherapy treatment as shown before [15].

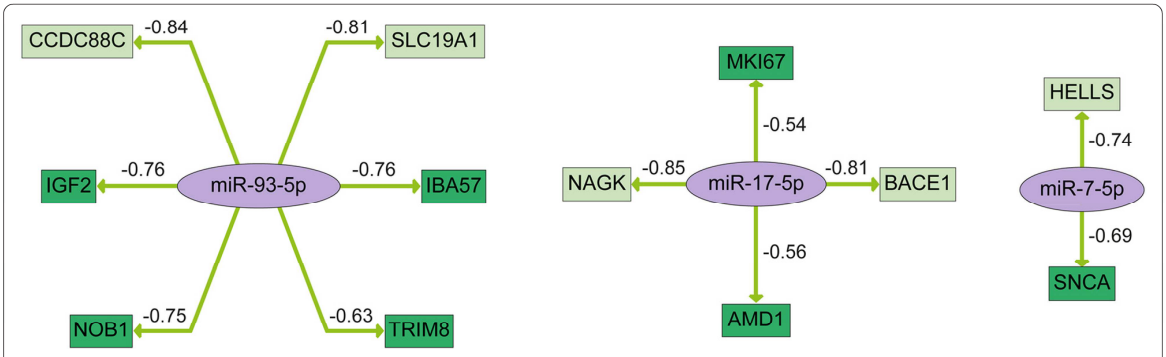

Fig. 5 Combined network reflecting common miRNA-mRNA interactions between HN1957 and HN2092 in response to radiochemotherapy treatment. MiRNA-mRNA pairs were generated based on the correlation coefficient (c ≤−0.5) of their expression levels. MiRNAs are shown in purple, potential target genes in HN1957 are shown in dark green, potential target genes in HN2092 in light green. Arrows indicate the direction of regulation. The numbers refer to the correlation values of the respective miRNA and mRNA expression levels

Table 2 Validation of deregulated miRNAs and correlating target mRNAs in HN1957 after radiochemotherapy treatment (analyzed with Agilent microarrays and TaqMan single qRT-PCR assays)

miRNA	Array	qRT-PCR	mRNA	Array	qRT-PCR
	FC (*p* value)	FC (*p* value)		FC (*p* value)	FC (*p* value)
miR-25-3p	0.88 (0.037)	0.89 (0.152)	-	-	-
miR-30a-3p	1.33 (0.013)	1.17 (0.294)	*FBLN1*	0.68 (<0.001)	0.98 (0.775)
miR-30e-5p	1.23 (0.010)	0.83 (0.002)	*TRAPPC9*	0.59 (<0.001)	0.56 (0.046)
miR-93-5p	0.92 (0.023)	1.03 (0.552)	*IGF2*	1.44 (<0.001)	not detected
miR-106b-5p	0.95 (0.042)	1.04 (0.830)	–	–	–
miR-125a-5p	1.17 (0.061)	0.99 (0.879)	–	–	–
miR-125b-5p	0.94 (0.072)	1.05 (0.599)	*ETS1*	1.48 (<0.001)	1.18 (0.509)
			IGF2	1.44 (<0.001)	not detected
			TNFAIP3	1.96 (<0.001)	2.14 (0.120)
miR-181b-5p	1.31 (<0.001)	1.12 (0.008)	*ASB13*	0.69 (<0.001)	0.64 (0.004)
			SEC24C	0.69 (<0.001)	0.62 (0.018)
miR-425-5p	1.27 (0.001)	1.28 (0.052)	–	–	–

FC Fold change

The short-term effect on cellular viability following radiochemotherapy treatment became apparent only in HN1957, but not in HN2092 [15]. Variations in the treatment response may be attributed to inter-tumor heterogeneity among the various types of HNSCC [6] with regard to the tumor site and the molecular profile of the tumors [21]. Accordingly, array CGH detected alterations in both primary cultures that are typical for HNSCC, such as gains on 5p, 8q, 11q, 9q and 20pq as well as losses on 3p and 18q (reviewed in [22]) (Additional files 1, 2, 3A and 4A). In addition, alterations that were unique to one of the primary cell cultures, such as chromosomal bands on chromosomes 4 and 14, which were affected only in HN2092 but not in HN1957, were observed. Structural rearrangements involving chromosomes 1, 3, 8 and 13 that were detected in HN1957 or HN2092 are in accordance with previous karyotyping investigations of HNSCC [23]. In addition, so far unpublished rearrangements on chromosomes 4, 9, 10, 14 and 15 were discovered in the two primary cell cultures. Altogether, the cytogenetic analysis demonstrated that both primary cultures consisted of a rather homogenous cell population since most of the chromosomal alterations were shown to be clonal.

We further analyzed the mutational status of *P53* and *EGFR* since mutations in *P53* are common in head and neck cancers [24] and *EGFR* represents a key oncogene in HNSCC [25]. *EGFR* did not show any mutations in both primary cultures, whereas HN1957 showed a *P53*

Table 3 Validation of deregulated miRNAs and correlating target mRNAs in HN2092 after radiochemotherapy treatment (analyzed with Agilent microarrays and TaqMan single qRT-PCR assays)

miRNA	Array	qRT-PCR	mRNA	Array	qRT-PCR
	FC (*p* value)	FC (*p* value)		FC (*p* value)	FC (*p* value)
miR-93-5p	0.96 (0.001)	0.84 (<0.001)	*CCDC88C*	1.44 (<0.001)	1.04 (0.890)
miR-99b-5p	1.13 (<0.001)	1.10 (0.502)	*ACTR1B*	0.62 (<0.001)	0.61 (0.012)
miR-181a-5p	1.38 (<0.001)	1.37 (0.001)	–	–	–
miR-183-5p	1.18 (<0.001)	1.18 (0.071)	*ASNS*	0.52 (<0.001)	0.47 (0.017)
			IDH2	0.63 (<0.001)	0.62 (0.045)
			HSPA1B	0.52 (0.022)	0.81 (0.167)
miR-186-5p	1.15 (0.083)	1.10 (0.147)	*FASN*	0.66 (<0.001)	0.66 (0.007)
miR-197-3p	1.17 (0.025)	1.02 (0.273)	*FASN*	0.66 (<0.001)	0.66 (0.007)
			HSPA1B	0.52 (0.022)	0.81 (0.167)
miR-222-3p	1.10 (0.006)	0.95 (0.057)	*FASN*	0.66 (<0.001)	0.66 (0.007)
miR-320a	1.14 (<0.001)	1.07 (0.425)	*HES6*	0.65 (<0.001)	0.52 (0.004)

FC Fold change

/**Table 4** Validation of miRNA-mRNA interactions in HN1957 and HN2092 in response to radiochemotherapy treatment (analyzed with TaqMan single qRT-PCR assays)

	miRNA	FC	mRNA	FC	Spearman correlation
HN1957	*miR-7-5p*	1.30	*SNCA*	0.48	0.5
	miR-17-5p	1.21	*AMD1*	0.87	−1.0
			MKI67	0.62	1.0
HN2092	*miR-7-5p*	1.54	*HELLS*	1.26	−0.5
	miR-17-5p	1.13	*BACE1*	0.96	−1.0
			NAGK	0.81	−0.5
	miR-93-5p	0.84	*CCDC88C*	1.04	0.5
			SLC19A1	2.38	−1.0

FC Fold change

mutation in the SH3 ligand (P72R) and a nonsense mutation (Δ331) in the tetramerization domain (TD). The polymorphism at position 72 (P72R) in *P53* affects the interaction between some *P53* mutants and *P73*, a *P53* homologue that can transcriptionally activate *P53* target genes [26]. The binding ability of *P53* and *P73* affects the response to chemotherapy *in vitro*, which points to a possible impact of the polymorphism in codon 72 on the chemosensitivity of tumor cells. The second *P53* mutation (Δ331) leads to a truncated protein, due to a stop codon in the TD. Most of the mutations in the TD lead to defects in oligomerization of *P53*, DNA binding, stimulation of the transcription of reporter genes and growth inhibition of tumor cells [27]. It has been shown that deletion of the TD, which impairs the ability of *P53* to tetramerize, does not abolish its ability to bind DNA and to stimulate transcription, but significantly decreases the overall affinity of *P53* for DNA, thus destabilizing the *P53*-DNA complexes [28].

Since *EGFR* is known to be overexpressed in up to 90 % of HNSCC [29] we determined the *EGFR* expression levels of HN1957 and HN2092 in comparison to normal human keratinocytes (OKF6-hTERT). Both primary HNSCC cultures demonstrated increased relative expression of *EGFR* (Additional file 5), which implies a potential impact of *EGFR* signaling suggesting an *EGFR*-targeted treatment for an improved therapy response. Additionally, the epithelial cell adhesion molecule (*EpCAM*), which is frequently overexpressed in HNSCC [30], showed higher expression in HN1957 and HN2092 cells relative to OKF6-hTERT cells (Additional file 5). *EpCAM* acts as a marker for metastasis and proliferation representing another potential target for the therapeutic response.

The two primary cell cultures, HN1957 and HN2092, in part showed the same molecular response to radiochemotherapy treatment. The similarities became clear after pathway enrichment analysis that resulted in six common pathways affected by combined treatment with ionizing radiation and 5-FU. Among these, the pathway *direct effectors of P53* is likely to represent effects of both ionizing radiation and 5-FU treatment. 5-FU is known to stabilize and activate *P53* promoting

Table 5 Pathway enrichment analysis of potential target genes in HN1957 for miRNAs responding to therapy in HNSCC patients (FDR < 0.05)

Pathway	Number of Proteins in Pathway	Proteins from Gene List	*P*-value	FDR	Genes
Pathways in cancer (K)	327	7	0.0004	1.40E-02	E2F1,PTEN,AKT2,MSH6,HSP90AA1,JUN,VEGFA
Direct p53 effectors (N)	133	5	0.0002	1.40E-02	E2F1,PTEN,SP1,JUN,SMARCA4
Hepatitis B (K)	146	5	0.0004	1.38E-02	E2F1,PTEN,AKT2,JUN,YWHAQ
Nonsense-mediated decay (R)	106	5	0.0001	1.55E-02	RPL30,UPF1,SMG7,RNPS1,RPL18A
RNA transport (K)	164	5	0.0006	1.50E-02	EEF1A1,UPF1,RNPS1,EIF4G2,NUP205
E2F transcription factor network (N)	68	4	0.0002	1.44E-02	E2F1,KAT2B,SP1,RRM2
Estrogen signaling pathway (K)	100	4	0.0009	1.69E-02	AKT2,HSP90AA1,SP1,JUN
Glucocorticoid receptor regulatory network (N)	77	4	0.0003	1.34E-02	SMARCD1,HSP90AA1,JUN,SMARCA4
HIF-1-alpha transcription factor network (N)	66	4	0.0002	2.03E-02	NPM1,SP1,JUN,VEGFA
Huntington disease (P)	121	4	0.0017	2.79E-02	GAPDH,AKT2,AP2A2,JUN
Processing of capped intron-containing pre-mRNA (R)	138	4	0.0028	3.33E-02	DDX23,PCBP1,RNPS1,NUP205
Prostate cancer (K)	89	4	0.0006	1.56E-02	E2F1,PTEN,AKT2,HSP90AA1
Regulation of androgen receptor activity (N)	49	4	0.0001	1.70E-02	KAT7,HSP90AA1,KAT2B,JUN
Regulation of telomerase (N)	68	4	0.0002	1.44E-02	E2F1,HSP90AA1,SP1,JUN

(B) BioCarta, (K) KEGG Pathway, (N) NCI - Nature Curated Data, (P) pantherdb, (R) Reactome

Table 6 Pathway enrichment analysis of potential target genes in HN2092 for miRNAs responding to therapy in HNSCC patients (FDR < 0.05)

Pathway	Number of Proteins in Pathway	Proteins from Gene List	*P*-value	FDR	Genes
ISG15 antiviral mechanism(R)	71	4	0	<1.000E-03	NUP153,EIF4G2,NUP205,KPNA2
Viral carcinogenesis(K)	206	4	0.0006	1.94E-02	KAT2B,RBL2,CCND2,JUN
HTLV-I infection(K)	260	4	0.0013	3.58E-02	KAT2B,MAD2L1,CCND2,JUN
Aurora B signaling(N)	40	3	0.0001	7.00E-03	BIRC5,NPM1,PSMA3
Signaling events mediated by HDAC Class I(N)	56	3	0.0002	1.17E-02	NUP153,KAT2B,YY1
E2F transcription factor network(N)	68	3	0.0003	1.34E-02	KAT2B,RBL2,YY1
Validated targets of C-MYC transcriptional activation(N)	72	3	0.0003	1.35E-02	BIRC5,CCND2,NPM1
Mitotic Prophase(R)	99	3	0.0009	2.79E-02	NUP153,SET,NUP205
Nonsense-Mediated Decay(R)	106	3	0.0010	3.07E-02	SMG7,RPL30,RPL7
Cell cycle(K)	124	3	0.0016	3.55E-02	RBL2,MAD2L1,CCND2
Mitotic G1-G1/S phases(R)	134	3	0.0020	3.66E-02	RBL2,CCND2,PSMA3
Mitotic Metaphase and Anaphase(R)	173	3	0.0042	4.77E-02	BIRC5,MAD2L1,PSMA3

(B) BioCarta, (K) KEGG Pathway, (N) NCI - Nature Curated Data, (P) pantherdb, (R) Reactome

P53-mediated apoptosis [31, 32]. *P53* is also activated by radiation-induced DNA-damage [33] and therefore represents an important cell cycle checkpoint. Another pathway affected by the treatment in our study was *apoptotic execution phase* including histones and molecules involved in DNA fragmentation and chromatin condensation. A further pathway, which was involved in the treatment response of both primary cell cultures, was *DNA damage/telomere stress induced senescence*. It is mainly based on histones that were damaged by the treatment and might reflect effects of ionizing radiation on the DNA structure. Molecules acting in the *cholesterol biosynthesis* also showed deregulation in both primary cell cultures, suggesting an involvement of membranes, probably due to an effect of 5-FU on lipids [34]. Further, the appearance of *dissolution of fibrin clot* as a result of the pathway analysis implies that cellular migration and inflammation was affected by the treatment since plasminogen activators and inhibitors regulate cellular adhesion and migration as well as inflammatory response [35]. *Unfolded protein response* was another pathway playing a role in the cellular treatment response due to deregulated chaperones, which are part of the cellular stress response [36]. Apart from that, we were able to validate deregulation of *miR-183-5p* and its target gene *ASNS* following radiochemotherapy (Table 3). Activation of *ASNS* transcription is part of the *unfolded protein response* and enhances the cellular resistance to drug treatment. Thus it represents a potential prognostic factor for the outcome of radiochemotherapy [37].

The miRNA-mRNA networks showing interactions that are part of the treatment response revealed three commonly deregulated miRNAs, *miR-7-5p*, *miR-17-5p* and *miR-93-5p*, in the two primary cell lines. For these miRNAs interactions with several target genes were validated for each primary cell line, which proves the significance of the treatment-responsive miRNA-mRNA interactions.

Genes, which are already known as key players in the response to 5-FU treatment, also appeared in the miRNA-mRNA networks of the two primary cell cultures. In particular, 5-FU is an anti-metabolite and inhibits thymidilate synthase, which catalyzes the synthesis of thymidylate and is an essential component of DNA replication and repair [31]. *SLC19A1* and *DHFR* are part of the folate metabolism, which is necessary for the reaction catalyzed by thymidilate synthase, and therefore they might represent predictive markers for the efficacy of 5-FU treatment [38]. Molecules, such as *ASNS* or *DHFR*, that show a response to treatment are potential candidates for stratification of patients with regard to their sensitivity to anti-tumor treatment and might be targets in a specific group of patients for a combinatorial treatment approach in order to enhance therapy success [7]. A systems-based prediction of such combinatorial treatment approaches has recently been reported for colon cancer by Klinger et al. [39], which would be also very promising in the case of HNSCC. Based on the

current study such a systems analysis of HNSCC cells in response to additional inhibitors and perturbations becomes feasible.

Despite many common features, differences in the molecular treatment response between the two primary cultures were observed. The pathway enrichment analysis of treatment-responsive genes revealed pathways that were only affected in one of the two primary cell cultures. The *TGF-beta signaling pathway* was affected in HN1957 as well as the *regulation of nuclear SMAD2/3 signaling*. The two pathways are closely connected since both *SMAD2* and *SMAD3* are regulated by *TGF-beta* [40]. *TGF-beta* signaling is involved in cellular processes such as cell growth, cell differentiation and apoptosis. Further pathways that distinguished the response of the two primary cell cultures were *TNF signaling pathway* and *IL6-mediated signaling events*. These pathways are both part of inflammatory processes which might point to an immunological response to treatment in HN1957 cells. The cytokines *TGF-beta*, *IL6* and *TNF-alpha* are all well-known biomarkers for treatment complications and prognosis of radiochemotherapy success [41, 42]. Accordingly, the miRNA analysis revealed many miRNAs regulating immune response and inflammatory molecules deregulated in HN1957, but not in HN2092. For example, *miR-18a-5p*, *miR-106b-5p*, *miR-92a-3p* and *miR-125b-5p* are known to play a role in inflammation or immune system [43] and showed a treatment response only in HN1957. Moreover, upregulation of *miR-181b-5p* following treatment was validated in HN1957. *MiR-181b-5p* is an oncogenic miRNA known to be overexpressed in HNSCC and represents a previously reported link between inflammation and cancer [44]. Taking all these differences between HN1957 and HN2092 concerning the pathways involved in the molecular treatment response into account, some of the discovered pathways might be important for prognosis of the individual therapy success. As a consequence this novel knowledge may be used to deduce more individualized treatment strategies, e.g. targeting inflammatory pathways which might lead to a better treatment response [39].

The fact that four miRNAs (*miR-21-5p*, *miR-93-5p*, *miR-106b-5p*, *miR-425-5p*) that have already been shown to be therapy-responsive in blood plasma of HNSCC patients [15] were also deregulated in the cell culture model, demonstrates the clinical impact of this study and links the results of the cell culture model to our *in vivo* findings. Therefore, we identified all possible target molecules of these miRNAs by correlation analysis of miRNA and mRNA expression values, including only target interactions that are validated in the miRTarBase [17, 18]. The four miRNAs were previously described to play a role in cancer and represent potential diagnostic or prognostic biomarkers. *MiR-106b-5p* and *miR-21-5p* were suggested as biomarkers in laryngeal carcinoma [45]. Moreover, *miR-106b-5p* has been shown to promote cell migration and invasion by targeting *PTEN* [46] while *miR-21-5p* is overexpressed in various cancer types and was reported as a prognostic biomarker in head and neck cancer [47]. *MiR-425-5p* and *miR-93-5p* are known as regulators in cell proliferation [48, 49]. *MiR-93-5p* is also targeting the *PTEN/AKT* signaling pathway, thus influencing drug sensitivity of cancer cells [50]. The pathway enrichment analysis based on the target genes of these miRNAs revealed mostly signaling molecules that represent *direct P53 effectors* such as *PTEN*, *JUN* and *E2F1* as well as *cell cycle* regulators such as *RBL2*, *CCND2*, *RRM2* and *E2F1*. The *E2F transcription factor network* including genes such as *E2F1*, *RRM2*, *RBL2*, *KAT2B* represents a crucial target of the four selected miRNAs in both primary HNSCC cultures, which might be due to the fact that *E2F1* impacts thymidilate synthase expression, which is a major target of 5-FU as already discussed [51]. Furthermore, several studies report an influence of deregulation of the *E2F transcription factor network* on the chemoradiation sensititvity of cancer cells [52–54]. Most of the genes, that are involved in many of the significantly enriched pathways, also play a role in *pathways in cancer* such as *PTEN*, *JUN*, *AKT2*, *HSP90AA1*, the latter of which was already described to influence radiosensitivity and chemosensitivity [55]. Also *PTEN* is a well-known radiosensitizer enhancing cell death through *AKT* signaling [56]. The results presented in this study open up the possibility of new treatment strategies that target the therapy-responsive signaling pathways either directly or on the level of the miRNAs regulating the signaling molecules.

Conclusions

Important progress in strategies for treatment of HNSCC has been made over the past decades, however, dose escalation studies revealed that classical radiochemotherapy has reached some sort of dead end [57]. Therefore, a combination of radiochemotherapy with molecularly targeted agents might open up new therapeutic possibilities. This requires the identification of prognostic targets that enable individualized treatment strategies and allow prevention of excessive therapy.

In the present study we showed that the main pathways affected by radiochemotherapy in two different HNSCC primary cultures are related to cell cycle and proliferation, cell death and stress response. As a difference between the two cell cultures we discovered an emphasis on inflammation in the treatment response of HN1957. This suggests the use of inflammatory pathways for stratification of HNSCC patients in order to

identify individuals who might benefit from an additional therapy targeting inflammatory pathways.

Similar pathways emerged from the analysis of potential targets of four miRNAs that showed a treatment response in the plasma of HNSCC patients and the cell culture model, suggesting potential molecular therapeutic targets in the *E2F transcription factor network* and the *PTEN/AKT* signaling pathway. This leads to the conclusion that promising prognostic markers and molecules for a targeted therapy approach in HNSCC patients are most likely to be found among those signaling molecules which needs to be further investigated on clinical samples.

Methods

Primary HNSCC cell cultures

The primary HNSCC cell cultures, HN1957 and HN2092, were previously described by Summerer et al. [15]. Characteristics of the two primary cell cultures are listed in Table 1. Molecular characterization of the primary cell cultures included array CGH, SKY, sequence analysis of *TP53* and *EGFR* and determination of EGFR and EpCAM protein expression levels on the cell surface.

High-Resolution Oligo Array CGH

For array CGH analysis of the primary cell cultures the SurePrint G3 human CGH Microarray Kit 4x180k (Agilent Technologies, Santa Clara, CA, AMADID: 022060) was used. Tumor DNA (250 ng) and sex-mismatched normal reference DNA (250 ng) (Promega, Madison, WI) were used for hybridization. Hybridization and data analysis were performed as described by Hess et al. [58].

SKY

Metaphase preparation was done with 3 h of colcemid (Roche) treatment followed by hypotonic treatment with KCl (75 mM) for 25 min and three fixation steps (20 min each) with methanol-acetic acid (3 + 1) on ice. After one week of ageing at room temperature metaphase preparations were treated with RNase A (50 μg/mL in 2 x SSC), digested with pepsin (1 mg/ml) for 2 min at 37 °C and dehydrated in a 70, 80, and 100 % ethanol series. After fixation with 1 % formaldehyde for 10 min metaphases were placed in denaturing solution (70 % formamide in 2 x SSC) at 72 °C for 7 min followed by dehydration. Hybridization steps and image analysis were previously described by Hieber et al. [59].

Sequencing

Complementary DNA was synthesized from cellular RNA using the SuperScript III First-Strand Synthesis System for RT-PCR (Invitrogen, Carlsbad, CA) according to the manufacturer's protocol using Oligo-dT primer and 1.6 μg RNA. Subsequently, PCR was performed using Q5 High-Fidelity DNA Polymerase (New England Biolabs, Ipswich, MA) with 1 μl of a 1:10 dilution of the cDNA using the primer combinations in Additional file 12. The protocol was optimized for a 50 μl reaction volume using 1 μl forward and 1 μl reverse primer and adding 5 μl of 10× cresol red and 1 μl of DMSO. The PCR was optimized as follows: denaturation for 10 min at 96 °C followed by 35 cycles of 15 s at 96 °C and 8 min at 68 °C and final extension for 10 min at 68 °C. The size of the PCR-products was checked on a 1 % agarose gel. The bands were cut out from the gel and DNA was purified on spin columns. The following BigDye PCR was performed using the BigDye Terminator V3.1 Kit (Applied Biosystems, Waltham, MA) with 6 μl of template DNA. PCR was carried out with 4 min of denaturation at 96 °C followed by 45 cycles of 30 s 95 °C, 20 s 50 °C and 4 min 60 °C. PCR products were sequenced on an ABI 3730 DNA Analyzer (Applied Biosystems, Waltham, MA).

EGFR and EpCAM expression

Surface expression levels of EGFR and EpCAM were assessed by flow cytometry using fluorescently labeled antibodies as described before [60]. Briefly, 1×10^5 cells were stained with anti-EGFR-PE (clone EGFR.1) and anti-EpCAM-APC (clone EBA-1) antibodies or the corresponding isotype controls (all from BD Biosciences, Franklin Lakes, NJ) in PBS supplemented with 2 % FCS for 20 min at 4 °C. Cells were washed twice and analyzed on an LSRII flow cytometer (BD Biosciences, Franklin Lakes, NJ). Relative surface expression levels are depicted as median fluorescence intensities subtracted by the matching isotype controls (means ± standard deviations of 3 technical replicates are given). Expression of EGFR and EpCAM was measured for HN1957 and HN2092 as well as for the immortalized keratinocytes OKF6-hTERT [61].

Treatment of HNSCC cells

The treatment of the primary HNSCC cells was designed to model radiochemotherapy treatment of a HNSCC patient cohort used in a previous study by Summerer et al. [15]. Briefly, cells were irradiated with 2 Gy using a ^{137}Cs source and treated with 5-FU (solved in DMSO; Sigma-Aldrich, St. Louis, MO). Controls were treated with the corresponding volumes of DMSO and sham-irradiated. 24 h after the first irradiation a second fraction of 2 Gy was applied to the 5-FU-treated cells followed by incubation for 1 h at 37 °C. Cells were harvested by trypsinization and stored at −20 °C until further processing.

RNA extraction and quality assessment

Total RNA was extracted from frozen cell pellets (−20 °C) of treated and untreated primary HNSCC cells using the miRNeasy mini kit (Qiagen, Venlo, Netherlands) according

to the manufacturer's protocol without DNase digest or small RNA enrichment. Optical density (OD) 260/280 ratios were measured with a Nanodrop ND-1000 (Thermo Scientific) and ranged from 1.92 to 2.04. RNA-concentrations were measured with a Qubit 2.0 Fluorometer (Invitrogen, Carlsbad, CA) using the RNA Broad Range Assay Kit (Invitrogen, Carlsbad, CA). Additionally, RNA quality was assessed prior to the Agilent microarray experiments using an Agilent 2100 Bioanalyzer (Agilent Technologies, Santa Clara, CA). The obtained RNA integrity numbers (RINs) ranged from 9.3 to 10.0. RNA samples were stored at −80 °C until further processing.

MicroRNA profiling

MiRNA profiling of primary HNSCC cell cultures was previously described by Summerer et al. [15].

Quantification of individual miRNAs by real-time PCR

Reverse transcription was performed on a Cyclone PCR system (Peqlab, Erlangen, Germany) using the TaqMan miRNA reverse transcription kit and miRNA-specific stem-loop primers (Applied Biosystems, Waltham, MA) according to the manufacturer's protocol. Quantitative real-time PCR (qRT-PCR) was performed in duplicates and included non-template negative controls. A ViiA 7 real-time PCR System (Applied Biosystems, Waltham, MA) was used according to the manufacturer's protocol. The U6 snRNA was used for normalization. Fold changes were calculated using the $2^{-\Delta\Delta Ct}$ method [62]. *P*-values were computed using the student's *t*-test.

Global gene expression analysis

To identify potential targets of deregulated miRNAs, a gene expression profiling was performed with G3 Human Gene Expression 8×60k v2 microarrays (Agilent Technologies, Santa Clara, CA, AMADID: 039494) covering over 40,000 transcripts. The gene expression analysis was carried out according to the manufacturer's protocol. Total RNA was extracted from untreated and treated cells as described above. A one-color microarray experiment with 60 ng of the same RNA samples that were used for the miRNA analysis was conducted with three biological and two technical replicates for each data point. A one-color RNA spike-in kit (Agilent Technologies, Santa Clara, CA) was used to monitor the workflow. In the first step copyDNA (cDNA) was generated from the RNA templates followed by transcription to copyRNA (cRNA) with incorporation of cyanine 3-CTP. After hybridization of the labeled cRNA on the arrays (17 h, 65 °C), the microarrays were scanned with a G2505C Sure Scan Microarray Scanner (Agilent Technologies, Santa Clara, CA). Data were extracted with the Feature Extraction 10.7 software (Agilent Technologies, Santa Clara, CA). Data quality assessment, preprocessing, and normalization were conducted in R using the Bioconductor AgiMicroRNA package [63]. In order to identify significantly differentially expressed genes between treated and untreated cells, statistical analyses were accomplished using the Bioconductor limma package [64]. A cut-off for FDR-adjusted *p*-values of 0.05 was applied.

Quantitative real-time PCR quantification of individual mRNAs

For validation of gene expression microarray data, individual mRNAs were quantified via qRT-PCR. 500 ng of RNA was reverse-transcribed using the QuantiTect Reverse Transcription Kit (Qiagen, Venlo, Netherlands) according to the manufacturer's protocol. qRT- PCR was performed on a ViiA 7 real-time PCR System (Applied Biosystems, Waltham, MA) using specific TaqMan gene expression assays (Applied Biosystems, Waltham, MA). PCR was carried out in 10 μl reactions consisting of 5 μl TaqMan PCR Master Mix (no AmpErase UNG), 3.5 μl H_2O, 0.5 μl TaqMan assay and 1 μl cDNA. All reactions were performed in triplicates and included non-template negative controls. *B2M* and *ACTB* were used as endogenous controls. Fold changes were calculated using the $2^{-\Delta\Delta Ct}$ method [62]. *P*-values were computed using the student's *t*-test.

Network analysis

MiRNA-mRNA networks were designed based on integrative analysis of the microarray data. A correlation matrix was calculated using the expression values of all significantly deregulated miRNAs and mRNAs, resulting in a correlation value for each miRNA-mRNA pair. Based on the assumption of a negative regulation mechanism Pearson correlation values of $-1 \leq c \leq -0.5$ were considered to indicate associations. This condition was used to convert the correlation matrix into a binary matrix to which we associated a false detection rate calculated after a permutation test. Only miRNA-mRNA pairs that represented validated interactions (with the annotation "strong evidence" or NGS-validated targets) in the miRTarBase [18, 17], were considered. The miRNA-mRNA pairs that showed significant negative correlation as well as validated functional interaction (according to miRTarBase) were visualized with the yED Graph Editor software [65]. All statistical analyses were performed using the R Project for Statistical Computing [66].

Pathway analysis of deregulated mRNAs

To analyze the functional context of the significantly deregulated genes in the radiochemotherapy cell culture model a pathway enrichment analysis was performed using the Reactome 4.0.1 application [14] in the Cytoscape 3.0.2 software [67].

Additional files

Additional file 1: Copy number alterations in HN1957. (PDF 37 kb)

Additional file 2: Copy number alterations in HN2092. (PDF 43 kb)

Additional file 3: Cytogenetic characterization of HN1957. (PDF 8257 kb)

Additional file 4: Cytogenetic characterization of HN2092. (PDF 8434 kb)

Additional file 5: EGFR and EpCAM surface expression of HN1957, HN2092 and OKF6-hTERT. (PDF 838 kb)

Additional file 6: Significantly deregulated mRNAs in primary HN1957 after *in vitro* radiochemotherapy treatment. (PDF 146 kb)

Additional file 7: Significantly deregulated mRNAs in primary HN2092 after *in vitro* radiochemotherapy treatment. (PDF 143 kb)

Additional file 8: Pathway enrichment analysis of differentially expressed genes in HN1957 after radiochemotherapy treatment. (PDF 66 kb)

Additional file 9: Pathway enrichment analysis of differentially expressed genes in HN2092 after radiochemotherapy treatment. (PDF 44 kb)

Additional file 10: Potential target genes in HN1957 for miRNAs responding to therapy in HNSCC patients. (PDF 72 kb)

Additional file 11: Potential target genes in HN2092 for miRNAs responding to therapy in HNSCC patients. (PDF 51 kb)

Additional file 12: Primer sequences for *TP53* and *EGFR* sequencing. (PDF 42 kb)

Abbreviations

^{137}Cs: ^{137}Cesium; 5-FU: 5-fluorouracil; APC: Allophycocyanin; CGH: Comparative genomic hybridization; cRNA: copyRNA; CTP: Cytosine triphosphate; DMSO: Dimethyl sulfoxide; EBA-1: EpCAM antibody 1; EBV: Ebstein Barr virus; FCS: Fetal calf serum; FDR: False discovery rate; HNSCC: Head and neck squamous cell carcinoma; HPV: Human papilloma virus; hTERT: Human telomerase reverse transcriptase; KCl: Potassium chloride; miRNA: microRNA; mRNA: messengerRNA; NGS: Next generation sequencing; OD: Optical density; PBS: Phosphate buffered saline; PCR: Polymerase chain reaction; PE: Phycoerythrin; qRT-PCR: Quantitative real-time PCR; SKY: Spectral karyotyping; snRNA: small nucleolar RNA; SSC: Saline sodium citrate; TD: Tetramerization domain; UNG: Uracil N-glycosylase.

Competing interests

The authors declare that they have no competing interests.

Authors' contributions

IS: experiments, establishment of radiochemotherapy cell culture model, Reactome pathway enrichment analysis, manuscript, JH: array CGH analysis, support for experimental design/concept, AP: biostatistics analysis, KU: bioinformatics and biostatistics analysis, LH: spectral karyotyping, MS: analysis of array CGH data, KL: EGFR/EpCAM analysis, support for experimental design/concept, HZ: study design and critical revision of the manuscript. All authors read and approved the final manuscript.

Acknowledgements

We thank Laura Dajka, Aaron Selmeier, Claire Innerlohinger, Isabella Zagorski and Elke Konhäuser for their excellent technical assistance. We further thank Steffen Heuer and Randolph Caldwell for their great support with the sequencing analysis. Tissue samples were obtained from the Wales Cancer Bank, which is funded by the Wales Assembly Government and Cancer Research Wales. Other investigators may have received specimens from the same subjects.
The study was supported by the federal ministry of education and research (Grant No.: 02NUK024B, 02NUK024C).

Author details

[1]Research Unit Radiation Cytogenetics, Helmholtz Center Munich, Ingolstaedter Landstr.1, 85764 Neuherberg, Germany. [2]Clinical Cooperation Group 'Personalized Radiotherapy of Head and Neck Cancer', Helmholtz Center Munich, Ingolstaedter Landstr. 1, 85764 Neuherberg, Germany. [3]Department of Radiation Oncology, University of Munich, Marchioninistr. 15, 81377 Munich, Germany.

Received: 17 October 2014 Accepted: 19 August 2015
Published online: 02 September 2015

References

1. Alibek K, Kakpenova A, Baiken Y. Role of infectious agents in the carcinogenesis of brain and head and neck cancers. Infect Agent Cancer. 2013;8(1):7.
2. Warnakulasuriya S. Global epidemiology of oral and oropharyngeal cancer. Oral Oncol. 2009;45(4–5):309–16. http://dx.doi.org/10.1016/j.oraloncology.2008.06.002.
3. Pulte D, Brenner H. Changes in survival in head and neck cancers in the Late 20th and Early 21st century: a period analysis. Oncologist. 2010;15(9):994–1001. doi:10.1634/theoncologist.2009-0289.
4. May JT, Rao N, Sabater RD, Boutrid H, Caudell JJ, Merchant F, et al. Intensity-modulated radiation therapy as primary treatment for oropharyngeal squamous cell carcinoma. Head Neck. 2013;35(12):1796–800. doi:10.1002/hed.23245.
5. Nagadia R, Pandit P, Coman W, Cooper-White J, Punyadeera C. miRNAs in head and neck cancer revisited. Cell Oncol. 2013;36(1):1–7. doi:10.1007/s13402-012-0122-4.
6. Baxi S, Fury M, Ganly I, Rao S, Pfister DG. Ten years of progress in head and neck cancers. J Natl Compr Canc Netw. 2012;10(7):806–10.
7. Orth M, Lauber K, Niyazi M, Friedl A, Li M, Maihöfer C, et al. Current concepts in clinical radiation oncology. Radiat Environ Biophys. 2014;53(1):1–29. doi:10.1007/s00411-013-0497-2.
8. Di Leva G, Garofalo M, Croce CM. MicroRNAs in cancer. Annu Rev Pathol. 2014;9:287–314. doi:10.1146/annurev-pathol-012513-104715.
9. Calin GA, Croce CM. MicroRNA signatures in human cancers. Nat Rev Cancer. 2006;6(11):857–66.
10. Babu JM, Prathibha R, Jijith VS, Hariharan R, Pillai MR. A miR-centric view of head and neck cancers. Biochim Biophys Acta Rev Cancer. 2011;1816(1):67–72. http://dx.doi.org/10.1016/j.bbcan.2011.04.003.
11. Salazar C, Nagadia R, Pandit P, Cooper-White J, Banerjee N, Dimitrova N, et al. A novel saliva-based microRNA biomarker panel to detect head and neck cancers. Cell Oncol (Dordr). 2014;37(5):331–8. doi:10.1007/s13402-014-0188-2.
12. Salazar C, Calvopina D, Punyadeera C. miRNAs in human papilloma virus associated oral and oropharyngeal squamous cell carcinomas. Expert Rev Mol Diagn. 2014;14(8):1033–40. doi:10.1586/14737159.2014.960519.
13. Stingo FC, Chen YA, Vannucci M, Barrier M, Mirkes PE. A Bayesian graphical modeling approach to microrna regulatory network inference. Ann Appl Stat. 2010;4(4):2024–48. doi:10.1214/10-aoas360.
14. Jupe S, Akkerman JW, Soranzo N, Ouwehand WH. Reactome – a curated knowledgebase of biological pathways: megakaryocytes and platelets. J Thromb Haemost. 2012;10(11):2399–402. doi:10.1111/j.1538-7836.2012.04930.x.
15. Summerer I, Niyazi M, Unger K, Pitea A, Zangen V, Hess J, et al. Changes in circulating microRNAs after radiochemotherapy in head and neck cancer patients. Radiat Oncol. 2013;8(1):296.
16. Petersson F. Nasopharyngeal carcinoma: a review. Semin Diagn Pathol. 2015;32(1):54–73. doi:10.1053/j.semdp.2015.02.021.
17. miRTarBase. The experimentally validated microRNA-target interactions database [database on the Internet]. Available from: http://mirtarbase.mbc.nctu.edu.tw/. Accessed: October 2013
18. Hsu S-D, Tseng Y-T, Shrestha S, Lin Y-L, Khaleel A, Chou C-H, et al. miRTarBase update 2014: an information resource for experimentally validated miRNA-target interactions. Nucleic Acids Res. 2014;42(D1):D78–85. doi:10.1093/nar/gkt1266.
19. Yamamoto Y, Yoshioka Y, Minoura K, Takahashi RU, Takeshita F, Taya T, et al. An integrative genomic analysis revealed the relevance of microRNA and gene expression for drug-resistance in human breast cancer cells. Mol Cancer. 2011;10:135. doi:10.1186/1476-4598-10-135.
20. Peng X, Li Y, Walters K-A, Rosenzweig E, Lederer S, Aicher L, et al. Computational identification of hepatitis C virus associated microRNA-mRNA regulatory modules in human livers. BMC Genomics. 2009;10(1):373.
21. Chung CH, Parker JS, Karaca G, Wu J, Funkhouser WK, Moore D, et al. Molecular classification of head and neck squamous cell carcinomas using

patterns of gene expression. Cancer Cell. 2004;5(5):489–500. http://dx.doi.org/10.1016/S1535-6108(04)00112-6.
22. Struski S, Doco-Fenzy M, Cornillet-Lefebvre P. Compilation of published comparative genomic hybridization studies. Cancer Genet Cytogenet. 2002;135(1):63–90. http://dx.doi.org/10.1016/S0165-4608(01)00624-0.
23. Singh B, Gogineni S, Goberdhan A, Sacks P, Shaha A, Shah J, et al. Spectral karyotyping analysis of head and neck squamous cell carcinoma. Laryngoscope. 2001;111(9):1545–50. doi:10.1097/00005537-200109000-00010.
24. Olshan AF, Weissler MC, Pei H, Conway K. p53 mutations in head and neck cancer: new data and evaluation of mutational spectra. Cancer Epidemiol Biomarkers Prev. 1997;6(7):499–504.
25. Safdari Y, Khalili M, Farajnia S, Asgharzadeh M, Yazdani Y, Sadeghi M. Recent advances in head and neck squamous cell carcinoma–a review. Clin Biochem. 2014;47(13–14):1195–202. doi:10.1016/j.clinbiochem.2014.05.066.
26. Marin MC, Jost CA, Brooks LA, Irwin MS, O'Nions J, Tidy JA, et al. A common polymorphism acts as an intragenic modifier of mutant p53 behaviour. Nat Genet. 2000;25(1):47–54. doi:10.1038/75586.
27. Chene P. The role of tetramerization in p53 function. Oncogene. 2001;20(21):2611–7. doi:10.1038/sj.onc.1204373.
28. Weinberg RL, Veprintsev DB, Fersht AR. Cooperative binding of tetrameric p53 to DNA. J Mol Biol. 2004;341(5):1145–59. http://dx.doi.org/10.1016/j.jmb.2004.06.071.
29. Boeckx C, Weyn C, Vanden Bempt I, Deschoolmeester V, Wouters A, Specenier P, et al. Mutation analysis of genes in the EGFR pathway in Head and Neck cancer patients: implications for anti-EGFR treatment response. BMC Res Notes. 2014;7:337. doi:10.1186/1756-0500-7-337.
30. Mu Y, Sa N, Yu L, Lu S, Wang H, Xu W. Epithelial cell adhesion molecule is overexpressed in hypopharyngeal carcinoma and suppresses the metastasis and proliferation of the disease when downregulated. Oncol Lett. 2014;8(1):175–82. doi:10.3892/ol.2014.2140.
31. Longley DB, Harkin DP, Johnston PG. 5-Fluorouracil: mechanisms of action and clinical strategies. Nat Rev Cancer. 2003;3(5):330–8.
32. Garcia MA, Carrasco E, Aguilera M, Alvarez P, Rivas C, Campos JM, et al. The chemotherapeutic drug 5-fluorouracil promotes PKR-mediated apoptosis in a p53-independent manner in colon and breast cancer cells. PLoS ONE. 2011;6(8), e23887. doi:10.1371/journal.pone.0023887.
33. Fei P, El-Deiry WS. P53 and radiation responses. Oncogene. 2003;22(37):5774–83. doi:10.1038/sj.onc.1206677.
34. Stathopoulos GP, Stergiou GS, Perrea-Kostarelis DN, Dontas IA, Karamanos BG, Karayiannacos PE. Influence of 5-fluorouracil on serum lipids. Acta Oncol. 1995;34(2):253–6.
35. Chapman HA. Plasminogen activators, integrins, and the coordinated regulation of cell adhesion and migration. Curr Opin Cell Biol. 1997;9(5):714–24.
36. Saibil H. Chaperone machines for protein folding, unfolding and disaggregation. Nat Rev Mol Cell Biol. 2013;14(10):630–42. doi:10.1038/nrm3658.
37. Balasubramanian MN, Butterworth EA, Kilberg MS. Asparagine synthetase: regulation by cell stress and involvement in tumor biology. Am J Physiol Endocrinol Metab. 2013;304(8):E789–99. doi:10.1152/ajpendo.00015.2013.
38. Galbiatti AL, Caldas HC, Maniglia JV, Pavarino EC, Goloni-Bertollo EM. Gene expression profile of 5-fluorouracil metabolic enzymes in laryngeal cancer cell line: predictive parameters for response to 5 fluorouracil based chemotherapy. Biomed Pharmacother. 2014;68(5):515–9. doi:10.1016/j.biopha.2014.03.015.
39. Klinger B, Sieber A, Fritsche-Guenther R, Witzel F, Berry L, Schumacher D, et al. Network quantification of EGFR signaling unveils potential for targeted combination therapy. Mol Syst Biol. 2013;9:673. doi:10.1038/msb.2013.29.
40. Moustakas A. Smad signalling network. J Cell Sci. 2002;115(17):3355–6.
41. Kong FM, Ao X, Wang L, Lawrence TS. The use of blood biomarkers to predict radiation lung toxicity: a potential strategy to individualize thoracic radiation therapy. Cancer Control. 2008;15(2):140–50.
42. Friedman E, Gold LI, Klimstra D, Zeng ZS, Winawer S, Cohen A. High levels of transforming growth factor beta 1 correlate with disease progression in human colon cancer. Cancer Epidemiol Biomarkers Prev. 1995;4(5):549–54.
43. Raisch J, Darfeuille-Michaud A, Nguyen HT. Role of microRNAs in the immune system, inflammation and cancer. World J Gastroenterol. 2013;19(20):2985–96. doi:10.3748/wjg.v19.i20.2985.
44. Liu J, Shi W, Wu C, Ju J, Jiang J. miR-181b as a key regulator of the oncogenic process and its clinical implications in cancer (Review). Biomed Rep. 2014;2(1):7–11. doi:10.3892/br.2013.199.
45. Yu X, Wu Y, Liu Y, Deng H, Shen Z, Xiao B, et al. miR-21, miR-106b and miR-375 as Novel Potential Biomarkers for Laryngeal Squamous Cell Carcinoma. Curr Pharm Biotechnol. 2014;15(5):503–8.
46. Yang TS, Yang XH, Chen X, Wang XD, Hua J, Zhou DL, et al. MicroRNA-106b in cancer-associated fibroblasts from gastric cancer promotes cell migration and invasion by targeting PTEN. FEBS Lett. 2014;588(13):2162–9. doi:10.1016/j.febslet.2014.04.050.
47. Fu X, Han Y, Wu Y, Zhu X, Lu X, Mao F, et al. Prognostic role of microRNA-21 in various carcinomas: a systematic review and meta-analysis. Eur J Clin Invest. 2011;41(11):1245–53. doi:10.1111/j.1365-2362.2011.02535.x.
48. Ma J, Liu J, Wang Z, Gu X, Fan Y, Zhang W, et al. NF-kappaB-dependent MicroRNA-425 upregulation promotes gastric cancer cell growth by targeting PTEN upon IL-1beta induction. Mol Cancer. 2014;13(1):40.
49. Liu S, Patel SH, Ginestier C, Ibarra I, Martin-Trevino R, Bai S, et al. MicroRNA93 regulates proliferation and differentiation of normal and malignant breast stem cells. PLoS Genet. 2012;8(6), e1002751. doi:10.1371/journal.pgen.1002751.
50. Fu X, Tian J, Zhang L, Chen Y, Hao Q. Involvement of microRNA-93, a new regulator of PTEN/Akt signaling pathway, in regulation of chemotherapeutic drug cisplatin chemosensitivity in ovarian cancer cells. FEBS Lett. 2012;586(9):1279–86. doi:10.1016/j.febslet.2012.03.006.
51. Sprio A, Di Scipio F, Ceppi P, Salamone P, Di Carlo F, Scagliotti G, et al. Differentiation-inducing factor-1 enhances 5-fluorouracil action on oral cancer cells inhibiting E2F1 and thymidylate synthase mRNAs accumulation. Cancer Chemother Pharmacol. 2012;69(4):983–9. doi:10.1007/s00280-011-1790-x.
52. Yan LH, Wang XT, Yang J, Kong FB, Lian C, Wei WY, et al. Reversal of multidrug resistance in gastric cancer cells by E2F-1 downregulation *in vitro* and *in vivo*. J Cell Biochem. 2014;115(1):34–41. doi:10.1002/jcb.24652.
53. Elliott MJ, Farmer MR, Atienza Jr C, Stilwell A, Dong YB, Yang HL, et al. E2F-1 gene therapy induces apoptosis and increases chemosensitivity in human pancreatic carcinoma cells. Tumour Biol. 2002;23(2):76–86.
54. Lee J, Park CK, Park JO, Lim T, Park YS, Lim HY, et al. Impact of E2F-1 expression on clinical outcome of gastric adenocarcinoma patients with adjuvant chemoradiation therapy. Clin Cancer Res. 2008;14(1):82–8. doi:10.1158/1078-0432.ccr-07-0612.
55. He S, Smith DL, Sequeira M, Sang J, Bates RC, Proia DA. The HSP90 inhibitor ganetespib has chemosensitizer and radiosensitizer activity in colorectal cancer. Invest New Drugs. 2014;32(4):577–86. doi:10.1007/s10637-014-0095-4.
56. Xue O, Sun K, Deng HJ, Lei ST, Dong JO, Li GX. Anti-miRNA-221 sensitizes human colorectal carcinoma cells to radiation by upregulating PTEN. World J Gastroenterol. 2013;19(48):9307–17. doi:10.3748/wjg.v19.i48.9307.
57. Budach W, Hehr T, Budach V, Belka C, Dietz K. A meta-analysis of hyperfractionated and accelerated radiotherapy and combined chemotherapy and radiotherapy regimens in unresected locally advanced squamous cell carcinoma of the head and neck. BMC Cancer. 2006;6:28. doi:10.1186/1471-2407-6-28.
58. Hess J, Thomas G, Braselmann H, Bauer V, Bogdanova T, Wienberg J, et al. Gain of chromosome band 7q11 in papillary thyroid carcinomas of young patients is associated with exposure to low-dose irradiation. Proc Natl Acad Sci U S A. 2011;108(23):9595–600. doi:10.1073/pnas.1017137108.
59. Hieber L, Huber R, Bauer V, Schaffner Q, Braselmann H, Thomas G, et al. Chromosomal rearrangements in post-Chernobyl papillary thyroid carcinomas: evaluation by spectral karyotyping and automated interphase FISH. J Biomed Biotechnol. 2011;2011:693691. doi:10.1155/2011/693691.
60. Hennel R, Brix N, Seidl K, Ernst A, Scheithauer H, Belka C, et al. Release of monocyte migration signals by breast cancer cell lines after ablative and fractionated gamma-irradiation. Radiat Oncol. 2014;9(1):85. doi:10.1186/1748-717x-9-85.
61. Dickson MA, Hahn WC, Ino Y, Ronfard V, Wu JY, Weinberg RA, et al. Human keratinocytes that express hTERT and also bypass a p16(INK4a)-enforced mechanism that limits life span become immortal yet retain normal growth and differentiation characteristics. Mol Cell Biol. 2000;20(4):1436–47.
62. Livak KJ, Schmittgen TD. Analysis of relative gene expression data using real-time quantitative PCR and the 2(-Delta Delta C(T)) Method. Methods. 2001;25(4):402–8. doi:10.1006/meth.2001.1262.
63. Bioconductor Open Source Software for Bioinformatics. http://www.bioconductor.org/. Accessed October 2013.
64. Smyth GK. limma: Linear Models for Microarray Data. In: Gentleman R, Carey V, Huber W, Irizarry R, Dudoit S, editors. Bioinformatics and Computational Biology Solutions Using R and Bioconductor. Statistics for Biology and Health. New York: Springer; 2005. p. 397–420.
65. yWorks - the diagramming company. http://www.yworks.com/en/products_yed_helpresources.html. Accessed October 2013.

66. The R Project for Statistical Computing. www.r-project.org. Accessed October 2013.
67. Shannon P, Markiel A, Ozier O, Baliga NS, Wang JT, Ramage D, et al. Cytoscape: a software environment for integrated models of biomolecular interaction networks. Genome Res. 2003;13(11):2498–504. doi:10.1101/gr.1239303.

Alle Additional files sind auf beiliegender CD verfügbar.

3 RESÜMEE UND AUSBLICK

Das Ziel der vorliegenden Arbeit war die Identifikation von miRNAs, die als Biomarker für eine Abschätzung der Prognose und den Therapieverlauf in der Radio(chemo)therapie von HNSCC (Plattenepithelkarzinom des Kopf-Hals Bereichs) Patienten genutzt werden können. Ein wesentlicher Vorteil von miRNA-Markern im Plasma gegenüber Markern im Tumorgewebe ist ihre minimalinvasive Zugänglichkeit. Die Ergebnisse dieser Arbeit zeigten, dass einige Plasma-miRNAs eine veränderte Expression nach radio(chemo)therapeutischer Behandlung aufweisen. Die Resultate wiesen zudem darauf hin, dass diese miRNAs die Antwort des Tumors auf die Therapie wiederspiegeln. Darüber hinaus konnte für fünf der Plasma-miRNAs eine Assoziation des Expressionslevels mit der lokoregionären Tumorkontrolle oder dem Überleben der Patienten nachgewiesen werden. Diese miRNAs sind somit vielversprechende Marker, die zur Stratifizierung von HNSCC Patienten genutzt werden können, um den individuellen Therapieerfolg zu prognostizieren und die Therapie gegebenenfalls individuell anzupassen.

Die Daten der vorliegenden Arbeit stellen die Grundlage für klinische Vorhersagen über den Erfolg einer Radio(chemo)therapie anhand von Plasma-miRNAs dar. Eine klinische Anwendung der nachgewiesenen prognostischen und Therapie-assoziierten miRNAs setzt jedoch deren Validierung in weiteren größeren unabhängigen Patientenkollektiven und eine Etablierung standardisierter Nachweisverfahren voraus. Darüber hinaus werden Analysen zum zeitlichen Verlauf der Marker-miRNA-Expression über den gesamten Zeitraum der Radio(chemo)therapie benötigt, um die Stabilität des Biomarkers im Verlauf der Therapie zu überprüfen. Da miRNAs von zahlreichen Faktoren, wie z. B. Ernährung, Nebenerkrankungen und anderen Stressoren, beeinflusst werden, muss die Stabilität der Marker-miRNAs im Plasma sichergestellt werden, um verlässliche Aussagen zu ermöglichen. Zudem sollten zusätzliche Analysen zum Ursprung der Marker-miRNAs im Plasma durchgeführt werden, da die hier gezeigten Resultate zwar einige indirekte Hinweise auf einen Tumorursprung dieser miRNAs liefern, wie z. B. der Nachweis der Expression aller Marker-miRNAs in Tumorbiopsien der Patienten, jedoch keinen direkten Nachweis des Ursprungs dieser miRNAs erbringen. Dafür sollten vergleichende miRNA-Expressionsanalysen an Tumorgewebe eines HNSCC Patientenkollektivs mit neoadjuvanter Radiochemotherapie vor einer Behandlung sowie an Tumorgewebe von Resektaten nach der Therapie durchgeführt werden. Dies würde die Identifikation von miRNAs ermöglichen, die sowohl im Plasma als auch im Tumorgewebe eine veränderte Expression nach Radiochemotherapie zeigen. Darüber hinaus kann im Zellkulturmodell mittels qRT-PCR der miRNAs im Überstand überprüft werden, ob die hier identifizierten Marker-miRNAs nach

simulierter Radiochemotherapie von HNSCC Zellen sezerniert werden, was die Hypothese eines Tumorursprungs der Marker-miRNAs im Plasma stützen würde.

Neben ihrer Funktion als Biomarker können miRNAs, die eine Therapieantwort zeigen, auch zur Identifikation potenzieller therapeutischer Zielstrukturen genutzt werden. Die Resultate der vorliegenden Arbeit deuten darauf hin, dass die Therapie-assoziierten miRNAs im Plasma der HNSCC Patienten die Therapieantwort des Tumors reflektieren und sogar vom Tumor in die Zirkulation gelangen. Dies lässt vermuten, dass diese miRNAs molekulare Prozesse regulieren, die die Therapiesensitivität des Tumors beeinflussen. Mithilfe eines integrativen Ansatzes wurde in der vorliegenden Arbeit die molekulare Therapieantwort zweier primärer HNSCC Zellkulturen exemplarisch charakterisiert. Eine Integration der miRNA-Daten, mRNA-Daten und der damit assoziierten molekularen Prozesse ermöglichte die Identifikation potenzieller therapeutischer Zielstrukturen. Es konnte gezeigt werden, dass Signalwege wie das *PTEN/AKT Signaling* und das *E2F transcription factor network*, eine wichtige Rolle in der Therapieantwort spielen. Eine Deregulation dieser Signalwege, auf mRNA- oder miRNA-Ebene stellt somit einen möglichen Ansatz dar die Therapie zu optimieren. Ein aktuelles Projekt, welches in großem Umfang molekulare Veränderungen in HNSCC zur Identifikation von Stratifizierungsmarkern und potenziellen therapeutischen Zielstrukturen analysierte, ist *The Cancer Genome Atlas* (TCGA) [33]. Dabei wurden die Daten von 500 HNSCC Fällen von mehreren molekularen Ebenen, wie Kopienzahlveränderungen, miRNA- und mRNA-Daten sowie klinischen Parametern in einem integrativen Ansatz zusammengeführt. In dieser Studie wurden neben den zentralen molekularen Markern *PIK3CA*, *TRAF3*, *CCND1*, *FADD*, *BIRC2* und *YAP1* auch Veränderungen der *E2F* Transkriptionsfaktoren und *PTEN*-assoziierte Signalwege als wichtige Veränderungen in HNSCC identifiziert. Basierend auf diesen Resultaten sollten im nächsten Schritt bereits bekannte *PTEN*-Inhibitoren, wie z. B. SF1670 [103], im HNSCC Zellkulturmodell eingesetzt werden, um Effekte auf das zelluläre Überleben und mögliche Auswirkungen auf die Sensitivität der Zellen gegenüber einer Radiochemotherapie zu analysieren. Einen weiteren Ansatz zur Überprüfung der Effekte einer gezielten molekularen Therapie stellt die Herunterregulierung von Zielgenen, wie z. B. *E2F* Transkriptionsfaktoren, mittels Transfektion der Zellen mit den bereits identifizierten regulatorischen miRNAs dar. In einem nächsten Schritt präklinischer Forschung sollten Mausmodelle eingesetzt werden, um weitere Hinweise auf eine mögliche klinische Nutzung der in der vorliegenden Arbeit identifizierten Zielgene und miRNAs als therapeutische Zielstrukturen zu erlangen. Durch Injektion humaner HNSCC Zellen in immunsupprimierte Mäuse können HNSCC Xenograft Tumore induziert werden. Zudem können orthotope Mausmodelle für eine genauere Abbildung der Tumorbiologie eingesetzt werden. Neue Technologien, wie die *Small Animal*

Radiation Research Platform (SARRP) [104] ermöglichen unter Verwendung integrierter bildgebender Verfahren eine präzise und reproduzierbare Bestrahlung von Kleintieren und somit eine sehr gute Simulation einer den aktuellen Standards entsprechenden Radiotherapie in der Klinik. Mithilfe dieser Techniken können die Tumore in den Mausmodellen einer simulierten Radiochemotherapie unterzogen werden. Durch Verabreichung der potenziell therapeutischen miRNAs oder direkter Signalwegsinhibitoren, wie z. B. *PTEN*-Inhibitoren, während der Radiochemotherapie kann deren Einfluss auf das Tumorvolumen sowie auf das Überleben der Mäuse untersucht werden.

Die Anwendung von miRNAs als therapeutische Zielstrukturen setzt eine eingehende funktionelle Analyse im Zellkulturmodell und im Mausmodell voraus, da eine miRNA meist zahlreiche Zielgene reguliert, wodurch unerwünschte Nebeneffekte auftreten können. Darüber hinaus ist für eine klinische Anwendung eine Optimierung der *in vivo* Transportsysteme für therapeutische miRNAs nötig, da unmodifizierte Nukleinsäuren eine geringe Lebensdauer aufweisen. Bei der Entwicklung dieser Transportvehikel stehen insbesondere die Spezifität für Tumorzellen, eine effektive Aufnahme in die Zielzellen sowie eine geringe Toxizität im Vordergrund. Neben den bereits bekannten Strategien mittels viraler Vektoren werden Lipidvesikel oder Polymer-Konstrukte sowie anorganische Nanopartikel als Transportsysteme untersucht [105].

Trotz der zahlreichen Herausforderungen bezüglich Gewebsspezifität, Abhängigkeit vom Krankheitsstatus oder Verabreichungsform, bergen miRNAs ein großes Potenzial zur klinischen Anwendung, was an der bereits in einer Phase 1 klinischen Studie befindlichen *miR-34* Familie [95] deutlich wird. Die Erforschung neuer Biomarker und molekularer Zielstrukturen ist für die Therapie von HNSCC Tumoren von großer Bedeutung, da die 5-Jahresüberlebensrate für HNSCC Patienten trotz der großen Fortschritte in der Weiterentwicklung der therapeutischen Maßnahmen erst bei ca. 65% liegt [5, 6]. Hinzu kommen unzureichende Erfolge bereits etablierter molekularer Therapien, wie die Inhibition von EGFR, die sich nur in bestimmten Patientengruppen mit einem spezifischen molekulargenetischen Hintergrund positiv auf den Therapieerfolg auswirkt [106]. Daher bedarf es neuer Stratifizierungsmarker und personalisierter Behandlungsstrategien basierend auf dem molekularen Profil des Tumors, um den notwendigen Fortschritt bei der Therapie von HNSCC zu erreichen.

4 LITERATURVERZEICHNIS

1. Parkin, D.M., F. Bray, J. Ferlay, et al. *Global Cancer Statistics, 2002.* CA Cancer J Clin, 2005. **55**(2): p. 74-108.
2. Warnakulasuriya, S. *Global epidemiology of oral and oropharyngeal cancer.* Oral Oncol, 2009. **45**(4–5): p. 309-316.
3. Jemal, A., F. Bray, M.M. Center, et al. *Global cancer statistics.* CA Cancer J Clin, 2011. **61**(2): p. 69-90.
4. Ferlay, J., I. Soerjomataram, M. Ervik, et al. *Cancer Incidence and Mortality Worldwide: IARC CancerBase No. 11.* GLOBOCAN 2012 v1.0, 2013.
5. Pulte, D. and H. Brenner *Changes in Survival in Head and Neck Cancers in the Late 20th and Early 21st Century: A Period Analysis.* The Oncologist, 2010. **15**(9): p. 994-1001.
6. Argiris, A., M.V. Karamouzis, D. Raben, et al. *Head and neck cancer.* Lancet, 2008. **371**(9625): p. 1695-709.
7. Ries LAG, M.D., Krapcho M, Mariotto A, Miller BA, Feuer EJ, Clegg L, Horner MJ, Howlader N, Eisner MP, Reichman M, Edwards BK *SEER Cancer Statistics Review, 1975–2004.* Bethesda, MD: National Cancer Institute, 2006.
8. Blot, W.J., J.K. McLaughlin, D.M. Winn, et al. *Smoking and drinking in relation to oral and pharyngeal cancer.* Cancer Res, 1988. **48**(11): p. 3282-7.
9. Warnakulasuriya, S. *Areca nut use following migration and its consequences.* Addict Biol, 2002. **7**(1): p. 127-32.
10. Pavia, M., C. Pileggi, C.G. Nobile, et al. *Association between fruit and vegetable consumption and oral cancer: a meta-analysis of observational studies.* Am J Clin Nutr, 2006. **83**(5): p. 1126-34.
11. Chuang, S.C., M. Jenab, J.E. Heck, et al. *Diet and the risk of head and neck cancer: a pooled analysis in the INHANCE consortium.* Cancer Causes Control, 2012. **23**(1): p. 69-88.
12. Gillison, M.L. *Current topics in the epidemiology of oral cavity and oropharyngeal cancers.* Head Neck, 2007. **29**(8): p. 779-92.
13. Shangina, O., P. Brennan, N. Szeszenia-Dabrowska, et al. *Occupational exposure and laryngeal and hypopharyngeal cancer risk in central and eastern Europe.* Am J Epidemiol, 2006. **164**(4): p. 367-75.
14. Langevin, S.M., M.H. O'Sullivan, J.L. Valerio, et al. *Occupational asbestos exposure is associated with pharyngeal squamous cell carcinoma in men from the greater Boston area.* Occup Environ Med, 2013. **70**(12): p. 858-63.
15. Yen, Y.C., C. Lin, S.W. Lin, et al. *Effect of metformin on the incidence of head and neck cancer in diabetics.* Head Neck, 2014.
16. Sandulache, V.C., J.S. Hamblin, H.D. Skinner, et al. *Association between metformin use and improved survival in patients with laryngeal squamous cell carcinoma.* Head Neck, 2014. **36**(7): p. 1039-1043.
17. Chaudhary, S.C., D. Kurundkar, C.A. Elmets, et al. *Metformin, an Antidiabetic Agent Reduces Growth of Cutaneous Squamous Cell Carcinoma by Targeting mTOR Signaling Pathway†.* Photochem Photobiol, 2012. **88**(5): p. 1149-1156.
18. Feng, Y., C. Ke, Q. Tang, et al. *Metformin promotes autophagy and apoptosis in esophageal squamous cell carcinoma by downregulating Stat3 signaling.* Cell Death Dis, 2014. **5**: p. e1088.
19. Cadoni, G., S. Boccia, L. Petrelli, et al. *A review of genetic epidemiology of head and neck cancer related to polymorphisms in metabolic genes, cell cycle control and alcohol metabolism.* Acta Otorhinolaryngol Ital, 2012. **32**(1): p. 1-11.

20. Khlifi, R., O. Messaoud, A. Rebai, et al. *Polymorphisms in the Human Cytochrome P450 and Arylamine N-Acetyltransferase: Susceptibility to Head and Neck Cancers.* Biomed Res Int, 2013. **2013**: p. 20.
21. Foulkes, W.D., J.S. Brunet, W. Sieh, et al. *Familial risks of squamous cell carcinoma of the head and neck: retrospective case-control study.* BMJ, 1996. **313**(7059): p. 716-21.
22. Trizna, Z. and S.P. Schantz *Hereditary and environmental factors associated with risk and progression of head and neck cancer.* Otolaryngol Clin North Am, 1992. **25**(5): p. 1089-103.
23. Kreimer, A.R., G.M. Clifford, P. Boyle, et al. *Human papillomavirus types in head and neck squamous cell carcinomas worldwide: a systematic review.* Cancer Epidemiol Biomarkers Prev, 2005. **14**(2): p. 467-75.
24. Huang, C.C., J.T. Qiu, M.L. Kashima, et al. *Generation of type-specific probes for the detection of single-copy human papillomavirus by a novel in situ hybridization method.* Mod Pathol, 1998. **11**(10): p. 971-977.
25. Gao, G., R.D. Chernock, H.A. Gay, et al. *A novel RT-PCR method for quantification of human papillomavirus transcripts in archived tissues and its application in oropharyngeal cancer prognosis.* Int J Cancer, 2013. **132**(4): p. 882-90.
26. Chaturvedi, A.K., E.A. Engels, R.M. Pfeiffer, et al. *Human papillomavirus and rising oropharyngeal cancer incidence in the United States.* J Clin Oncol, 2011. **29**(32): p. 4294-301.
27. D'Souza, G., A.R. Kreimer, R. Viscidi, et al. *Case-control study of human papillomavirus and oropharyngeal cancer.* N Engl J Med, 2007. **356**(19): p. 1944-1956.
28. Ghittoni, R., R. Accardi, U. Hasan, et al. *The biological properties of E6 and E7 oncoproteins from human papillomaviruses.* Virus Genes, 2010. **40**(1): p. 1-13.
29. Giarre, M., S. Caldeira, I. Malanchi, et al. *Induction of pRb degradation by the human papillomavirus type 16 E7 protein is essential to efficiently overcome p16INK4a-imposed G1 cell cycle Arrest.* J Virol, 2001. **75**(10): p. 4705-12.
30. Garbuglia, A.R. *Human papillomavirus in head and neck cancer.* Cancers (Basel), 2014. **6**(3): p. 1705-26.
31. Friedman, J.M., M.J. Stavas and A.J. Cmelak *Clinical and scientific impact of human papillomavirus on head and neck cancer.* World J Clin Oncol, 2014. **5**(4): p. 781-91.
32. Leemans, C.R., B.J. Braakhuis and R.H. Brakenhoff *The molecular biology of head and neck cancer.* Nat Rev Cancer, 2011. **11**(1): p. 9-22.
33. The Cancer Genome Atlas, N. *Comprehensive genomic characterization of head and neck squamous cell carcinomas.* Nature, 2015. **517**(7536): p. 576-582.
34. Smeets, S.J., B.J. Braakhuis, S. Abbas, et al. *Genome-wide DNA copy number alterations in head and neck squamous cell carcinomas with or without oncogene-expressing human papillomavirus.* Oncogene, 2006. **25**(17): p. 2558-64.
35. Ntziachristos, P., J.S. Lim, J. Sage, et al. *From fly wings to targeted cancer therapies: a centennial for notch signaling.* Cancer Cell, 2014. **25**(3): p. 318-34.
36. Agrawal, N., M.J. Frederick, C.R. Pickering, et al. *Exome sequencing of head and neck squamous cell carcinoma reveals inactivating mutations in NOTCH1.* Science, 2011. **333**(6046): p. 1154-7.
37. McCaul, J.A., K.E. Gordon, L.J. Clark, et al. *Telomerase inhibition and the future management of head-and-neck cancer.* Lancet Oncol, 2002. **3**(5): p. 280-288.
38. Lui, V.W., M.L. Hedberg, H. Li, et al. *Frequent mutation of the PI3K pathway in head and neck cancer defines predictive biomarkers.* Cancer Discov, 2013. **3**(7): p. 761-9.
39. Patel, S.G. and J.P. Shah *TNM Staging of Cancers of the Head and Neck: Striving for Uniformity Among Diversity.* CA Cancer J Clin, 2005. **55**(4): p. 242-258.
40. Sobin LH, G.M., Wittekind Ch, eds., *International Union Against Cancer (UICC) TNM Classification of Malignant Tumors.* 7th Edition ed. 2009: Wiley-Blackwell.

41. Ng, S.H., T.C. Yen, J.T. Chang, et al. *Prospective study of [18F]fluorodeoxyglucose positron emission tomography and computed tomography and magnetic resonance imaging in oral cavity squamous cell carcinoma with palpably negative neck.* J Clin Oncol, 2006. **24**(27): p. 4371-6.
42. Machiels, J.P., M. Lambrecht, F.X. Hanin, et al. *Advances in the management of squamous cell carcinoma of the head and neck.* F1000Prime Rep, 2014. **6**: p. 44.
43. Eisbruch, A., L.H. Marsh, M.K. Martel, et al. *Comprehensive irradiation of head and neck cancer using conformal multisegmental fields: assessment of target coverage and noninvolved tissue sparing.* Int J Radiat Oncol Biol Phys, 1998. **41**(3): p. 559-68.
44. Bourhis, J., J. Overgaard, H. Audry, et al. *Hyperfractionated or accelerated radiotherapy in head and neck cancer: a meta-analysis.* Lancet, 2006. **368**(9538): p. 843-54.
45. Yamazaki, H., M. Ogita, K. Himei, et al. *Hypofractionated stereotactic radiotherapy using CyberKnife as a boost treatment for head and neck cancer, a multi-institutional survey: impact of planning target volume.* Anticancer Res, 2014. **34**(10): p. 5755-9.
46. May, J.T., N. Rao, R.D. Sabater, et al. *Intensity-modulated radiation therapy as primary treatment for oropharyngeal squamous cell carcinoma.* Head Neck, 2013. **35**(12): p. 1796-800.
47. Cohen, E.E., M.W. Lingen and E.E. Vokes *The expanding role of systemic therapy in head and neck cancer.* J Clin Oncol, 2004. **22**(9): p. 1743-52.
48. Georges, P., K. Rajagopalan, C. Leon, et al. *Chemotherapy advances in locally advanced head and neck cancer.* World J Clin Oncol, 2014. **5**(5): p. 966-72.
49. Pendleton, K.P. and J.R. Grandis *Cisplatin-Based Chemotherapy Options for Recurrent and/or Metastatic Squamous Cell Cancer of the Head and Neck.* Clin Med Insights Ther, 2013. **2013**(5).
50. Pui, C.H. and M.V. Relling *Can the genotoxicity of chemotherapy be predicted?* Lancet, 2004. **364**(9438): p. 917-8.
51. Loong, H.H., E. Winquist, J. Waldron, et al. *Phase 1 study of nab-paclitaxel, cisplatin and 5-fluorouracil as induction chemotherapy followed by concurrent chemoradiotherapy in locoregionally advanced squamous cell carcinoma of the oropharynx.* Eur J Cancer, 2014. **50**(13): p. 2263-70.
52. Peitzsch, C., R. Perrin, R.P. Hill, et al. *Hypoxia as a biomarker for radioresistant cancer stem cells.* Int J Radiat Biol, 2014. **90**(8): p. 636-52.
53. Perri, F., R. Pacelli, G. Della Vittoria Scarpati, et al. *Radioresistance in head and neck squamous cell carcinoma: Biological bases and therapeutic implications.* Head Neck, 2014.
54. Karamouzis, M.V., J.R. Grandis and A. Argiris *Therapies directed against epidermal growth factor receptor in aerodigestive carcinomas.* JAMA, 2007. **298**(1): p. 70-82.
55. Jenab-Wolcott, J. and B.J. Giantonio *Bevacizumab: current indications and future development for management of solid tumors.* Expert Opin Biol Ther, 2009. **9**(4): p. 507-17.
56. Khan, A.J., B.L. King, B.D. Smith, et al. *Characterization of the HER-2/neu oncogene by immunohistochemical and fluorescence in situ hybridization analysis in oral and oropharyngeal squamous cell carcinoma.* Clin Cancer Res, 2002. **8**(2): p. 540-8.
57. Gandhi, M.D. and M. Agulnik *Targeted treatment of head and neck squamous-cell carcinoma: potential of lapatinib.* Onco Targets Ther, 2014. **7**: p. 245-51.
58. Simpson, D.R., L.K. Mell and E.E. Cohen *Targeting the PI3K/AKT/mTOR pathway in squamous cell carcinoma of the head and neck.* Oral Oncol, 2014.
59. Yadav, A., B. Kumar, T.N. Teknos, et al. *Sorafenib enhances the antitumor effects of chemoradiation treatment by downregulating ERCC-1 and XRCC-1 DNA repair proteins.* Mol Cancer Ther, 2011. **10**(7): p. 1241-51.
60. Biomarkers_Definitions_Working_Group *Biomarkers and surrogate endpoints: preferred definitions and conceptual framework.* Clin Pharmacol Ther, 2001. **69**(3): p. 89-95.

61. de Gramont, A., S. Watson, L.M. Ellis, et al. *Pragmatic issues in biomarker evaluation for targeted therapies in cancer.* Nat Rev Clin Oncol, 2014.
62. Sethi, S., S. Ali, P. Philip, et al. *Clinical Advances in Molecular Biomarkers for Cancer Diagnosis and Therapy.* Int J Mol Sci, 2013. **14**(7): p. 14771-14784.
63. Arantes, L.M., A.C. de Carvalho, M.E. Melendez, et al. *Methylation as a biomarker for head and neck cancer.* Oral Oncol, 2014. **50**(6): p. 587-92.
64. Nordsmark, M., S.M. Bentzen, V. Rudat, et al. *Prognostic value of tumor oxygenation in 397 head and neck tumors after primary radiation therapy. An international multi-center study.* Radiother Oncol, 2005. **77**(1): p. 18-24.
65. Chung, C.H., K. Ely, L. McGavran, et al. *Increased epidermal growth factor receptor gene copy number is associated with poor prognosis in head and neck squamous cell carcinomas.* J Clin Oncol, 2006. **24**(25): p. 4170-6.
66. Klinger, B., A. Sieber, R. Fritsche-Guenther, et al. *Network quantification of EGFR signaling unveils potential for targeted combination therapy.* Mol Syst Biol, 2013. **9**: p. 673.
67. Burtness, B., J.E. Bauman and T. Galloway *Novel targets in HPV-negative head and neck cancer: overcoming resistance to EGFR inhibition.* Lancet Oncol, 2013. **14**(8): p. e302-9.
68. Chen, J., J. Zhou, J. Lu, et al. *Significance of CD44 expression in head and neck cancer: a systemic review and meta-analysis.* BMC Cancer, 2014. **14**: p. 15.
69. Yang, Q.Q. and Y.F. Deng *Long non-coding RNAs as novel biomarkers and therapeutic targets in head and neck cancers.* Int J Clin Exp Pathol, 2014. **7**(4): p. 1286-92.
70. Ganci, F., A. Sacconi, V. Manciocco, et al. *microRNAs expression predicts local recurrence risk in oral squamous cell carcinoma.* Head Neck, 2014.
71. Alexander, R.P., G. Fang, J. Rozowsky, et al. *Annotating non-coding regions of the genome.* Nat Rev Genet, 2010. **11**(8): p. 559-71.
72. Saxena, A. and P. Carninci *Long non-coding RNA modifies chromatin: epigenetic silencing by long non-coding RNAs.* Bioessays, 2011. **33**(11): p. 830-9.
73. Tang, J.Y., J.C. Lee, Y.T. Chang, et al. *Long noncoding RNAs-related diseases, cancers, and drugs.* ScientificWorldJournal, 2013. **2013**: p. 943539.
74. Huntzinger, E. and E. Izaurralde *Gene silencing by microRNAs: contributions of translational repression and mRNA decay.* Nat Rev Genet, 2011. **12**(2): p. 99-110.
75. Lee, R.C., R.L. Feinbaum and V. Ambros *The C. elegans heterochronic gene lin-4 encodes small RNAs with antisense complementarity to lin-14.* Cell, 1993. **75**(5): p. 843-54.
76. *miRBase: the microRNA database*. Available from: www.miRbase.org.
77. Friedman, R.C., K.K.-H. Farh, C.B. Burge, et al. *Most mammalian mRNAs are conserved targets of microRNAs.* Genome Res, 2009. **19**(1): p. 92-105.
78. Zhao, Y. and D. Srivastava *A developmental view of microRNA function.* Trends Biochem Sci, 2007. **32**(4): p. 189-97.
79. Krol, J., I. Loedige and W. Filipowicz *The widespread regulation of microRNA biogenesis, function and decay.* Nat Rev Genet, 2010. **11**(9): p. 597-610.
80. Bartel, D.P. *MicroRNAs: target recognition and regulatory functions.* Cell, 2009. **136**(2): p. 215-33.
81. Grimson, A., K.K.-H. Farh, W.K. Johnston, et al. *MicroRNA Targeting Specificity in Mammals: Determinants beyond Seed Pairing.* Molecular Cell, 2007. **27**(1): p. 91-105.
82. Pasquinelli, A.E. *MicroRNAs and their targets: recognition, regulation and an emerging reciprocal relationship.* Nat Rev Genet, 2012. **13**(4): p. 271-82.
83. Leung, A.K.L. and P.A. Sharp *microRNAs: A Safeguard against Turmoil?* Cell, 2007. **130**(4): p. 581-585.
84. Esteller, M. *Non-coding RNAs in human disease.* Nat Rev Genet, 2011. **12**(12): p. 861-74.
85. Deng, G. and G. Sui *Noncoding RNA in oncogenesis: a new era of identifying key players.* Int J Mol Sci, 2013. **14**(9): p. 18319-49.

86. Di Leva, G., M. Garofalo and C.M. Croce *MicroRNAs in cancer.* Annu Rev Pathol, 2014. **9**: p. 287-314.
87. Calin, G.A. and C.M. Croce *MicroRNA signatures in human cancers.* Nat Rev Cancer, 2006. **6**(11): p. 857-866.
88. Gandellini, P., T. Rancati, R. Valdagni, et al. *miRNAs in tumor radiation response: bystanders or participants?* Trends Mol Med, 2014. **20**(9): p. 529-39.
89. Hansen, T.F., A.L. Carlsen, N.H. Heegaard, et al. *Changes in circulating microRNA-126 during treatment with chemotherapy and bevacizumab predicts treatment response in patients with metastatic colorectal cancer.* Br J Cancer, 2015. **112**(4): p. 624-9.
90. Xiao-chun, W., W. Wei, Z. Zhu-Bo, et al. *Overexpression of miRNA-21 promotes radiation-resistance of non-small cell lung cancer.* Radiat Oncol, 2013. **8**(1): p. 146.
91. Babu, J.M., R. Prathibha, V.S. Jijith, et al. *A miR-centric view of head and neck cancers.* Biochim Biophys Acta, 2011. **1816**(1): p. 67-72.
92. Courthod, G., P. Franco, L. Palermo, et al. *The role of microRNA in head and neck cancer: current knowledge and perspectives.* Molecules, 2014. **19**(5): p. 5704-16.
93. Zacharewicz, E., S. Lamon and A.P. Russell *MicroRNAs in skeletal muscle and their regulation with exercise, ageing, and disease.* Front Physiol, 2013. **4**: p. 266.
94. Ross, S.A. and C.D. Davis *MicroRNA, nutrition, and cancer prevention.* Adv Nutr, 2011. **2**(6): p. 472-85.
95. Agostini, M. and R.A. Knight *miR-34: from bench to bedside.* Oncotarget, 2014. **5**(4): p. 872-81.
96. Chen, X., Y. Ba, L. Ma, et al. *Characterization of microRNAs in serum: a novel class of biomarkers for diagnosis of cancer and other diseases.* Cell Res, 2008. **18**(10): p. 997-1006.
97. Selth, L.A., W.D. Tilley and L.M. Butler *Circulating microRNAs: macro-utility as markers of prostate cancer?* Endocr Relat Cancer, 2012. **19**(4): p. R99-R113.
98. Cortez, M.A., C. Bueso-Ramos, J. Ferdin, et al. *MicroRNAs in body fluids--the mix of hormones and biomarkers.* Nat Rev Clin Oncol, 2011. **8**(8): p. 467-77.
99. Hsu, C.M., P.M. Lin, Y.M. Wang, et al. *Circulating miRNA is a novel marker for head and neck squamous cell carcinoma.* Tumour Biol, 2012. **33**(6): p. 1933-42.
100. Heneghan, H.M., N. Miller, A.J. Lowery, et al. *Circulating microRNAs as novel minimally invasive biomarkers for breast cancer.* Ann Surg, 2010. **251**(3): p. 499-505.
101. Cui, W., J. Ma, Y. Wang, et al. *Plasma miRNA as biomarkers for assessment of total-body radiation exposure dosimetry.* PLoS One, 2011. **6**(8): p. e22988.
102. Zhao, L., W. Liu, J. Xiao, et al. *The role of exosomes and "exosomal shuttle microRNA" in tumorigenesis and drug resistance.* Cancer Lett, 2015. **356**(2 Pt B): p. 339-46.
103. Spinelli, L., Y.E. Lindsay and N.R. Leslie *PTEN inhibitors: an evaluation of current compounds.* Adv Biol Regul, 2015. **57**: p. 102-11.
104. Wong, J., E. Armour, P. Kazanzides, et al. *High-resolution, small animal radiation research platform with x-ray tomographic guidance capabilities.* Int J Radiat Oncol Biol Phys, 2008. **71**(5): p. 1591-9.
105. Zhang, Y., Z. Wang and R.A. Gemeinhart *Progress in microRNA delivery.* J Control Release, 2013. **172**(3): p. 962-74.
106. Moon, C., Y.K. Chae and J. Lee *Targeting epidermal growth factor receptor in head and neck cancer: lessons learned from cetuximab.* Exp Biol Med (Maywood), 2010. **235**(8): p. 907-20.

5 DANKSAGUNG

Mein besonderer Dank gilt Herrn Prof. Dr. Horst Zitzelsberger für die sehr gute Betreuung, die großartige Unterstützung unter schwierigen Umständen und das außerordentliche Engagement für einen erfolgreichen Abschluss meines Promotionsprojektes.

Des Weiteren möchte ich mich ganz herzlich bei meinen Kolleginnen und Kollegen in der Abteilung für Strahlenzytogenetik für die gute Zusammenarbeit und jegliche Unterstützung bedanken.

Insbesondere gilt mein Dank Dr. Julia Heß für ihre stets außergewöhnliche Hilfsbereitschaft und ihren unermüdlichen fachlichen und moralischen Beistand.

Ein großes Dankeschön geht an dieser Stelle auch an Dr. Kristian Unger, Herbert Braselmann, Laura Dajka, Randolph Caldwell, Steffen Heuer, Dr. Ludwig Hieber, Aaron Selmeier, Claire Innerlohinger, Elke Konhäuser, Adriana Pitea, Martin Selmansberger, Sebastian Kuger und Dr. Verena Zangen. Darüber hinaus möchte ich mich besonders bei Daniel Piehlmaier, Christina Wilke und Ludmila Schneider für die schöne Zeit während und neben der Arbeitszeit bedanken.

Außerdem bedanke ich mich bei Prof. Dr. Kirsten Lauber, Dr. Maximilian Niyazi, Dr. Lars Schüttrumpf und Maya Flieger, sowie bei Prof. Dr. Gabriele Multhoff, Dr. Thomas Schmid und Eva Sage.

Auch bei den Kolleginnen und Kollegen des Instituts für Strahlenbiologie bedanke ich mich für die Zusammenarbeit, insbesondere bei Dr. Anne Völler, Dr. Ines Höfig, Dr. Alfred Ahne, Stefanie Winkler und Lisa Mutschelknaus.

Ganz besonders herzlich möchte ich mich bei Klaudia Winkler bedanken, die nicht nur stets ein offenes Ohr für jegliche Fragen im Laboralltag hatte, sondern auch eine sehr wichtige moralische Stütze für mich in allen Höhen und Tiefen meiner Doktorandenzeit war.

Ein riesiges Dankeschön geht an meine lieben (Zimmer-)Kollegen, Dr. Arundhathi Sriharshan, Basti Busch, Sabine Richter, Vanja Radulovic und Theresa Heider für den unverzichtbaren moralischen Beistand und die wundervolle Bereicherung meiner Zeit während und neben der Arbeit.

Ganz herzlich möchte ich mich bei meinen Eltern, meinem Bruder und meinem Freund Stefan für die ausnahmslose Unterstützung auf meinem Weg bedanken.

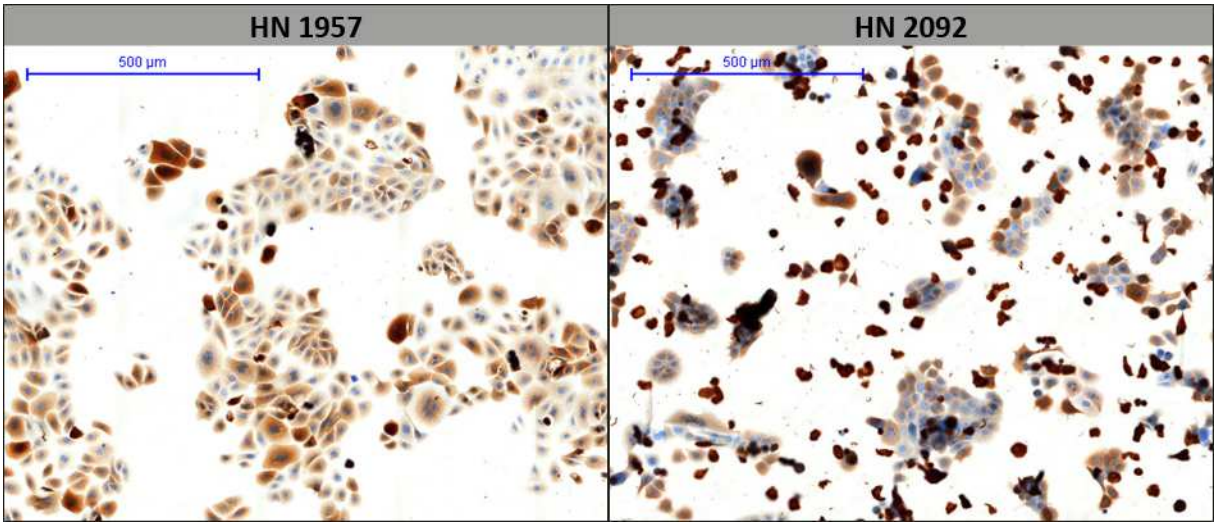

Additional file 1 Immunohistochemical cytokeratin-staining of primary HNSCC cell cultures. The positive cytokeratin-staining confirms the epithelial origin of the tumor cells.

Additional file 2 Therapy-responsive microRNAs in plasma samples of 18 head and neck cancer patients

miRNA	number of patients with ≥ 2 fold up-regulation	number of patients with ≥ 2 fold down-regulation	*p* value
miR-590-5p	1	11	0.021
miR-574-3p	1	7	0.043
miR-425-5p	2	9	0.048
miR-885-3p	0	7	0.048
miR-21-5p	3	10	0.054
miR-106b-5p	2	6	0.067
miR-28-3p	0	5	0.074
miR-223-5p	1	5	0.081
miR-195-5p	2	8	0.119
miR-191-5p	3	9	0.142
miR-93-5p	8	5	0.154
miR-29c-3p	2	7	0.181
miR-25-3p	5	3	0.196
miR-486-3p	7	3	0.196
miR-197-3p	1	5	0.212
miR-222-3p	1	7	0.212
let-7g-5p	0	3	0.304
miR-146b-5p	3	6	0.304
let-7b-5p	2	8	0.325
miR-628-5p	1	6	0.325
miR-146a-5p	5	7	0.347
miR-381-3p	0	4	0.347
miR-26b-5p	3	6	0.370
miR-374b-5p	3	4	0.370
miR-140-5p	3	5	0.393
miR-885-5p	3	6	0.393
miR-26a-5p	3	5	0.417
miR-19a-3p	3	5	0.442
miR-30c-5p	4	2	0.442
miR-454-3p	3	5	0.442
miR-186-5p	4	6	0.468
miR-483-5p	1	5	0.468
miR-92a-3p	6	6	0.523
miR-150-5p	7	5	0.523
miR-323-3p	3	2	0.609
miR-29a-3p	4	3	0.671

miR-320a	5	4	0.671
miR-451a	5	3	0.671
miR-24-3p	5	6	0.702
miR-19b-3p	5	4	0.766
miR-126-3p	3	5	0.766
miR-20b-5p	4	5	0.799
let-7e-5p	5	3	0.832
miR-17-5p	4	5	0.832
miR-30b-5p	6	5	0.832
miR-122-5p	3	4	0.832
miR-199a-3p	3	4	0.832
miR-106a-5p	3	5	0.932
miR-486-5p	5	5	0.932
miR-16-5p	5	4	0.966
miR-20a-5p	5	6	0.966
miR-142-3p	5	7	0.966
miR-484	6	5	0.966
miR-342-3p	3	4	1

Additional file 3 Correlation coefficients of normalized Ct values (ΔCt) of plasma miRNAs analyzed with arrays and single assays

	Correlation coefficient (*p* value)	
miRNA	**ΔCt values prior to treatment**	**ΔCt values post treatment**
miR-590-5p	0.56 (0.029)	0.85 (0.001)
miR-574-3p	0.75 (0.000)	0.75 (0.000)
miR-425-5p	-0.06 (0.842)	0.71 (0.003)
miR-885-3p	-0.13 (0.652)	0.00 (--------)
miR-21-5p	0.55 (0.034)	0.42 (0.122)
miR-28-3p	0.83 (0.000)	0.85 (0.000)
miR-195-5p	0.49 (0.061)	0.69 (0.004)
miR-191-5p	0.91 (0.000)	0.92 (0.000)
miR-150-5p	0.79 (0.001)	0.65 (0.009)
miR-142-3p	0.63 (0.012)	0.45 (0.094)

Additional file 4 Correlation coefficients of normalized Ct values (ΔCt) of miRNAs analyzed with TaqMan single assays in PBMC and plasma

miRNA	Correlation coefficient (*p* value)	
	ΔCt values prior to treatment	ΔCt values post treatment
miR-574-3p	0.47 (0.109)	0.32 (0.294)
miR-425-5p	0.28 (0.350)	0.00 (0.997)
miR-21-5p	0.24 (0.429)	-0.09 (0.770)
miR-28-3p	0.50 (0.083)	0.30 (0.317)
miR-195-5p	0.36 (0.231)	-0.05 (0.871)
miR-191-5p	0.23 (0.459)	0.13 (0.676)
miR-150-5p	0.43 (0.141)	0.38 (0.206)
miR-142-3p	0.14 (0.652)	0.11 (0.712)

PBMC = peripheral blood mononuclear cells

Additional file 5 Significantly deregulated microRNAs in HN1957 primary cell cultures after *in vitro* radiochemotherapy

miRNA	fold change	*p* value	adjusted *p* value
miR-181a-3p	6.71	0.002	0.018
miR-7-1-3p	6.09	0.002	0.018
miR-181a-2-3p	6.08	0.000	0.003
miR-454-3p	3.39	0.020	0.059
miR-335-5p	3.18	0.019	0.059
miR-362-5p	2.77	0.026	0.069
miR-29b-1-5p	1.95	0.000	0.006
miR-182-5p	1.83	0.015	0.055
miR-23a-5p	1.74	0.000	0.001
miR-20a-3p	1.65	0.011	0.045
miR-4298	1.62	0.001	0.010
miR-224-5p	1.56	0.037	0.086
miR-221-5p	1.55	0.004	0.026
miR-19b-1-5p	1.53	0.010	0.042
miR-148b-3p	1.46	0.012	0.045
miR-181a-5p	1.40	0.000	0.000
miR-455-5p	1.38	0.005	0.027
miR-642b-3p	1.36	0.004	0.027
miR-21-3p	1.34	0.000	0.009
miR-30a-3p	1.33	0.001	0.013
miR-4261	1.32	0.026	0.069
miR-181b-5p	1.31	0.000	0.000
miR-23a-3p	1.27	0.005	0.027
miR-155-5p	1.27	0.013	0.047
miR-425-5p	1.27	0.004	0.026
miR-1280_v18.0	1.25	0.001	0.013
miR-98-5p	1.24	0.019	0.059
miR-30e-5p	1.23	0.001	0.010
miR-1274b_v16.0	1.23	0.009	0.041
miR-7-5p	1.21	0.011	0.044
miR-342-3p	1.21	0.008	0.039
miR-331-3p	1.20	0.020	0.060
miR-151a-5p	1.20	0.009	0.041
miR-203a	1.19	0.028	0.071
miR-138-5p	1.18	0.027	0.071
miR-200a-3p	1.18	0.008	0.040
miR-205-3p	1.17	0.000	0.006

miR-301a-3p	1.17	0.044	0.099
miR-125a-5p	1.17	0.021	0.061
let-7f-5p	1.16	0.009	0.040
miR-423-5p	1.15	0.001	0.011
miR-151a-3p	1.15	0.001	0.010
miR-1260a	1.15	0.002	0.018
miR-200b-3p	1.15	0.002	0.018
miR-4306	1.15	0.012	0.045
miR-503-5p	1.15	0.018	0.058
miR-30d-5p	1.14	0.002	0.018
miR-31-5p	1.13	0.001	0.010
let-7b-5p	1.13	0.020	0.059
miR-17-3p	1.13	0.006	0.030
miR-31-3p	1.12	0.005	0.027
let-7a-5p	1.11	0.021	0.061
miR-21-5p	1.11	0.031	0.076
miR-1274a_v16.0	1.11	0.000	0.007
miR-320e	1.11	0.001	0.011
miR-29b-3p	1.11	0.003	0.024
miR-17-5p	1.09	0.019	0.059
miR-106b-5p	0.95	0.042	0.095
miR-125b-5p	0.94	0.028	0.072
miR-92a-3p	0.92	0.022	0.061
miR-93-5p	0.92	0.023	0.063
miR-141-3p	0.92	0.032	0.076
miR-22-3p	0.91	0.012	0.045
miR-18a-5p	0.90	0.010	0.041
miR-320b	0.90	0.020	0.059
miR-24-3p	0.89	0.016	0.055
miR-25-3p	0.88	0.007	0.037
miR-1260b	0.87	0.001	0.010
miR-3911	0.84	0.014	0.050
miR-1914-3p	0.80	0.017	0.056
miR-2861	0.76	0.029	0.072
miR-638	0.75	0.023	0.063
miR-3125	0.75	0.021	0.061
miR-940	0.75	0.008	0.040
miR-1305	0.74	0.018	0.058
miR-572	0.72	0.035	0.083
miR-3198	0.71	0.009	0.040
miR-1288	0.69	0.005	0.027

miR-575	0.67	0.003	0.020
miR-324-3p	0.65	0.000	0.010
miR-630	0.63	0.008	0.040
miR-4299	0.58	0.000	0.000
miR-1973	0.53	0.027	0.071
miR-1275	0.53	0.002	0.018
miR-1225-5p	0.52	0.004	0.025
miR-3663-3p	0.50	0.016	0.056
miR-4313	0.47	0.040	0.091
miR-513a-5p	0.42	0.003	0.021
miR-494	0.41	0.010	0.042
miR-188-5p	0.32	0.032	0.077
miR-3652	0.29	0.032	0.076
miR-513b	0.19	0.002	0.016
miR-135a-3p	0.12	0.004	0.026

Additional file 6 Significantly deregulated microRNAs in HN2092 primary cell cultures after *in vitro* radiochemotherapy

miRNA	fold change	*p* value	adjusted *p* value
miR-193a-5p	1.66	0.000	0.000
miR-7-5p	1.59	0.000	0.000
miR-532-5p	1.46	0.014	0.040
miR-30e-3p	1.40	0.001	0.005
miR-181a-5p	1.38	0.000	0.000
miR-224-3p	1.35	0.003	0.012
miR-181b-5p	1.31	0.000	0.000
miR-4298	1.30	0.003	0.012
miR-1274b_v16.0	1.26	0.000	0.000
miR-21-3p	1.19	0.000	0.000
miR-584-5p	1.19	0.013	0.038
miR-17-3p	1.19	0.001	0.003
miR-183-5p	1.18	0.000	0.001
miR-30a-3p	1.18	0.000	0.002
miR-3653	1.18	0.000	0.002
miR-151a-3p	1.17	0.000	0.000
miR-101-3p	1.17	0.006	0.021
miR-197-3p	1.17	0.008	0.025
miR-452-5p	1.16	0.000	0.000
miR-320e	1.16	0.000	0.000
miR-30e-5p	1.15	0.000	0.000
miR-18b-5p	1.15	0.003	0.012
miR-182-5p	1.15	0.004	0.013
miR-33a-5p	1.15	0.021	0.055
miR-186-5p	1.15	0.035	0.083
miR-30d-5p	1.15	0.000	0.001
miR-320a	1.14	0.000	0.000
miR-454-3p	1.14	0.040	0.093
miR-149-5p	1.14	0.003	0.011
miR-378_v17.0	1.14	0.000	0.000
miR-335-5p	1.14	0.029	0.071
miR-99b-5p	1.13	0.000	0.000
miR-1274a_v16.0	1.13	0.000	0.002
miR-320d	1.12	0.002	0.008
miR-4286	1.12	0.001	0.004
miR-1280_v18.0	1.11	0.028	0.070
miR-362-5p	1.11	0.022	0.058

miR-128	1.11	0.036	0.085
miR-222-3p	1.10	0.001	0.006
miR-151a-5p	1.10	0.000	0.000
miR-98-5p	1.10	0.007	0.023
miR-320c	1.10	0.003	0.012
let-7f-5p	1.09	0.041	0.095
miR-20b-5p	1.09	0.029	0.071
miR-1260a	1.08	0.000	0.002
miR-423-5p	1.08	0.011	0.031
miR-15a-5p	1.08	0.009	0.027
miR-148b-3p	1.08	0.011	0.032
miR-17-5p	1.07	0.002	0.008
miR-125a-5p	1.06	0.002	0.009
miR-130b-3p	1.06	0.017	0.046
miR-19a-3p	1.06	0.015	0.041
miR-3651	1.06	0.005	0.019
miR-455-3p	1.05	0.029	0.071
miR-193b-3p	1.05	0.003	0.012
miR-30a-5p	1.04	0.008	0.025
miR-96-5p	0.97	0.037	0.085
miR-30b-5p	0.97	0.043	0.098
miR-93-5p	0.96	0.001	0.003
let-7i-5p	0.95	0.027	0.070
miR-100-5p	0.94	0.009	0.027
miR-135b-5p	0.93	0.002	0.009
miR-29c-3p	0.92	0.026	0.067
miR-3659	0.91	0.036	0.085
miR-3656	0.90	0.009	0.028
miR-1202	0.88	0.005	0.019
miR-4284	0.87	0.002	0.008
miR-762	0.85	0.006	0.022
miR-494	0.84	0.017	0.046
miR-3665	0.83	0.000	0.003
miR-3911	0.83	0.000	0.000
miR-939-5p	0.81	0.000	0.000
miR-4281	0.81	0.001	0.005
miR-1207-5p	0.80	0.000	0.002
miR-3679-5p	0.80	0.010	0.030
miR-324-3p	0.79	0.002	0.008
miR-940	0.79	0.002	0.008
miR-1972	0.78	0.001	0.004

miR-3663-3p	0.77	0.003	0.012
miR-1915-3p	0.76	0.000	0.000
miR-575	0.76	0.000	0.002
miR-1275	0.76	0.000	0.000
miR-4299	0.75	0.000	0.001
miR-638	0.73	0.000	0.000
miR-1225-5p	0.73	0.000	0.000
miR-630	0.72	0.000	0.001
miR-513a-5p	0.68	0.001	0.005
miR-2861	0.65	0.000	0.001
miR-150-3p	0.64	0.023	0.060
miR-572	0.63	0.000	0.000
miR-16-2-3p	0.60	0.004	0.014
miR-15b-3p	0.56	0.006	0.021
miR-188-5p	0.50	0.000	0.003
miR-513b	0.33	0.000	0.002
miR-1181	0.29	0.009	0.027

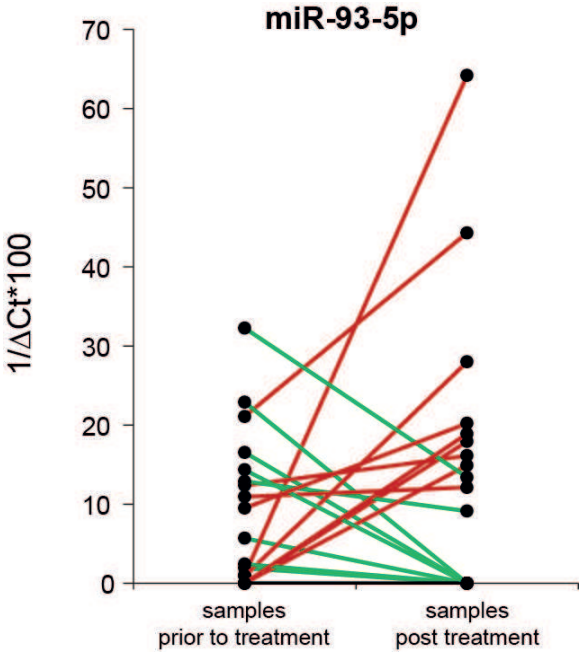

Additional file 7 Expression levels of miR-93-5p in plasma of 18 head and neck cancer patients prior and post treatment. Green lines mark down-regulation, red lines show up-regulation of the plasma miRNA.

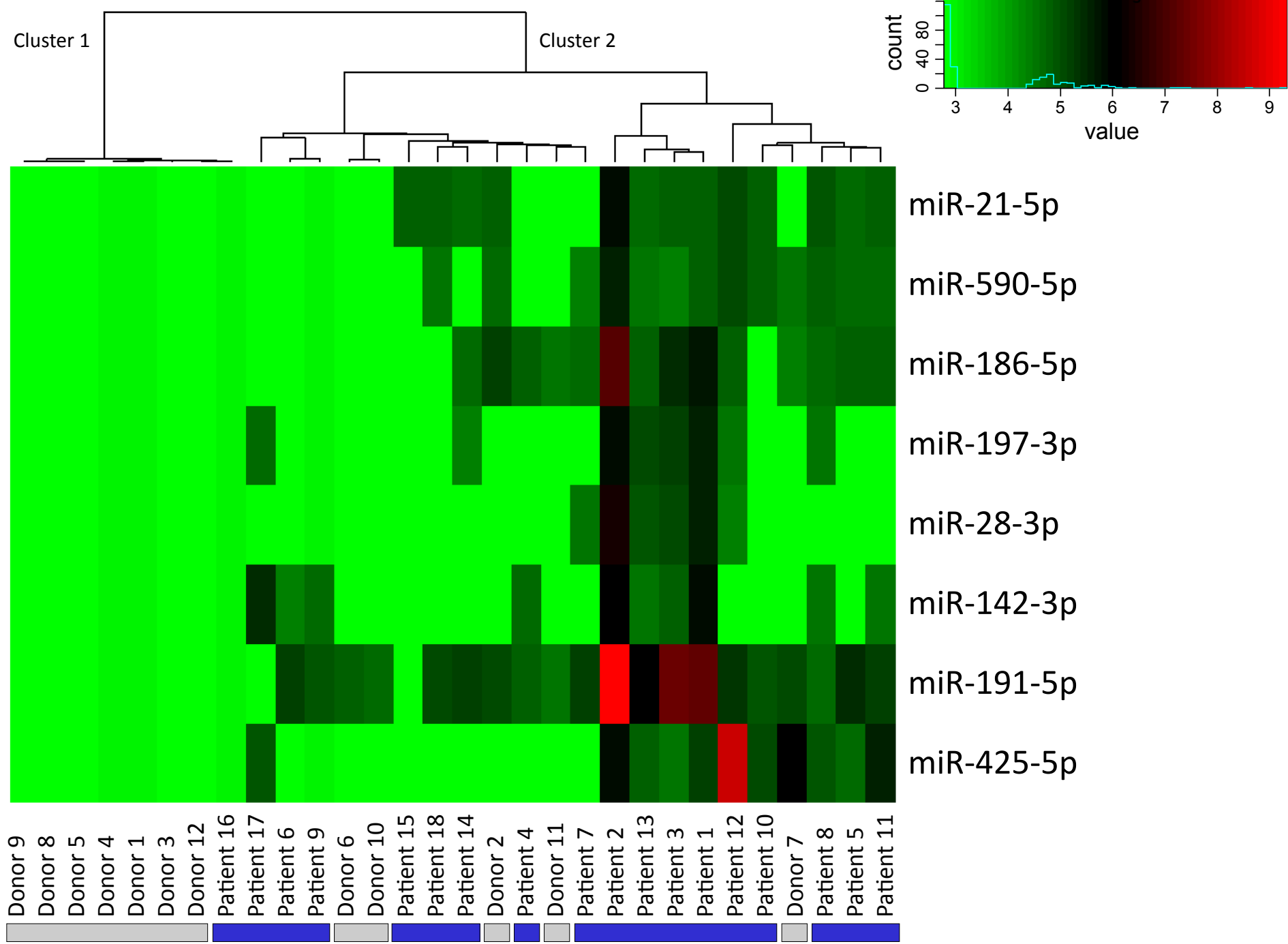

Supplementary Fig. 1 Unsupervised hierarchical cluster analysis of HNSCC patient samples collected before therapy and samples of healthy donors. Expression values of the plasma miRNAs were determined with TaqMan arrays. Patient samples collected prior to treatment are marked with blue bars, healthy donor samples are marked with grey bars. Cluster 1 and Cluster 2 indicate the two main clusters emerging from unsupervised cluster analysis using expression levels of the top eight distinctive miRNAs.

Supplementary Table 1 Patient-specific microRNAs in plasma samples of 18 HNSCC patients compared to 12 healthy controls analyzed with TaqMan arrays

miRNA	Normalized Ct values in plasma of HNSCC patients [mean ± SEM]	Normalized Ct values in plasma of healthy controls [mean ± SEM]	p value
miR-21-5p	5.23 ± 1.55	13.78 ± 1.10	0.001
miR-191-5p	0.86 ± 1.55	8.99 ± 1.95	0.001
miR-142-3p	6.98 ± 1.71	undetected	0.007
miR-197-3p	8.40 ± 1.69	undetected	0.007
miR-425-5p	6.14 ± 1.86	13.46 ± 1.41	0.019
miR-590-5p	6.47 ± 1.55	12.70 ± 1.38	0.022
miR-28-3p	9.81 ± 1.68	undetected	0.031
miR-186-5p	5.56 ± 1.73	11.46 ± 1.65	0.031
miR-24-3p	0.71 ± 1.28	5.32 ± 1.86	0.035
miR-126-3p	-1.08 ± 1.03	1.98 ± 1.61	0.039
miR-195-5p	7.33 ± 1.55	12.68 ± 1.41	0.039
miR-374b-5p	6.29 ± 2.31	13.79 ± 1.14	0.043
miR-16-5p	-5.39 ± 0.37	-4.10 ± 0.51	0.053
miR-26a-5p	6.54 ± 1.80	12.76 ± 1.35	0.053
let-7e-5p	8.88 ± 1.75	13.71 ± 1.18	0.065
miR-19b-3p	-3.46 ± 0.38	-2.32 ± 0.41	0.072
miR-106b-5p	7.57 ± 1.69	12.64 ± 1.42	0.072
miR-222-3p	-1.53 ± 0.43	0.90 ± 1.13	0.072
let-7g-5p	9.92 ± 1.67	undetected	0.079
miR-17-5p	-3.08 ± 0.47	-0.54 ± 1.27	0.079
miR-342-3p	5.64 ± 1.72	9.48 ± 1.79	0.087
miR-885-5p	5.11 ± 1.65	11.31 ± 1.70	0.087
miR-92a-3p	0.70 ± 1.23	3.63 ± 1.83	0.104
miR-146a-5p	0.26 ± 0.99	4.19 ± 1.72	0.104
miR-19a-3p	0.78 ± 1.18	3.59 ± 1.86	0.113
miR-320a	1.73 ± 1.65	2.22 ± 1.60	0.113
miR-106a-5p	-1.07 ± 1.36	-0.25 ± 1.37	0.124
miR-146b-5p	7.77 ± 1.95	12.68 ± 1.50	0.124
miR-483-5p	10.55 ± 1.55	undetected	0.146
miR-484	1.09 ± 1.52	3.86 ± 1.79	0.146
miR-486-5p	-3.93 ± 0.31	-3.09 ± 0.49	0.146
miR-26b-5p	5.31 ± 1.59	9.21 ± 1.88	0.172
miR-574-3p	8.12 ± 1.81	12.73 ± 1.38	0.172
let-7b-5p	3.51 ± 1.72	6.49 ± 1.99	0.200
miR-30c-5p	8.96 ± 1.75	11.71 ± 1.60	0.215
miR-323-3p	3.50 ± 1.65	3.93 ± 1.70	0.215

miR-454-3p	9.07 ± 1.70	12.54 ± 1.48	0.215
miR-885-3p	8.08 ± 2.10	11.59 ± 2.19	0.267
miR-140-5p	9.39 ± 1.60	11.48 ± 1.71	0.285
miR-29c-3p	5.61 ± 1.70	8.72 ± 2.00	0.325
miR-20a-5p	0.65 ± 1.49	1.42 ± 1.64	0.391
miR-628-5p	8.45 ± 1.90	11.07 ± 1.91	0.391
miR-30b-5p	6.75 ± 1.78	10.34 ± 1.77	0.415
miR-93-5p	8.56 ± 1.79	11.48 ± 1.71	0.465
miR-122-5p	6.12 ± 1.77	9.00 ± 1.89	0.518
miR-503-5p	12.88 ± 1.26	9.24 ± 1.98	0.545
miR-150-5p	4.05 ± 1.82	5.43 ± 1.81	0.632
miR-424-5p	10.80 ± 1.68	7.48 ± 2.16	0.632
miR-199a-3p	9.95 ± 1.64	11.43 ± 1.65	0.755
miR-20b-5p	7.39 ± 1.75	7.47 ± 2.08	0.787
miR-381-3p	7.30 ± 2.31	7.47 ± 2.47	0.851
miR-223-5p	-7.15 ± 0.76	-7.39 ± 1.30	0.884
miR-486-3p	7.22 ± 1.62	7.78 ± 1.94	0.884
miR-451a	2.35 ± 1.33	3.32 ± 1.88	0.917
miR-888-5p	11.43 ± 1.64	8.19 ± 2.34	0.917
miR-25-3p	8.89 ± 1.62	11.14 ± 1.80	0.950

SEM = standard error of the mean

Supplementary Table 2 Patient-specific plasma miRNAs in 15 HNSCC patients (discovery cohort) and 12 healthy donors analyzed with single assays

miRNA	Normalized Ct values in plasma of HNSCC patients [mean ± SEM]	Normalized Ct values in plasma of healthy controls [mean ± SEM]	p value
miR-21-5p	0.86 ± 0.54	5.24 ± 0.30	<0.001
miR-28-3p	10.22 ± 1.40	undetected	0.001
miR-126-3p	1.87 ± 0.68	6.19 ± 0.26	<0.001
miR-142-3p	5.76 ± 0.96	9.14 ± 0.26	0.006
miR-186-5p	7.43 ± 0.91	15.37 ± 0.58	<0.001
miR-191-5p	3.48 ± 0.83	8.64 ± 0.33	<0.001
miR-195-5p	11.98 ± 0.98	undetected	0.002
miR-197-3p	4.61 ± 0.65	9.01 ± 0.25	<0.001
miR-374b-5p	12.80 ± 1.32	undetected	0.046
miR-425-5p	5.85 ± 0.93	10.94 ± 0.72	<0.001
miR-590-5p	13.14 ± 1.14	undetected	0.040

SEM = standard error of the mean

Supplementary Table 3 Therapy-responsive miRNAs in plasma samples of 11 HNSCC patients (validation cohort)

miRNA	Number of patients with ≥ 1.33-fold upregulation	Number of patients with ≤ 0.75-fold downregulation
miR-21-5p	5	3
miR-28-3p	3	4
miR-93-5p	6	4
miR-142-3p	3	5
miR-150-5p	3	5
miR-191-5p	4	3
miR-195-5p	4	4
miR-425-5p	5	4
miR-574-3p	5	3

Supplementary Table 4 Patient-specific microRNAs in plasma samples of 11 HNSCC patients (validation cohort) compared to healthy donors

miRNA	Normalized Ct values in plasma of HNSCC patients [mean ± SEM]	Normalized Ct values in plasma of healthy controls [mean ± SEM]	p value
miR-21-5p	3.43 ± 0.32	5.24 ± 0.30	0.003
miR-28-3p	0.04 ± 0.30	undetected	<0.001
miR-126-3p	3.42 ± 0.38	6.19 ± 0.26	<0.001
miR-142-3p	5.59 ± 0.31	9.14 ± 0.26	<0.001
miR-186-5p	6.60 ± 0.37	15.37 ± 0.58	<0.001
miR-191-5p	5.34 ± 0.50	8.64 ± 0.33	<0.001
miR-195-5p	9.70 ± 1.06	undetected	0.001
miR-197-3p	6.18 ± 0.40	9.01 ± 0.25	<0.001
miR-374b-5p	10.21 ± 1.00	undetected	0.001
miR-425-5p	6.60 ± 0.37	10.94 ± 0.72	<0.001

SEM = standard error of the mean

Supplementary Table 5 Correlation of miRNA expression in FFPE-tumor-tissue and matched plasma of 14 HNSCC patients analyzed with single assays

miRNA	Pearson correlation coefficient	p value
miR-21-5p	0.13	0.65
miR-28-3p	-0.31	0.29
miR-126-3p	-0.21	0.47
miR-142-3p	-0.17	0.56
miR-186-5p	-0.15	0.62
miR-191-5p	0.21	0.48
miR-195-5p	-0.32	0.27
miR-197-3p	0.22	0.45
miR-374b-5p	-0.38	0.17
miR-425-5p	-0.01	0.96
miR-150-5p	0.06	0.84
miR-574-3p	0.21	0.46

Additional file 1 Copy number alterations in HN1957

Chromosome	Location	Start (bp)	End (bp)	Size (Mb)	Gain/loss
1	p31.3	64137196	64574378	437	Loss
1	q21.1	145009491	145291681	282	Loss
1	q21.2	147404182	149243878	1840	Loss
2	p22.3	34702900	34714858	12	Loss
2	p11.2 - 11.1	89427335	91815649	2388	Loss
2	q21.2	133817872	134013314	195	Loss
3	p26.3 - 11.1	73884	90282026	90208	Loss
5	p15.33 - 12	26112	45872739	45847	Gain
5	q35.3	177059894	178434885	1375	Loss
7	p22.3 - 11.2	830127	56021762	55192	Gain
8	p23.3 - 23.1	161442	7786619	7625	Loss
8	p11.22	39237408	39345390	108	Loss
8	q11.1 - 24.3	46943427	146294012	99351	Gain
9	p24.3 - q21.13	204163	75759274	75555	Gain
9	q21.13	75773390	75785187	12	Gain
9	q21.13 - 34.3	75793096	139521304	63728	Gain
10	p15.3 - 11.21	136331	37912674	37776	Loss
11	p15.5 - q25	210270	134927025	134717	Gain
12	p11.22 - q13.11	29394531	47149663	17755	Gain
13	q21.1 - 34	56908708	115105208	58197	Gain
15	q11.1 - 11.2	20102511	22409302	2307	Loss
15	q11.2 - 26.3	22425868	102480799	80055	Gain
16	p13.3 - q24.3	106241	90163040	90057	Gain
17	q11.1 - 25.3	25403416	81098955	55696	Gain
18	p11.32 - q23	118730	78009943	77891	Loss
20	p13 - q13.33	67748	62949060	62881	Gain
21	p11.2 - q11.2	9832418	15499817	5667	Loss
21	q11.2 - 21.1	15513138	17895158	2382	Gain
22	q11.21 - 12.1	17927733	28915008	10987	Gain
22	q12.2 - 13.33	31001795	51218920	20217	Gain

Additional file 2 Copy number alterations in HN2092

Chromosome	Location	Start (bp)	End (bp)	Size (Mb)	Gain/loss
1	p34.1	45638843	46411830	773	Loss
2	p11.2 - 11.1	89129502	91815649	2686	Loss
3	p26.3 - 14.2	73884	60431612	60358	Loss
3	p14.2	60445716	60856997	411	Loss
3	p14.2	60877532	61256461	379	Loss
3	p14.2 - 14.1	61279362	65309302	4030	Gain
3	p14.1 - 13	65329274	71064421	5735	Gain
3	p12.1	85375309	85527808	152	Loss
4	p16.3 - 11	45852	49032819	48987	Loss
4	q13.2	69392515	69438151	46	Gain
4	q32.1	159836338	160477505	641	Gain
5	p15.33 - 12	26112	45872739	45847	Gain
5	q15	92922745	92925263	3	Loss
7	q21.11 - 31.1	85927890	111030944	25103	Gain
7	q31.1	111044005	111303942	260	Gain
7	q31.1 - 31.31	111316562	120348264	9032	Gain
7	q31.31 - 36.3	120355583	159118477	38763	Loss
8	p23.3 - 23.2	161442	3379024	3218	Loss
8	p23.2	3395242	3614215	219	Loss
8	p23.2	3623018	4532958	910	Loss
8	p12 - 11.23	30428574	37449311	7021	Gain
8	p11.23 - 11.22	37498547	39222337	1724	Gain
8	p11.22	39237408	39345390	108	Loss
8	p11.22	39392445	39587449	195	Gain
8	p11.22 - q24.3	39607186	146294012	106687	Gain
9	p24.3 - q13	204163	68452996	68249	Loss
9	q21.11 - 34.3	70984451	141018895	70034	Gain
11	q13.2 - 25	68090440	134927025	66837	Gain
12	q21.31 - 24.33	83072415	133291385	50219	Gain
13	q11 - 14.3	19296514	51173255	31877	Loss
13	q14.3 - 31.2	51212860	89898466	38686	Gain
14	q11.2	19376732	20414143	1037	Loss
14	q11.2	20465917	22428569	1963	Loss
14	q11.2 - 12	23016509	25424295	2408	Loss
14	q12 - 24.3	25443991	75707870	50264	Gain
14	q24.3	75727607	78086326	2359	Gain
14	q24.3 - 32.33	78104995	107278681	29174	Gain
16	p13.3	6754631	6982630	228	Loss

16	p11.2 - q24.3	29652969	90163040	60510	Gain
17	q25.3	80111187	81098955	988	Loss
18	p11.32 - q23	118730	78009943	77891	Loss
19	q13.2 - 13.43	42737047	59092485	16355	Gain
20	p13 - q13.33	67748	62949060	62881	Gain
21	p11.2	9832418	15347165	5515	Loss
22	q11.23	24347929	24390165	42	Loss
22	q11.23 - 12.1	25664588	25911562	247	Loss

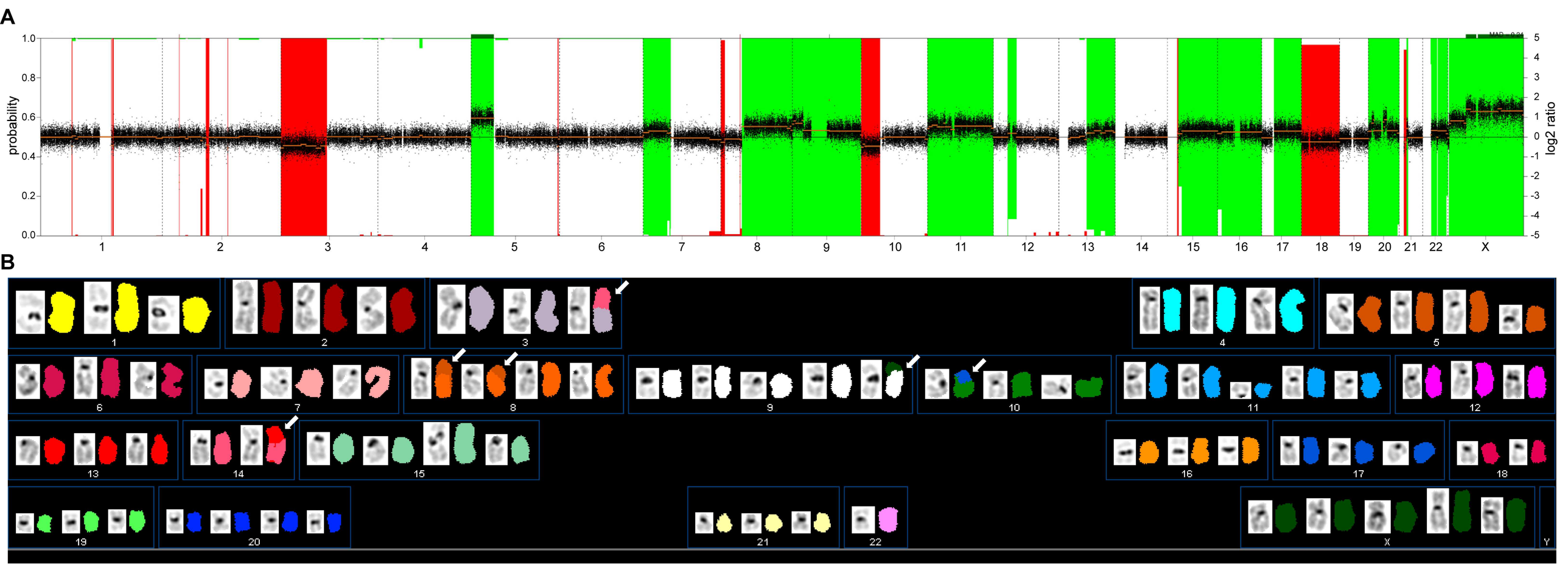

Cytogenetic characterization of HN1957. (A) The array CGH profile shows copy number alterations on several chromosomes. Green bars (top down) represent copy number gains at the corresponding position in the genome. Red bars (bottom up) indicate copy number losses. Bars reaching beyond the middle axis (probability >0.5) were called as gains or losses. (B) The spectral karyotype of a representative metaphase reveals various chromosomal alterations: 75,XX,+X,+2xdel(X)(p13→qter),+1,+2,+der(3)t(3;14)(p11→qter;qter→q11),+4,+5,+i(5)(p10),+6,+7,+2xder(8)t(5;8)(?;p10→qter),+2x9,+der(9)t(X;9)(?;p13→qter),+der(10)t(10;17)(p10→qter;qter→q10),+2x11,+del(11)(pter→q10?),+12,+13,der(14)t(13;14)(qter→q11;p11→qter),+15,+i(15)(q10),+16,+17,+19,+2x20,+21,i(22)(q10). White arrows indicate chromosomes with color junctions.

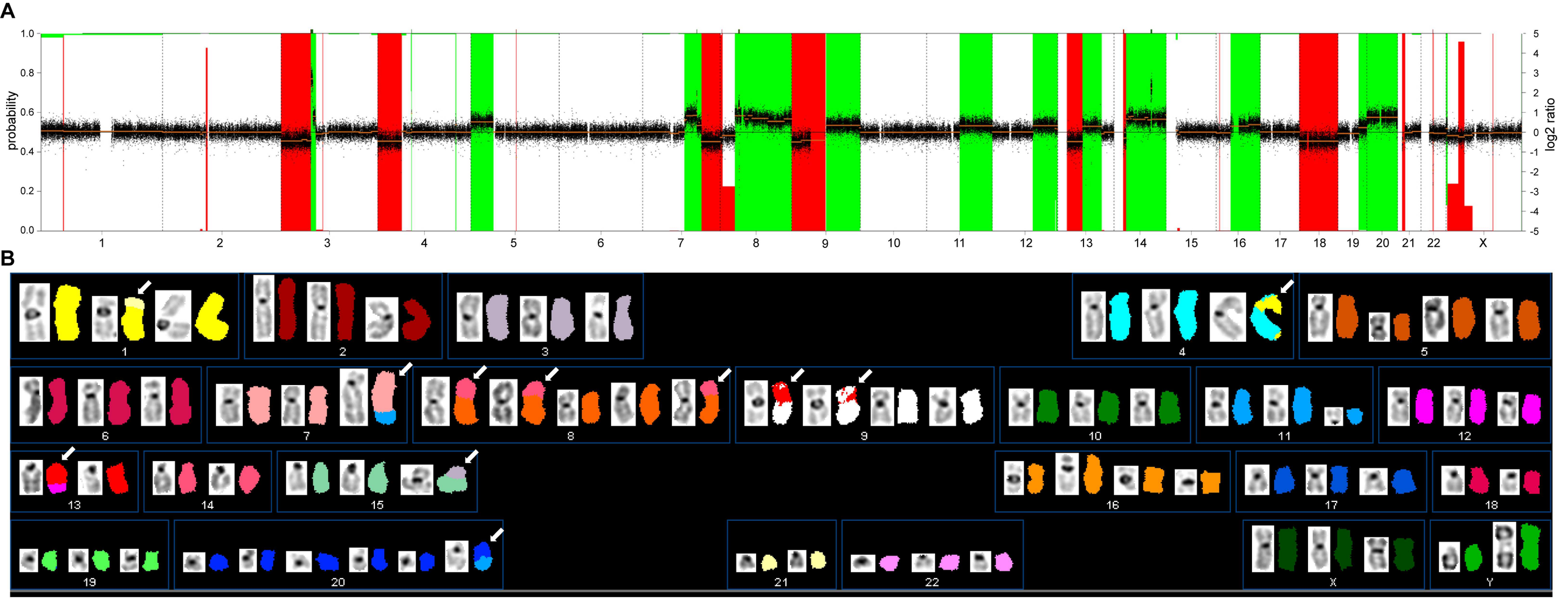

Cytogenetic characterization of HN2092. (A) The array CGH profile shows copy number alterations on several chromosomes. Green bars (top down) represent copy number gains at the corresponding position in the genome. Red bars (bottom up) indicate copy number losses. Bars reaching beyond the middle axis (probability >0.5) were called as gains or losses. (B) The spectral karyotype of a representative metaphase reveals various chromosomal alterations: 75,XY,+X,+del(X)(p21→pter),+i(X)(q10),+i(Y)(q10),+der(1)t(1;21)(p11→qter;qter→q11),+2,+3,+der(4)t(1;4)(pter→q21;?),+5,+i(5)(p10),+6,+der(7)add(7)(q31)t(7;11),+3xder(8)t(8;14)(p11→qter;qter→q11),+2xder(9)t(9;13)(p11→qter;qter→q14),+10,+del(11)(q11),+12,der(13)t(12;13)(?;p13→q22),+der(15)t(3;15)(?;p11→qter),+16,+der(16)(?),+17,+19,+3x20,+der(20)t(11;20)(?),+22. White arrows indicate chromosomes with color junctions.

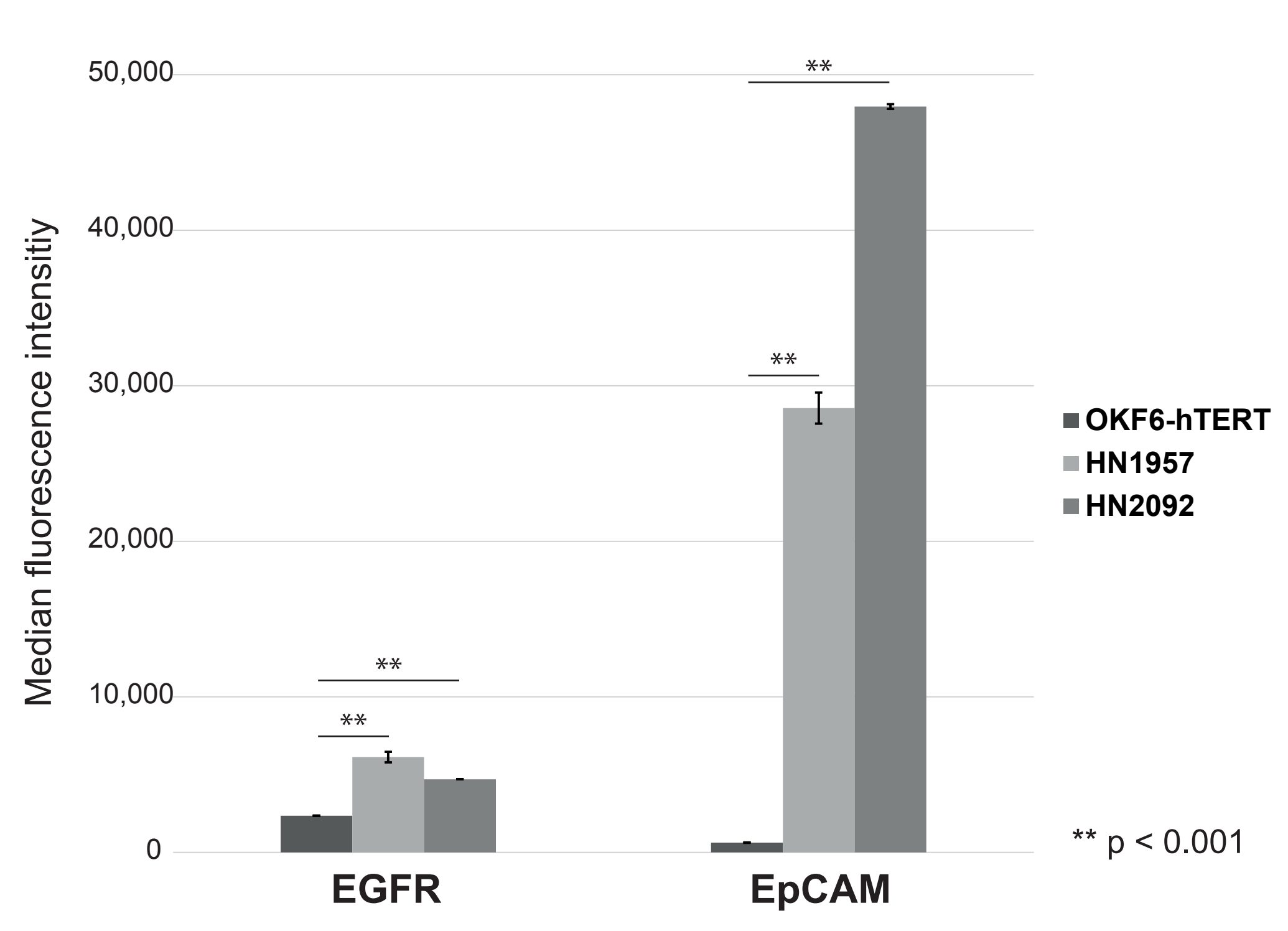
50,000
40,000
30,000
20,000
10,000
0
Median fluorescence intensitiy
**
**
**
**
OKF6-hTERT
HN1957
HN2092
** p < 0.001
EGFR
EpCAM

Additional file 6 Significantly deregulated mRNAs in HN1957 after radiochemotherapy treatment (adjusted p-value<0.05)

Gene	adjusted p-value	fold-change
TXNIP	6.35E-13	0.31
C8orf55	7.54E-12	2.19
RHBDF2	7.54E-12	1.96
IFIT1	7.54E-12	0.49
SNRPA1	7.54E-12	0.45
IFIT2	7.54E-12	0.31
SDF2L1	1.17E-11	1.91
OASL	1.17E-11	0.33
IL24	1.17E-11	0.28
MANF	1.27E-11	2.21
CTSC	1.84E-11	0.51
SLFN11	2.21E-11	2.13
IFRD1	2.23E-11	0.52
LHPP	2.62E-11	2.04
ARRDC4	2.62E-11	0.45
AGR2	2.81E-11	3.01
E2F2	3.08E-11	1.82
HMGA2	3.08E-11	0.46
GADD45A	3.94E-11	0.53
HSPA1A	4.72E-11	2.20
CALR	4.72E-11	1.81
RPL28	4.72E-11	0.45
TNFSF9	4.96E-11	2.25
KREMEN1	4.96E-11	1.79
INF2	7.46E-11	1.91
FADS2	8.67E-11	2.32
TET1	9.49E-11	2.36
C6orf48	9.49E-11	0.52
IFIT3	1.30E-10	0.50
HSPA1B	1.39E-10	1.96
DDX58	1.39E-10	0.52
BIRC3	1.39E-10	0.45
MVD	1.57E-10	2.31
FAM20C	1.65E-10	1.84
INSIG1	1.67E-10	2.32
LSS	1.67E-10	2.25
TMEM97	1.67E-10	2.01

OSBPL5	1.67E-10	1.95
CDK2AP2	1.67E-10	1.66
ANTXR2	1.67E-10	0.53
CH25H	1.67E-10	0.26
ABCB6	2.03E-10	1.66
ADAMTS6	2.03E-10	0.55
HIST1H2AG	2.65E-10	2.08
MEGF8	2.73E-10	1.89
LAMA3	2.77E-10	0.57
MAST1	2.95E-10	1.72
C6orf1	2.95E-10	1.58
IL23A	3.91E-10	0.58
HS3ST1	4.00E-10	0.60
ISG15	4.15E-10	0.64
TMEM79	4.15E-10	0.57
DDIT3	4.15E-10	0.52
B3GAT3	5.30E-10	1.55
COMTD1	5.34E-10	1.90
RGS2	5.34E-10	0.54
RUNX1	5.34E-10	0.45
PRR7	5.81E-10	1.63
HSP90B1	5.87E-10	1.67
CIDEC	6.29E-10	0.62
CRELD2	6.62E-10	1.69
PIF1	6.69E-10	1.71
TMEM187	6.91E-10	2.08
ETS2	7.04E-10	0.55
CMTM4	7.05E-10	1.61
ISG20	7.05E-10	0.64
SERPINB2	7.05E-10	0.39
PRMT7	7.26E-10	1.63
HR	7.26E-10	0.52
CBX6	7.35E-10	1.73
DUSP12	7.47E-10	0.63
ST6GALNAC2	7.97E-10	2.39
MYLK	8.49E-10	1.53
SEC24D	8.58E-10	1.82
CKLF	8.95E-10	1.61
FYB	8.95E-10	0.57
NLRP3	9.00E-10	0.53
LRP8	9.06E-10	1.93

PSKH1	1.04E-09	1.75
MYO5C	1.04E-09	1.73
NUAK2	1.04E-09	0.60
JDP2	1.10E-09	1.97
PLAU	1.10E-09	0.60
RPL10A	1.13E-09	1.47
HSD11B1	1.34E-09	0.48
XBP1	1.37E-09	1.68
BRD4	1.37E-09	0.66
NOG	1.37E-09	0.55
CELSR1	1.40E-09	1.55
FAM83A	1.40E-09	0.61
ANGPTL4	1.63E-09	0.61
DUX4	1.67E-09	1.60
PLEKHA6	1.81E-09	1.61
HTRA1	1.81E-09	1.58
PDLIM5	1.81E-09	0.69
BMP2	1.81E-09	0.65
UBAP1	1.81E-09	0.65
GADD45B	1.87E-09	0.57
PSAT1	2.08E-09	1.65
LAMB3	2.08E-09	0.60
SNN	2.16E-09	1.52
SP5	2.26E-09	1.62
C15orf42	2.26E-09	1.51
NKX2-5	2.29E-09	1.55
SGK1	2.29E-09	0.62
ZC3HAV1	2.31E-09	0.61
TST	2.39E-09	1.71
EDN1	2.42E-09	0.64
APOL6	2.66E-09	1.49
PCSK9	2.70E-09	1.80
HSD17B8	2.76E-09	1.55
BAIAP2	2.76E-09	0.69
SFI1	2.95E-09	1.64
C22orf40	3.22E-09	1.55
PSMG4	3.22E-09	1.50
IGFBP3	3.22E-09	0.59
NT5C3	3.24E-09	0.68
LFNG	3.29E-09	2.08
ZBED2	3.94E-09	0.61

RBM14	3.94E-09	0.63
B4GALNT1	4.01E-09	1.84
PHACTR3	4.04E-09	0.59
PHF13	4.10E-09	1.72
IMPA2	4.10E-09	1.61
TRAPPC9	4.45E-09	1.70
IDE	4.45E-09	1.54
PTGS2	4.45E-09	0.52
FGFR3	4.47E-09	1.66
METTL3	4.78E-09	1.53
ALDH4A1	5.06E-09	1.64
SYTL1	5.11E-09	1.57
TRIOBP	5.33E-09	1.82
MMD	5.33E-09	1.45
PNPLA3	5.42E-09	1.64
RNF145	5.49E-09	1.59
GTPBP5	5.49E-09	0.66
RTN4R	5.52E-09	1.56
EVL	5.66E-09	1.46
SPTLC2	5.84E-09	1.72
PRDM1	5.84E-09	0.51
FXYD3	6.19E-09	0.60
IDH1	6.45E-09	1.45
ASF1B	6.71E-09	1.64
PLAUR	6.71E-09	0.56
FGD3	6.83E-09	1.69
CYP27B1	6.83E-09	0.50
TUFT1	6.94E-09	0.70
RNF43	6.94E-09	0.63
TMEM40	6.96E-09	0.59
ANKRD52	7.00E-09	1.54
HES2	7.00E-09	0.64
C12orf23	7.11E-09	1.47
PTPN18	7.28E-09	1.43
HSPA8	7.77E-09	1.56
SLC6A9	7.80E-09	1.56
MYEOV	7.80E-09	0.63
CALB1	7.80E-09	0.60
LEPREL2	7.98E-09	1.55
HYAL2	7.98E-09	1.47
CYP27C1	8.23E-09	0.63

ATG16L2	8.46E-09	1.58
SERPINE1	8.57E-09	0.52
SLC48A1	8.79E-09	1.42
VEGFC	8.85E-09	0.69
IBA57	9.07E-09	0.55
CBX2	1.02E-08	1.54
PGLS	1.03E-08	1.49
ELFN2	1.03E-08	1.48
HSPG2	1.08E-08	1.64
PMAIP1	1.09E-08	0.60
SPC25	1.11E-08	1.54
MOB3B	1.11E-08	0.67
B9D1	1.12E-08	1.42
CAMKK1	1.14E-08	1.84
DUX4L4	1.14E-08	1.72
APOBEC3F	1.17E-08	1.58
NLRP2	1.18E-08	1.46
INHBA	1.18E-08	0.55
ANP32E	1.22E-08	1.56
TRIM8	1.25E-08	0.66
PANK1	1.30E-08	1.76
ZNF502	1.41E-08	0.64
HMGCR	1.42E-08	1.57
EVI5L	1.44E-08	1.80
SLC17A5	1.44E-08	1.54
LMNB1	1.44E-08	1.51
HES6	1.48E-08	1.57
HSBP1L1	1.50E-08	0.66
TMBIM4	1.51E-08	1.42
ADAMTS1	1.51E-08	0.61
IL1A	1.55E-08	0.66
NUDT8	1.60E-08	1.55
ARHGAP27	1.60E-08	0.69
MVK	1.68E-08	1.57
ITFG3	1.68E-08	1.43
MICA	1.72E-08	1.46
SMARCC2	1.72E-08	1.42
FADS1	1.72E-08	1.60
PCYOX1L	1.83E-08	1.46
HIST1H4L	1.88E-08	1.45
DHCR7	1.93E-08	1.49

SMOX	1.93E-08	0.63
MRPS30	1.98E-08	0.68
VNN1	2.00E-08	0.64
MCM6	2.05E-08	1.45
FLRT3	2.13E-08	0.62
XXYLT1	2.17E-08	1.45
FAT1	2.17E-08	0.70
ACP1	2.18E-08	0.68
C12orf34	2.18E-08	1.46
C16orf7	2.18E-08	1.58
TNFAIP3	2.20E-08	0.51
WWC3	2.21E-08	1.48
NFKBIL1	2.23E-08	1.60
NUCB2	2.30E-08	1.51
NSDHL	2.31E-08	1.51
IL1RL1	2.33E-08	0.49
TRIB1	2.35E-08	0.60
TLCD1	2.35E-08	1.50
OSBPL7	2.39E-08	1.50
BTG1	2.48E-08	0.64
CARS	2.50E-08	1.44
HMGCS1	2.52E-08	1.60
MAOA	2.52E-08	0.68
TMEM143	2.54E-08	1.57
ELOVL6	2.55E-08	1.50
CREB3L2	2.55E-08	1.48
FBLN1	2.59E-08	1.46
SNCA	2.61E-08	1.51
NECAB3	2.67E-08	1.49
D2HGDH	2.68E-08	1.55
IRAK2	2.70E-08	0.58
DUSP4	2.71E-08	0.70
SLC16A5	2.74E-08	1.50
FAM206A	2.74E-08	0.69
TTC9C	2.74E-08	0.69
IL11	2.74E-08	0.61
DNAJB9	2.79E-08	1.61
SUV420H1	2.79E-08	0.66
FN1	2.79E-08	0.57
RNPEPL1	2.88E-08	1.42
NEDD4L	2.97E-08	0.69

TSTD2	3.02E-08	0.67
CAMKK2	3.03E-08	1.48
ASB13	3.23E-08	1.45
FOSL1	3.31E-08	0.66
UGDH	3.35E-08	1.53
SEC24C	3.35E-08	1.45
IRS2	3.50E-08	0.62
CCNE2	3.52E-08	1.42
CRYL1	3.55E-08	1.52
TRMT61A	3.55E-08	0.61
CALHM3	3.60E-08	1.84
PCK2	3.60E-08	1.71
FSTL3	3.60E-08	0.67
MFSD3	3.66E-08	1.58
SMAD7	3.68E-08	0.65
BDKRB2	3.72E-08	1.41
CXCL1	3.82E-08	0.55
TOR2A	3.88E-08	1.62
COL13A1	3.98E-08	1.74
BIRC2	4.01E-08	0.66
TIMP4	4.01E-08	1.50
CC2D2A	4.01E-08	0.60
CNFN	4.07E-08	0.67
UPF3B	4.09E-08	0.62
DSCAM	4.13E-08	0.68
PCYT2	4.14E-08	1.47
RNF114	4.22E-08	0.67
UBAP2L	4.35E-08	1.53
TSPYL4	4.35E-08	0.70
CITED2	4.53E-08	0.68
CD274	4.63E-08	0.68
COL5A1	4.80E-08	1.56
RIOK3	4.94E-08	0.66
FLJ22184	5.08E-08	1.57
KLF4	5.10E-08	0.59
LIPE	5.18E-08	1.51
SERF2	5.18E-08	0.65
ACSS2	5.29E-08	1.61
FAM167A	5.44E-08	0.65
KDM4C	5.56E-08	0.69
OR51B5	6.07E-08	1.42

STMN1	6.24E-08	0.68
TCFL5	6.48E-08	1.64
PTPRK	6.48E-08	0.70
HCAR2	6.48E-08	0.63
HCAR3	6.49E-08	0.68
TIPARP	6.49E-08	0.67
TXNL4B	6.50E-08	0.60
AKR1B10	6.59E-08	1.57
ANKRD2	6.74E-08	1.42
BDH1	6.76E-08	1.42
KCNJ15	6.85E-08	0.67
NR3C1	6.93E-08	0.61
ACTR1B	7.19E-08	1.51
MSMO1	7.30E-08	1.46
TMEM129	7.38E-08	1.56
PSIP1	7.77E-08	1.55
GFOD1	7.85E-08	0.52
C20orf201	7.85E-08	1.76
INPP5A	7.86E-08	0.66
WIBG	7.96E-08	1.43
WWP2	8.13E-08	0.62
CALM3	8.55E-08	1.46
USO1	8.64E-08	1.45
JUN	8.66E-08	0.64
KHDRBS1	8.71E-08	1.46
MKRN1	8.78E-08	0.67
A2LD1	8.79E-08	1.47
TAF15	9.01E-08	1.80
AEN	9.01E-08	0.69
KRT6C	9.10E-08	0.67
PPP1R15A	9.24E-08	0.55
LOC728392	9.30E-08	1.65
GDF15	9.65E-08	1.44
RNF222	1.02E-07	1.97
PIR	1.02E-07	1.53
PLS3	1.03E-07	0.70
PLEKHJ1	1.04E-07	1.50
ABTB2	1.04E-07	0.68
HSD17B7	1.04E-07	1.43
AREG	1.04E-07	0.68
TMX4	1.07E-07	1.42

CALY	1.10E-07	1.62
RAB11FIP4	1.12E-07	1.52
C3orf52	1.12E-07	0.70
CERCAM	1.14E-07	1.48
SPRY2	1.14E-07	0.59
FLYWCH1	1.14E-07	1.55
EPPK1	1.14E-07	1.51
CDC42EP5	1.14E-07	1.48
ELL	1.14E-07	0.70
FAM55C	1.15E-07	1.44
SERINC1	1.15E-07	0.67
KCNE1L	1.15E-07	0.64
C6orf62	1.16E-07	1.48
SMG1	1.18E-07	0.67
ZNF488	1.24E-07	1.61
C11orf75	1.26E-07	1.69
KIAA0232	1.28E-07	1.56
EEF2K	1.30E-07	1.45
PER2	1.30E-07	0.69
BCL2L1	1.33E-07	0.64
ASB1	1.35E-07	0.69
HCFC1R1	1.36E-07	1.52
RPP30	1.44E-07	0.70
C14orf1	1.50E-07	1.42
C9orf69	1.50E-07	1.54
MKI67	1.51E-07	1.43
CCDC76	1.52E-07	0.70
SEMA4C	1.52E-07	1.45
SNAI2	1.55E-07	0.59
CEACAM1	1.59E-07	0.64
VSX1	1.59E-07	1.61
KAT7	1.61E-07	0.70
BATF2	1.61E-07	0.69
CSF2	1.62E-07	0.64
AKAP12	1.65E-07	0.69
UPP1	1.65E-07	0.65
MMP1	1.71E-07	0.59
ZC3HAV1L	1.79E-07	1.59
AMD1	1.85E-07	1.45
HCN2	1.87E-07	1.65
DNMT3B	1.87E-07	1.58

MICB	1.88E-07	1.51
LBR	1.97E-07	1.55
ZFC3H1	1.98E-07	1.45
UNKL	1.98E-07	1.73
HGSNAT	2.16E-07	1.48
IDH2	2.17E-07	1.48
LAMTOR2	2.20E-07	1.44
SPATA5L1	2.23E-07	0.70
BAMBI	2.32E-07	0.61
HBEGF	2.33E-07	0.60
NEDD9	2.38E-07	0.64
AKAP8L	2.40E-07	0.67
C12orf4	2.42E-07	0.70
CLMP	2.44E-07	0.68
ABL2	2.44E-07	0.62
AHNAK2	2.47E-07	0.70
FAM120B	2.58E-07	1.43
CDKN2D	2.62E-07	1.46
DOK7	2.62E-07	0.68
CCDC18	2.71E-07	1.56
HIST1H1A	2.75E-07	1.56
MAFB	2.87E-07	0.59
FDPS	2.92E-07	1.62
ERP27	2.93E-07	0.61
IGFLR1	2.93E-07	1.43
CHIC2	3.04E-07	0.63
PNLIPRP3	3.07E-07	0.67
IDI1	3.23E-07	1.49
GATSL3	3.33E-07	1.50
IL1R2	3.35E-07	0.59
ASNS	3.37E-07	1.57
ETS1	3.48E-07	0.68
DAPP1	3.52E-07	0.64
ABCB10	3.53E-07	1.48
NUDT18	3.56E-07	1.43
NDUFC2	3.81E-07	0.66
SLC25A38	3.83E-07	0.70
TREX1	3.91E-07	1.44
TM7SF2	3.92E-07	1.60
LSP1	4.00E-07	1.67
ZZZ3	4.02E-07	0.68

SMG7	4.17E-07	0.70
ANK3	4.31E-07	1.44
E2F1	4.33E-07	1.43
FOXP4	4.47E-07	1.44
MBOAT2	4.50E-07	0.71
ZFAND2A	4.70E-07	0.69
HDAC9	4.78E-07	0.57
RND3	4.78E-07	0.70
NFIC	4.84E-07	1.47
IP6K1	4.87E-07	1.54
CASP10	4.90E-07	0.67
ID1	4.91E-07	1.61
ELK3	4.95E-07	0.65
TPSG1	4.99E-07	1.42
REEP6	5.13E-07	1.45
RSF1	5.13E-07	0.68
LIMK1	5.21E-07	1.42
KPNA4	5.32E-07	0.71
COX19	5.76E-07	0.65
LY9	5.77E-07	1.56
IFITM10	5.95E-07	1.51
C17orf108	6.30E-07	1.70
CREB3L4	6.33E-07	1.51
SFXN5	6.43E-07	1.50
HIVEP3	6.44E-07	1.46
TSC22D1	6.44E-07	0.63
RALGDS	6.82E-07	1.52
GALR3	6.91E-07	1.57
HIST1H1B	6.96E-07	1.69
CD44	7.24E-07	0.67
KCTD19	7.33E-07	1.71
ITGA5	7.54E-07	0.70
NAV3	7.69E-07	0.64
GRHL3	7.80E-07	0.68
OSR2	7.82E-07	0.60
ZFP57	8.10E-07	0.67
IGF2	8.15E-07	0.69
CEBPD	8.16E-07	1.64
EIF4EBP2	8.16E-07	1.46
CYP1A1	8.16E-07	0.61
C19orf60	8.57E-07	1.47

RBM4	8.76E-07	0.69
ADA	9.48E-07	1.49
PRMT5	9.71E-07	0.70
PANK2	9.73E-07	0.69
WIPI1	9.93E-07	1.45
IFFO1	1.02E-06	0.68
RIMBP3	1.03E-06	1.46
C20orf160	1.16E-06	1.61
FBRSL1	1.17E-06	1.47
BTBD7	1.24E-06	0.70
HEXDC	1.26E-06	1.47
CISH	1.27E-06	1.49
AKAP2	1.29E-06	0.67
LRP3	1.31E-06	1.75
GJC2	1.31E-06	1.51
ACCN2	1.33E-06	1.48
CDKN2AIP	1.35E-06	0.70
RAB26	1.40E-06	1.61
TRAPPC6A	1.40E-06	1.48
C1orf116	1.42E-06	0.69
RNF32	1.46E-06	1.62
SMG9	1.46E-06	0.67
ARHGEF3	1.47E-06	0.69
SCG5	1.48E-06	0.65
DOCK4	1.53E-06	0.69
IL6	1.53E-06	0.56
DUSP10	1.59E-06	0.70
DST	1.60E-06	0.70
TMCO4	1.63E-06	1.45
ATF3	1.65E-06	0.66
LYNX1	1.70E-06	1.86
SFXN2	1.73E-06	1.44
SOCS3	1.80E-06	0.62
MAP1S	1.88E-06	1.49
MARCH4	1.93E-06	0.70
ZNF497	1.97E-06	1.79
EPHX2	2.01E-06	1.44
MON1B	2.03E-06	1.67
SMARCA2	2.05E-06	1.47
SDCBP2	2.11E-06	0.68
ARHGAP33	2.18E-06	1.54

KLHL21	2.19E-06	0.71
DIABLO	2.21E-06	1.48
EPHA4	2.24E-06	0.67
SPRR1B	2.31E-06	0.70
NOB1	2.32E-06	0.68
PTX3	2.37E-06	0.67
SYT12	2.56E-06	1.48
SGSM3	2.57E-06	1.42
AKR1B15	2.67E-06	1.43
ITGB2	2.67E-06	1.57
TMC8	2.74E-06	0.65
PEAR1	2.79E-06	0.70
ZCCHC2	2.83E-06	1.45
GATA3	2.86E-06	0.63
DGCR14	2.88E-06	0.70
JUNB	2.90E-06	0.70
CD59	2.95E-06	0.70
KCNQ2	2.98E-06	1.96
SYNGR4	2.98E-06	1.60
HAGHL	3.02E-06	1.42
SGK3	3.03E-06	1.59
TRAK2	3.04E-06	1.51
DNM1	3.27E-06	1.43
PRRG1	3.37E-06	0.63
IL37	3.50E-06	0.65
HIST1H1D	3.52E-06	1.44
SLC37A1	3.90E-06	1.42
LIMA1	4.06E-06	0.70
HMGB2	4.12E-06	1.43
HIST1H2AH	4.38E-06	1.43
PER1	4.38E-06	0.66
DNMBP	4.85E-06	0.66
GDA	4.97E-06	0.70
SERPINB7	5.17E-06	0.70
CD86	5.43E-06	1.81
STEAP4	5.81E-06	0.65
PNPLA2	6.17E-06	1.57
IQGAP3	6.61E-06	1.41
CSF3	6.76E-06	0.68
PI4K2B	7.03E-06	1.49
ACACB	7.88E-06	1.44

PFKL	8.67E-06	1.73
PARVB	8.67E-06	1.43
ZNF350	8.77E-06	0.70
HCN3	8.79E-06	1.47
IBTK	9.32E-06	1.43
EMILIN1	1.01E-05	1.61
AOX1	1.01E-05	0.65
RUSC1-AS1	1.09E-05	1.52
C11orf9	1.15E-05	1.54
RDM1	1.17E-05	1.54
HMG20B	1.30E-05	1.63
PHTF1	1.30E-05	1.44
CRCT1	1.34E-05	0.69
TMEM50B	1.37E-05	1.44
NFAT5	1.37E-05	0.66
ATXN10	1.42E-05	1.44
KLF5	1.43E-05	0.69
LHX3	1.48E-05	1.58
C16orf93	1.50E-05	1.45
NUPR1	1.85E-05	1.45
HMX1	1.92E-05	1.44
VGLL3	1.93E-05	0.61
RSAD2	2.18E-05	0.68
HERC5	2.29E-05	0.49
C1orf27	2.37E-05	0.67
NFKBIZ	2.41E-05	0.63
MOCOS	2.48E-05	1.50
CD70	2.63E-05	1.53
FICD	3.27E-05	1.42
ABCA1	3.27E-05	0.69
HIST1H2AL	3.36E-05	1.45
GPR150	3.70E-05	1.58
TINAGL1	3.98E-05	1.65
SCARF2	4.08E-05	1.48
HUS1B	4.19E-05	0.67
YJEFN3	4.62E-05	1.68
MED10	4.74E-05	0.71
PTMS	4.79E-05	1.44
LRRC45	4.83E-05	1.47
METTL7A	5.13E-05	1.62
RAVER1	5.58E-05	1.51

SBNO2	6.62E-05	1.43
TMEM52	7.14E-05	1.52
PCSK1N	9.27E-05	1.69
RBAK-LOC389458	9.28E-05	1.46
PKD1	9.53E-05	1.48
SPRR2A	1.03E-04	0.67
MEX3D	1.07E-04	1.45
ELFN1	1.09E-04	1.49
RHBDL1	1.18E-04	1.48
PRR25	1.33E-04	1.50
C11orf91	1.42E-04	0.66
KRTAP3-3	1.45E-04	1.51
TGFA	1.53E-04	0.71
ANKRD10	1.67E-04	0.70
RFX8	2.19E-04	1.58
UTS2R	2.44E-04	1.75
UNCX	2.48E-04	1.46
MOB1B	2.62E-04	1.42
PPP1R14A	2.66E-04	1.60
C1orf229	2.98E-04	1.51
ZNF699	3.11E-04	0.70
HOXA10	3.42E-04	1.45
HKR1	3.52E-04	0.68
DPF2	4.63E-04	0.65
TPP1	5.60E-04	1.52
TMEM156	7.79E-04	0.69
CISD3	1.11E-03	2.09
UCP3	1.18E-03	1.78
BHLHE23	1.32E-03	1.54
P2RY1	1.75E-03	1.47
MOCS3	2.39E-03	1.53
GP9	2.58E-03	1.45
C3AR1	3.68E-03	1.81
VAMP2	9.57E-03	1.51
ZNF467	1.07E-02	1.47
SSTR3	1.52E-02	1.77
MTRNR2L10	1.88E-02	1.45
ATXN7L2	2.02E-02	1.42
KLRG2	3.37E-02	1.53
FAM57B	3.72E-02	1.52
EVX1	3.82E-02	1.57

LRRIQ3	4.86E-02	1.44

Additional file 7 Significantly deregulated mRNAs in HN2092 after radiochemotherapy treatment (adjusted p-value<0.05)

Gene	adjusted p-value	fold-change
RPL28	3.68E-08	0.44
TRMT61A	6.87E-08	0.49
WLS	6.87E-08	0.52
ASNS	6.87E-08	1.91
SLC38A10	6.87E-08	1.98
HEXDC	6.87E-08	2.16
PCK2	6.87E-08	2.25
JDP2	6.87E-08	2.39
HS1BP3	7.11E-08	1.90
ZBTB24	8.78E-08	0.53
C1S	8.78E-08	1.83
IFRD1	1.07E-07	0.48
LIG1	1.22E-07	1.71
SFXN2	1.37E-07	1.67
DHRS1	1.52E-07	1.58
CDC45	1.52E-07	1.66
CPT2	1.52E-07	1.73
NINL	1.52E-07	1.76
CBS	1.52E-07	1.96
KCNE1L	1.65E-07	0.34
RUNX1	1.65E-07	0.57
RPL22L1	1.65E-07	0.61
GFOD1	1.93E-07	0.57
TRIOBP	1.93E-07	1.98
SFI1	1.95E-07	1.79
HSPA1A	2.02E-07	1.59
FUT1	2.02E-07	1.60
PACS2	2.12E-07	1.81
CC2D2A	2.44E-07	0.48
TMEM143	2.44E-07	1.94
RPL3	2.47E-07	1.68
MEGF6	2.60E-07	1.76
EDN1	2.80E-07	0.59
CREB3L4	2.80E-07	1.58
NOTCH3	2.81E-07	1.75
SYTL1	3.01E-07	1.64
LOC100287177	3.09E-07	1.66

CTF1	3.09E-07	1.67
STAG3	3.52E-07	1.53
C8orf33	3.76E-07	0.63
PHGDH	4.36E-07	1.85
CBX6	4.68E-07	1.73
PLD6	5.12E-07	0.61
MYLK2	5.38E-07	0.57
FASN	5.74E-07	1.52
RHBDF2	5.74E-07	1.67
TRADD	5.99E-07	1.61
MSRB2	6.72E-07	1.52
GPT2	6.94E-07	1.51
TROAP	8.06E-07	0.59
HGSNAT	8.06E-07	1.58
PIGZ	8.53E-07	1.66
HES6	8.56E-07	1.53
HMGA2	8.94E-07	0.64
LLGL2	9.67E-07	1.48
SHANK3	9.67E-07	1.50
MVD	9.67E-07	1.69
IDH2	1.00E-06	1.58
ANKRD10	1.01E-06	0.54
SNRPA1	1.01E-06	0.64
PDRG1	1.01E-06	0.67
ALDH1L2	1.01E-06	1.87
OSBPL5	1.01E-06	2.13
HIST1H1D	1.01E-06	2.41
PLAT	1.01E-06	1.55
ZDHHC12	1.08E-06	1.46
ZNF256	1.15E-06	0.65
ZNF672	1.15E-06	1.59
METTL3	1.15E-06	1.62
LEPROT	1.18E-06	0.54
ITPK1	1.18E-06	0.59
ABL2	1.18E-06	0.63
SLC6A15	1.18E-06	0.67
BRF2	1.18E-06	0.70
MKRN1	1.24E-06	0.57
RECQL	1.27E-06	1.46
CLEC16A	1.30E-06	1.52
POLA2	1.30E-06	1.54

NLRP7	1.30E-06	1.59
ZNF502	1.35E-06	0.63
DUSP12	1.36E-06	0.65
TST	1.36E-06	1.83
TDRD9	1.38E-06	1.49
GAA	1.43E-06	1.52
RMI2	1.43E-06	1.73
KLHL29	1.45E-06	1.61
ASF1B	1.49E-06	1.75
ARHGAP27	1.50E-06	0.64
RPL17	1.56E-06	0.64
PDSS2	1.72E-06	0.66
TMEM201	1.72E-06	0.70
PGLS	1.81E-06	1.54
ADCK5	1.81E-06	1.49
SDF2L1	1.82E-06	1.46
TAF9	1.82E-06	0.69
HKDC1	1.84E-06	1.52
CYCS	1.99E-06	0.68
SLMO1	1.99E-06	0.70
PARVB	2.01E-06	1.53
PGAP3	2.07E-06	0.66
EPHX2	2.16E-06	1.71
IRF5	2.16E-06	1.44
CTH	2.16E-06	1.73
NRP2	2.20E-06	0.64
ZZZ3	2.20E-06	0.68
NOXA1	2.20E-06	1.73
PPP1R35	2.37E-06	1.50
MLH1	2.53E-06	1.63
CYR61	2.63E-06	0.66
ADM	2.72E-06	0.60
CRELD2	2.72E-06	1.66
HABP4	2.73E-06	1.49
UBE2C	2.76E-06	0.70
SGK1	2.79E-06	0.61
MBIP	2.98E-06	0.63
PER1	2.98E-06	0.69
PTPN18	3.00E-06	1.49
TMEM129	3.02E-06	1.61
SETD3	3.07E-06	0.70

REEP6	3.07E-06	1.61
PRRT3	3.15E-06	1.51
SLC6A9	3.22E-06	1.62
HIST2H2AC	3.27E-06	1.87
DNMT3B	3.38E-06	1.57
TRMU	3.44E-06	0.65
RNF213	3.44E-06	1.47
HKR1	3.49E-06	0.65
SPTLC2	3.49E-06	2.12
PPOX	3.54E-06	1.44
C17orf90	3.54E-06	1.44
C1orf56	3.58E-06	1.42
EVL	3.60E-06	1.52
GIT2	3.60E-06	1.54
POLA1	3.64E-06	1.54
KIAA1432	3.90E-06	0.58
CREG2	3.92E-06	1.58
CDK2AP2	4.28E-06	1.42
HEATR7A	4.28E-06	1.51
IGFLR1	4.30E-06	1.62
ARHGEF9	4.34E-06	1.43
MTR	4.34E-06	1.44
SPATA5L1	4.42E-06	0.70
SERF2	4.45E-06	0.66
UCN2	4.82E-06	0.60
C5orf45	4.82E-06	1.42
PRR4	4.88E-06	0.67
C11orf75	4.88E-06	1.56
TXNL4B	5.04E-06	0.61
CABLES2	5.05E-06	1.59
ACTR1B	5.08E-06	1.61
ZNF614	5.09E-06	0.61
SFXN5	5.12E-06	1.45
NUP210	5.12E-06	1.55
KCNG1	5.14E-06	1.73
NLGN4Y	5.21E-06	0.64
C1orf51	5.22E-06	0.68
DLG3	5.22E-06	1.44
C1orf55	5.23E-06	0.65
MAP3K9	5.29E-06	0.58
PLEKHJ1	5.29E-06	1.66

SH2D3C	5.32E-06	1.52
UBOX5	5.46E-06	0.71
ZNF775	5.46E-06	1.52
C8orf40	5.75E-06	1.42
ZNF362	5.80E-06	1.53
HSD17B7	6.04E-06	1.50
ZNF750	6.29E-06	0.60
ARL8B	6.29E-06	0.65
SETDB1	6.29E-06	0.70
COMTD1	6.29E-06	1.52
CALHM3	6.50E-06	1.42
PIP5KL1	6.51E-06	1.46
SPRY2	6.54E-06	0.68
NCAPH2	6.60E-06	0.68
RGS16	6.84E-06	0.60
BCCIP	6.84E-06	0.66
GINS1	6.84E-06	1.44
ZNF789	6.84E-06	1.58
SLC7A11	6.94E-06	1.62
ARMCX2	7.03E-06	1.48
C16orf72	7.11E-06	0.67
ACOX3	7.19E-06	1.45
BRD4	7.23E-06	0.63
ESPL1	7.23E-06	1.49
NECAB3	7.31E-06	1.43
SLC35F2	7.37E-06	0.67
FLVCR1	7.37E-06	0.69
IFFO1	7.84E-06	0.69
DOCK9	7.90E-06	0.66
B3GNT3	7.90E-06	1.48
NT5C3	7.91E-06	0.67
ZNF720	8.40E-06	1.86
DAPP1	8.49E-06	0.66
HIST1H4D	8.51E-06	1.98
GET4	8.54E-06	0.70
HIST1H1A	8.88E-06	3.50
STAT2	9.08E-06	1.55
ZSCAN5A	9.17E-06	0.68
FXYD3	9.22E-06	0.61
LEPR	9.23E-06	0.58
RPL27A	9.23E-06	0.64

LOXL1	9.23E-06	1.47
C2orf43	9.38E-06	0.64
GLS	9.38E-06	0.67
PER2	9.54E-06	0.70
HEATR5A	9.54E-06	1.46
C9orf40	9.73E-06	1.47
AGRN	9.76E-06	1.65
HNRPDL	9.79E-06	0.57
TMSB15B	9.79E-06	1.50
SEPT10	9.79E-06	1.54
FEM1B	1.03E-05	0.68
ARHGEF17	1.03E-05	1.45
C15orf52	1.03E-05	1.52
GNAZ	1.07E-05	1.42
SPG11	1.07E-05	1.43
CHAC1	1.07E-05	1.62
DNAJC2	1.09E-05	0.70
HSD17B8	1.09E-05	1.51
ST6GALNAC2	1.09E-05	1.64
FXC1	1.10E-05	0.71
PRSS16	1.16E-05	1.51
EGFR	1.18E-05	0.70
KANK2	1.18E-05	1.42
APCDD1	1.18E-05	1.46
SHMT2	1.18E-05	1.50
UPF3B	1.21E-05	0.67
TFB2M	1.22E-05	0.62
OXCT1	1.27E-05	1.60
NAT8L	1.31E-05	0.69
MIPEP	1.32E-05	1.43
ATG16L2	1.34E-05	1.49
CERCAM	1.40E-05	1.53
IQGAP3	1.40E-05	1.53
MEGF8	1.41E-05	1.73
C2orf55	1.42E-05	1.69
KIAA0101	1.48E-05	1.46
HCAR3	1.49E-05	0.69
MFAP3	1.50E-05	0.68
KLHL22	1.52E-05	1.46
PSMG4	1.53E-05	1.52
AHNAK	1.55E-05	0.70

WHAMM	1.59E-05	0.70
ABCB6	1.59E-05	1.47
EEF2K	1.62E-05	1.60
MBLAC2	1.62E-05	1.60
ZNF777	1.66E-05	0.70
UBFD1	1.69E-05	0.65
CWC27	1.69E-05	0.69
OVGP1	1.70E-05	0.70
ACCS	1.71E-05	1.50
C5orf42	1.75E-05	1.52
C8orf55	1.76E-05	1.47
ACSS2	1.77E-05	1.55
ANKRD35	1.78E-05	1.54
HOOK2	1.80E-05	1.43
ACOT11	1.80E-05	1.44
HAGH	1.80E-05	1.49
RECQL5	1.84E-05	0.69
GARS	2.03E-05	1.49
DOK1	2.03E-05	1.57
DTNBP1	2.03E-05	1.48
HIST1H4L	2.13E-05	1.90
NAGK	2.16E-05	1.44
HIST1H1B	2.26E-05	2.99
PLK2	2.27E-05	0.68
C7orf53	2.32E-05	0.58
FAM126A	2.33E-05	0.65
RNF114	2.33E-05	0.70
TMSB15A	2.33E-05	1.42
C1orf226	2.33E-05	1.48
THUMPD2	2.44E-05	0.61
N4BP2L2	2.46E-05	0.64
KCNRG	2.48E-05	0.70
BACE1	2.50E-05	1.65
LSS	2.54E-05	1.49
CLEC2B	2.54E-05	0.66
RGS2	2.60E-05	0.56
ANKRD2	2.60E-05	1.50
NDUFC2	2.61E-05	0.61
ZNF837	2.70E-05	1.56
G2E3	2.71E-05	0.59
PLK3	2.71E-05	0.69

ALDH4A1	2.75E-05	1.51
TCP1	2.76E-05	0.63
TET1	2.78E-05	1.58
ACSF3	2.78E-05	1.45
FLG	2.80E-05	0.63
ADM2	2.97E-05	1.54
HSPG2	2.97E-05	1.67
PLAU	3.00E-05	0.70
LHPP	3.04E-05	1.44
STMN1	3.19E-05	0.68
C18orf21	3.20E-05	0.67
ARL6IP1	3.30E-05	0.64
CCR10	3.31E-05	1.42
EVI5L	3.31E-05	1.54
CCDC88C	3.32E-05	0.70
B9D1	3.32E-05	1.46
C17orf109	3.36E-05	0.65
TUBB3	3.44E-05	1.45
C1orf109	3.47E-05	0.64
ZNF354B	3.47E-05	0.69
WDR3	3.56E-05	0.68
AHSA2	3.67E-05	1.60
ZNF317	3.68E-05	0.68
SAP25	3.72E-05	1.45
ELF3	3.82E-05	0.64
RPAP2	3.92E-05	0.70
CNOT1	4.03E-05	0.69
MSI2	4.03E-05	0.65
SERPINB2	4.03E-05	0.63
C17orf108	4.14E-05	1.61
ACY1	4.15E-05	1.44
MANF	4.16E-05	1.74
HERPUD1	4.27E-05	1.59
PTGER4	4.28E-05	0.61
SEPT6	4.31E-05	1.46
SLC19A1	4.34E-05	0.68
HIST1H1E	4.34E-05	2.18
GNGT1	4.37E-05	0.67
CCDC92	4.40E-05	1.47
PRH2	4.41E-05	0.67
HMGCS1	4.42E-05	1.59

DHRS2	4.52E-05	1.43
MICALCL	4.73E-05	1.46
PCSK9	4.95E-05	1.52
RSPH3	5.19E-05	1.46
HIST1H2AJ	5.23E-05	1.94
PSAT1	5.45E-05	1.54
HIST1H2AL	5.51E-05	2.65
NUDT8	5.83E-05	1.47
CAT	5.94E-05	1.80
OVOL1	6.10E-05	0.64
FDPS	6.15E-05	1.45
D2HGDH	6.18E-05	1.47
HIST1H2AB	6.21E-05	1.54
EEFSEC	6.34E-05	1.50
C3orf52	6.43E-05	0.69
CD55	6.52E-05	0.70
PDE5A	6.54E-05	1.46
CBY1	6.71E-05	1.46
ATHL1	6.93E-05	1.45
NEK1	7.08E-05	1.47
ANKRD36B	7.08E-05	1.59
GRHL3	7.10E-05	0.68
RDM1	7.25E-05	1.45
DDX10	7.29E-05	0.68
BCAR3	7.30E-05	0.69
DHFR	7.38E-05	1.46
STK17B	7.41E-05	0.70
GDF15	7.46E-05	1.45
AARS	7.54E-05	1.50
ANKRD36	7.68E-05	1.70
SLX1A	8.24E-05	1.46
HSPA5	8.53E-05	2.02
TMEM187	8.56E-05	1.59
KATNAL1	8.56E-05	1.57
SMNDC1	8.66E-05	0.62
ASL	8.82E-05	1.69
MLXIP	8.89E-05	0.67
MMD	8.91E-05	1.58
ACAD11	8.98E-05	1.42
HIST1H2AK	9.12E-05	1.93
IBA57	9.32E-05	0.63

HIST1H2AI	9.37E-05	1.94
HSBP1L1	9.39E-05	0.69
CARS	9.56E-05	1.93
ULBP1	1.01E-04	1.42
S100PBP	1.03E-04	1.43
PSKH1	1.04E-04	1.85
FOSB	1.04E-04	0.67
C21orf91	1.12E-04	0.66
HIST1H2AG	1.14E-04	3.10
IFIT2	1.15E-04	0.60
RPS6KA2	1.17E-04	1.87
PRODH	1.17E-04	1.43
ATAT1	1.21E-04	1.53
PDCD6IP	1.23E-04	1.43
IRS2	1.27E-04	0.66
GEMIN2	1.27E-04	0.68
LYSMD2	1.27E-04	0.69
SLC30A1	1.33E-04	0.69
MICB	1.36E-04	1.45
RABL2A	1.36E-04	1.49
NIPSNAP3A	1.40E-04	1.46
MMP28	1.43E-04	1.48
SLC13A3	1.43E-04	1.48
ASS1	1.45E-04	1.44
BLOC1S3	1.48E-04	0.71
B4GALNT1	1.48E-04	1.43
CCDC50	1.50E-04	0.70
PASK	1.52E-04	1.46
CSNK1A1L	1.55E-04	0.70
HIST1H2AH	1.67E-04	2.11
ITFG2	1.71E-04	0.70
ACADM	1.76E-04	1.44
CHP2	1.76E-04	1.63
CLSPN	1.76E-04	1.72
OASL	1.79E-04	0.57
TIMM13	1.82E-04	0.68
FAT1	1.95E-04	0.63
USP53	1.99E-04	0.69
HSP90B1	2.03E-04	2.01
PIDD	2.09E-04	1.42
HIST1H2BJ	2.13E-04	1.44

ATF3	2.17E-04	0.66
SEL1L3	2.20E-04	1.43
CCDC18	2.32E-04	1.49
EIF4A2	2.32E-04	0.67
VEGFA	2.38E-04	1.61
CTHRC1	2.40E-04	1.47
AVPR1A	2.43E-04	0.65
CBR4	2.44E-04	1.45
CCNE2	2.45E-04	1.58
EXPH5	2.49E-04	0.69
TMEM107	2.50E-04	1.50
NDUFA7	2.57E-04	1.43
INSIG1	2.58E-04	1.61
CALB1	2.69E-04	0.65
YBX2	2.69E-04	1.42
DNMT3A	2.82E-04	1.46
ASB7	2.84E-04	0.63
KRR1	2.85E-04	0.65
HIST1H2AM	3.03E-04	1.73
FRS2	3.06E-04	0.66
EFNB2	3.11E-04	0.68
TMX4	3.42E-04	1.45
C18orf56	3.54E-04	1.55
TCFL5	3.58E-04	1.48
KIAA0513	3.61E-04	1.45
ID1	3.72E-04	1.44
EGR4	3.80E-04	0.69
HIST1H4E	3.89E-04	2.21
CHM	3.95E-04	0.63
NRAS	3.96E-04	0.67
HIST1H4A	3.96E-04	1.86
CRELD1	4.10E-04	1.56
SHMT1	4.15E-04	1.60
HIST1H2BB	4.31E-04	1.41
ANK1	4.42E-04	1.44
HIST1H2BD	4.52E-04	1.44
GBP5	4.54E-04	1.42
ZNF426	4.64E-04	0.71
POLR1C	4.67E-04	0.68
MED10	4.80E-04	0.67
FZR1	5.04E-04	0.71

C11orf82	5.06E-04	0.71
CHODL	5.06E-04	0.67
STX12	5.06E-04	1.45
HIST1H2AD	5.11E-04	1.46
RABGGTB	5.40E-04	0.68
ACACB	5.42E-04	1.62
HIST1H4C	5.42E-04	1.55
HIST1H3D	5.55E-04	1.95
MRPL44	5.83E-04	0.69
TOR2A	5.84E-04	1.42
RND3	5.88E-04	0.52
EFNA1	6.19E-04	0.68
ENC1	6.28E-04	0.61
CNFN	6.57E-04	0.60
ZFC3H1	6.72E-04	1.44
HIST1H3B	6.83E-04	1.83
HIST1H3H	6.96E-04	1.86
CCNB1	7.25E-04	0.68
FOSL1	7.59E-04	0.71
AEN	7.77E-04	0.70
HIST1H4K	7.94E-04	1.94
MOCOS	8.01E-04	1.46
RRN3	8.05E-04	0.67
PMS1	8.12E-04	1.43
MCMBP	8.43E-04	0.68
HIST1H4I	8.58E-04	1.89
DCBLD1	9.27E-04	1.64
FAM111B	9.51E-04	1.66
CT45A1	9.57E-04	0.68
RNF39	9.70E-04	0.65
TMEM63C	9.72E-04	1.47
IKZF5	9.84E-04	0.69
CAPRIN1	9.85E-04	0.70
CXCR7	1.06E-03	0.68
SLC25A33	1.16E-03	0.66
HIST1H3I	1.17E-03	1.81
C9orf3	1.21E-03	0.71
RBM17	1.22E-03	0.69
METTL21D	1.23E-03	0.61
RNF222	1.32E-03	0.68
PHF20L1	1.40E-03	0.70

MDM4	1.52E-03	0.71
HOXB9	1.52E-03	1.41
HIST1H3G	1.58E-03	1.55
MRE11A	1.58E-03	1.52
GADD45A	1.65E-03	0.70
RIOK3	1.77E-03	0.70
PIGX	1.80E-03	1.56
C1orf52	1.80E-03	0.66
TMEM175	1.95E-03	1.42
SOX9	1.97E-03	0.67
SGK3	2.02E-03	1.45
GNAQ	2.08E-03	0.70
HSPA8	2.14E-03	1.43
HIST2H2AB	2.24E-03	1.68
EHF	2.28E-03	0.70
NR2F1	2.30E-03	1.45
HECTD3	2.38E-03	1.50
HIST1H3F	2.39E-03	1.84
HIST1H2AC	2.41E-03	2.11
HIST1H2BF	2.54E-03	2.11
PTPRZ1	2.55E-03	0.69
UBAP2	2.65E-03	1.47
MBTPS2	2.81E-03	0.70
HIST1H4J	3.04E-03	1.89
MEF2BNB	3.13E-03	0.66
SIK1	3.13E-03	0.70
TTYH3	3.17E-03	1.47
EIF4G3	3.32E-03	1.42
C11orf9	3.38E-03	1.45
PSIP1	3.45E-03	1.47
HIST1H4H	3.48E-03	1.81
HIST2H4B	3.60E-03	1.82
HIST1H2BN	3.69E-03	1.42
PRDM1	4.12E-03	0.70
PKD1	4.22E-03	1.51
NR1D2	4.29E-03	0.69
PGD	4.30E-03	1.44
HIST1H4F	4.44E-03	1.83
EWSR1	4.54E-03	0.69
HIST1H2BE	4.71E-03	1.88
NFATC2IP	4.89E-03	1.58

SPARCL1	4.94E-03	0.63
TINAGL1	5.07E-03	1.63
IMMT	5.28E-03	1.62
RBMS1	5.45E-03	0.70
FAM135A	5.79E-03	0.69
RRM2	5.82E-03	1.60
PIM1	6.50E-03	0.65
STIL	6.53E-03	1.49
KLRG2	6.66E-03	1.44
DNAJC10	6.89E-03	1.43
MRGPRG	7.04E-03	1.43
HIST1H4B	7.51E-03	1.77
PINX1	7.55E-03	1.47
HELLS	7.99E-03	1.43
SPRR2B	8.14E-03	0.69
PBX3	8.14E-03	1.49
BRD3	8.90E-03	1.51
C12orf5	9.47E-03	0.70
TTC7A	1.05E-02	1.43
CLK1	1.12E-02	0.66
CD86	1.12E-02	1.50
MYOF	1.18E-02	1.52
MAP1S	1.26E-02	1.64
ABCB10	1.35E-02	1.42
HERC2	1.43E-02	1.61
NRIP1	1.49E-02	0.68
MOCS3	1.59E-02	1.47
TAF15	1.63E-02	1.61
HMG20B	1.72E-02	1.43
SMC1A	1.82E-02	1.56
ZHX3	1.85E-02	1.66
CYP17A1	1.88E-02	1.43
SNAI2	1.95E-02	0.64
MKI67IP	2.03E-02	0.68
CCDC59	2.17E-02	0.70
HIST1H3J	2.17E-02	1.55
HSPA1B	2.19E-02	1.93
PFKL	2.27E-02	1.75
ZC3HAV1L	2.36E-02	1.56
ARPC1B	2.49E-02	1.48
FBRSL1	2.53E-02	1.74

RBAK-LOC389458	2.58E-02	1.49
ZKSCAN1	2.66E-02	1.44
EPPK1	2.91E-02	2.11
TXNIP	2.93E-02	0.66
UCP3	2.98E-02	1.77
EMILIN1	2.98E-02	1.82
UNCX	3.41E-02	1.70
TMEM167B	3.46E-02	0.64
VAMP2	3.47E-02	1.80
HAPLN2	3.52E-02	2.07
MEX3D	3.59E-02	1.46
PARP1	3.59E-02	1.42
CISD3	3.61E-02	2.06
PPP1R14A	3.76E-02	1.62
SMG5	4.04E-02	0.67
TMEM95	4.11E-02	2.21
IQSEC3	4.14E-02	1.59
KCTD19	4.16E-02	1.55
C20orf201	4.19E-02	1.77
PNPLA2	4.20E-02	1.59
HIST4H4	4.20E-02	1.54
ZNF497	4.34E-02	1.75
TPP1	4.39E-02	1.59
DUX4L4	4.56E-02	1.76
COPG	4.73E-02	1.49
DUX4	4.75E-02	1.74
RAVER1	4.94E-02	1.76
ELFN1	4.96E-02	1.67

Additional file 8 Pathway enrichment analysis of differentially expressed genes in HN1957 after radiochemotherapy treatment (FDR<0.05)

Gene Set	Number of Proteins in GeneSet	Proteins from Network	p-value	FDR	Nodes
Direct p53 effectors(N)	133	12	0	<1.250E-04	PMAIP1,SERPINE1,JUN,HSPA1A,BCL2L1,ATF3,E2F1,E2F2,GADD45A, CASP10,GDF15,IGFBP3
Small cell lung cancer(K)	86	10	0	<1.429E-04	PTGS2,BCL2L1,LAMB3,FN1,LAMA3,E2F1,E2F2,CCNE2,BIRC3,BIRC2
Regulation of Cholesterol Biosynthesis by SREBP (SREBF)(R)	50	9	0	<1.667E-04	HMGCR,INSIG1,MVK,MVD,HMGCS1,FDPS,SEC24C,SEC24D,DHCR7
Validated transcriptional targets of AP1 family members Fra1 and Fra2(N)	36	8	0	<2.000E-04	MMP1,JUNB,PLAUR,JUN,LAMA3,PLAU,FOSL1,IL6
AP-1 transcription factor network(N)	70	11	0	<2.500E-04	EDN1,MMP1,JUNB,JUN,ATF3,ETS1,PLAU,FOSL1,CSF2,NR3C1,IL6
TNF signaling pathway(K)	110	14	0	<3.333E-04	PTGS2,EDN1,CREB3L4,SOCS3,JUNB,VEGFC,JUN,TNFAIP3,CXCL1,C SF2,IL6,BIRC3,BIRC2,CASP10
ATF-2 transcription factor network(N)	58	11	0	<5.000E-04	JDP2,SOCS3,JUNB,DDIT3,JUN,BCL2L1,IL23A,ATF3,PLAU,GADD45A,I L6
Cholesterol biosynthesis(R)	19	9	0	<1.000E-03	HMGCR,MVK,MVD,HMGCS1,MSMO1,FDPS,DHCR7,HSD17B7,NSDHL
Pathways in cancer(K)	327	19	0	1.11E-04	PTGS2,MMP1,VEGFC,JUN,FGFR3,BCL2L1,LAMB3,RUNX1,FN1,BMP2, LAMA3,ETS1,E2F1,E2F2,CCNE2,IL6,BIRC3,BIRC2,HSP90B1
TGF-beta signaling pathway(P)	80	9	0	1.82E-04	CITED2,JUNB,JUN,BMP2,SMAD7,FOSL1,INHBA,GDF15,BAMBI
Glucocorticoid receptor regulatory network(N)	77	9	0	2.00E-04	MMP1,GATA3,JUN,SMARCC2,SGK1,CSF2,NR3C1,IL6,PCK2
C-MYB transcription factor network(N)	82	9	0	3.33E-04	PTGS2,GATA3,SMARCA2,ADA,ETS1,ETS2,HSPA8,CEBPD,BIRC3
Nucleotide-binding domain, leucine rich repeat containing	47	7	0	6.00E-04	TNFAIP3,BCL2L1,IRAK2,NLRP3,TXNIP,BIRC3,BIRC2

receptor (NLR) signaling pathways(R)					
IL6-mediated signaling events(N)	47	7	0	6.00E-04	SOCS3,JUNB,JUN,BCL2L1,IL6,CEBPD,HSP90B1
Calcineurin-regulated NFAT-dependent transcription in lymphocytes(N)	46	7	0	6.15E-04	PTGS2,GATA3,JUNB,JUN,E2F1,FOSL1,CSF2
Steroid biosynthesis(K)	20	5	0	1.00E-03	MSMO1,CYP27B1,DHCR7,HSD17B7,NSDHL
Amoebiasis(K)	109	10	0	1.06E-03	IL1R2,ITGB2,LAMB3,FN1,LAMA3,SERPINB2,CXCL1,CSF2,IL6,COL5A1
Terpenoid backbone biosynthesis(K)	21	5	0	1.17E-03	HMGCR,MVK,MVD,HMGCS1,FDPS
Dissolution of Fibrin Clot(R)	11	4	0.0001	1.37E-03	SERPINE1,PLAUR,PLAU,SERPINB2
NOD-like receptor signaling pathway(K)	57	7	0.0001	1.70E-03	TNFAIP3,NLRP3,CXCL1,IL6,BIRC3,BIRC2,HSP90B1
HTLV-I infection(K)	260	15	0.0001	1.70E-03	JUN,IL1R2,ITGB2,BCL2L1,CALR,FDPS,ATF3,ETS1,ETS2,E2F1,E2F2,FOSL1,CSF2,XBP1,IL6
Extracellular matrix organization(R)	263	15	0.0001	1.77E-03	MMP1,CD44,SERPINE1,DST,ITGB2,LAMB3,FN1,BMP2,LAMA3,ITGA5,LEPREL2,COL13A1,HSPG2,COL5A1,FBLN1
Regulation of nuclear SMAD2/3 signaling(N)	77	8	0.0001	1.81E-03	GATA3,SERPINE1,JUN,RUNX1,NKX2-5,SMAD7,NR3C1,HSPA8
Urokinase-type plasminogen activator (uPA) and uPAR-mediated signaling(N)	42	6	0.0001	2.32E-03	SERPINE1,PLAUR,ITGB2,FN1,ITGA5,PLAU
Calcium signaling in the CD4+ TCR pathway(N)	26	5	0.0001	2.38E-03	PTGS2,JUNB,JUN,FOSL1,CSF2
Validated transcriptional targets of deltaNp63 isoforms(N)	44	6	0.0002	2.73E-03	IL1A,ADA,RUNX1,CEBPD,COL5A1,IGFBP3
HIF-1-alpha transcription factor network(N)	66	7	0.0002	3.24E-03	EDN1,CITED2,SERPINE1,JUN,ITGB2,ETS1,PFKL
Beta1 integrin cell surface interactions(N)	66	7	0.0002	3.24E-03	PLAUR,LAMB3,FN1,LAMA3,ITGA5,PLAU,COL5A1

Rheumatoid arthritis(K)	90	8	0.0002	3.42E-03	MMP1,IL1A,JUN,ITGB2,IL23A,CXCL1,CSF2,IL6
Oncogene Induced Senescence(R)	30	5	0.0002	3.43E-03	ETS1,ETS2,E2F1,E2F2,ID1
CD40/CD40L signaling(N)	29	5	0.0002	3.44E-03	JUN,TNFAIP3,BCL2L1,BIRC3,BIRC2
E2F transcription factor network(N)	68	7	0.0002	3.50E-03	SERPINE1,SMARCA2,PLAU,E2F1,E2F2,CCNE2,PRMT5
NF-kappa B signaling pathway(K)	91	8	0.0002	3.67E-03	PTGS2,TNFAIP3,BCL2L1,DDX58,PLAU,GADD45B,BIRC3,BIRC2
Validated transcriptional targets of TAp63 isoforms(N)	49	6	0.0003	3.71E-03	PMAIP1,DST,ADA,GADD45A,GDF15,IGFBP3
mets effect on macrophage differentiation(B)	18	4	0.0003	4.20E-03	JUN,ETS1,ETS2,E2F1
Caspase cascade in apoptosis(N)	52	6	0.0004	4.64E-03	LMNB1,DIABLO,LIMK1,BIRC3,BIRC2,CASP10
Transcriptional misregulation in cancer(K)	179	11	0.0004	4.84E-03	DDIT3,IL1R2,BCL2L1,RUNX1,PLAU,HMGA2,CSF2,PER2,IL6,BIRC3,IGFBP3
Unfolded Protein Response(R)	74	7	0.0004	4.92E-03	DDIT3,CALR,ATF3,TPP1,ASNS,XBP1,HSP90B1
Pertussis(K)	75	7	0.0004	4.97E-03	IL1A,JUN,ITGB2,IL23A,ITGA5,NLRP3,IL6
IL23-mediated signaling events(N)	35	5	0.0004	5.05E-03	SOCS3,IL24,IL23A,CXCL1,IL6
Plasminogen activating cascade(P)	9	3	0.0006	7.10E-03	MMP1,PLAUR,SERPINB2
DNA Damage/Telomere Stress Induced Senescence(R)	58	6	0.0007	7.71E-03	LMNB1,CCNE2,HIST1H1D,HIST1H1B,HIST1H1A,HMGA2
BMP receptor signaling(N)	41	5	0.0009	1.01E-02	NOG,BMP2,SMAD7,PPP1R15A,BAMBI
ECM-receptor interaction(K)	86	7	0.0009	1.06E-02	CD44,LAMB3,FN1,LAMA3,ITGA5,HSPG2,COL5A1
Interferon alpha/beta signaling(R)	63	6	0.001	1.10E-02	ISG15,SOCS3,OASL,IFIT3,IFIT2,IFIT1
Hematopoietic cell lineage(K)	88	7	0.0011	1.18E-02	CD44,IL1A,IL1R2,ITGA5,CD59,CSF2,IL6

Hepatitis B(K)	146	9	0.0013	1.35E-02	CREB3L4,JUN,DDX58,E2F1,E2F2,CCNE2,IL6,HSPG2,CASP10
Influenza A(K)	176	10	0.0013	1.38E-02	IL1A,SOCS3,JUN,HSPA1A,FDPS,DDX58,NLRP3,RSAD2,HSPA8,IL6
PI3K-Akt signaling pathway(K)	346	15	0.0014	1.40E-02	CREB3L4,VEGFC,FGFR3,BCL2L1,LAMB3,FN1,LAMA3,ITGA5,CCNE2, SGK1,SGK3,IL6,PCK2,COL5A1,HSP90B1
FGF signaling pathway(N)	46	5	0.0015	1.44E-02	PLAUR,JUN,FGFR3,PLAU,SPRY2
p53 signaling pathway(K)	68	6	0.0015	1.45E-02	PMAIP1,SERPINE1,CCNE2,GADD45B,GADD45A,IGFBP3
role of mitochondria in apoptotic signaling(B)	13	3	0.0017	1.58E-02	BCL2L1,DIABLO,BIRC3
Signaling by TGF-beta Receptor Complex(R)	70	6	0.0017	1.61E-02	SERPINE1,JUNB,SMAD7,PPP1R15A,NEDD4L,BAMBI
Apoptotic execution phase(R)	52	5	0.0025	2.33E-02	LMNB1,HIST1H1D,HIST1H1B,HIST1H1A,BIRC2
Cytokine-cytokine receptor interaction(K)	265	12	0.0029	2.70E-02	IL1A,IL24,VEGFC,IL1R2,CD70,IL23A,BMP2,INHBA,CXCL1,CSF2,IL6,T NFSF9
Protein processing in endoplasmic reticulum(K)	167	9	0.0032	2.80E-02	DDIT3,HSPA1A,CALR,SEC24C,SEC24D,PPP1R15A,XBP1,HSPA8,HSP 90B1
TGF-beta signaling pathway(K)	80	6	0.0033	2.80E-02	NOG,BMP2,SMAD7,INHBA,ID1,BAMBI
Legionellosis(K)	55	5	0.0032	2.84E-02	ITGB2,HSPA1A,CXCL1,HSPA8,IL6
Beta5 beta6 beta7 and beta8 integrin cell surface interactions(N)	17	3	0.0036	3.10E-02	PLAUR,FN1,PLAU
signal transduction through il1r(B)	35	4	0.0037	3.16E-02	IL1A,JUN,IRAK2,IL6
Focal adhesion(K)	206	10	0.004	3.43E-02	VEGFC,JUN,LAMB3,FN1,LAMA3,ITGA5,PARVB,BIRC3,BIRC2,COL5A1
gata3 participate in activating the th2 cytokine genes expression(B)	18	3	0.0042	3.56E-02	GATA3,IL1A,JUNB
nfat and hypertrophy of the heart (B)	37	4	0.0045	3.75E-02	EDN1,NKX2-5,HDAC9,HBEGF
Apoptosis(K)	86	6	0.0046	3.78E-02	IL1A,BCL2L1,IRAK2,BIRC3,BIRC2,CASP10

Bladder cancer(K)	38	4	0.0049	3.89E-02	MMP1,FGFR3,E2F1,E2F2
Intrinsic Pathway for Apoptosis(R)	38	4	0.0049	3.89E-02	PMAIP1,BCL2L1,DIABLO,E2F1
Parkinson disease(P)	61	5	0.0049	3.99E-02	SNCA,HSPA1A,CCNE2,TOR2A,HSPA8
Regulation of retinoblastoma protein(N)	62	5	0.0053	4.05E-02	JUN,E2F1,E2F2,CSF2,CEBPD
Vitamin B6 metabolism(K)	6	2	0.0053	4.11E-02	AOX1,PSAT1
Toxoplasmosis(K)	119	7	0.0057	4.30E-02	HSPA1A,BCL2L1,LAMB3,LAMA3,HSPA8,BIRC3,BIRC2
Regulation of Insulin-like Growth Factor (IGF) Transport and Uptake by Insulin-like Growth Factor Binding Proteins (IGFBPs)(R)	21	3	0.0065	4.89E-02	MMP1,IGF2,IGFBP3

(B) BioCarta, (K) KEGG Pathway, (N) NCI - Nature Curated Data, (P) pantherdb, (R) Reactome

Additional file 9 Pathway enrichment analysis of differentially expressed genes in HN2092 after radiochemotherapy treatment
(FDR<0.05)

Gene Set	Number of Proteins in GeneSet	Proteins from Network	p-value	FDR	Nodes
RNA Polymerase I, RNA Polymerase III, and Mitochondrial Transcription(R)	109	13	0	<1.000E-04	HIST1H2BN,HIST1H2BJ,HIST1H4A,RRN3,HIST2H2AC,BRF2,POLR1C,HIST1H2AB,HIST1H2AC,HIST1H2AD,HIST1H2BB,HIST1H2BD,HIST1H2AJ
Mitotic Prophase(R)	99	13	0	<1.111E-04	HIST1H2BN,HIST1H2BJ,HIST1H4A,HIST2H2AC,NCAPH2,HIST1H2AB,HIST1H2AC,HIST1H2AD,NUP210,HIST1H2BB,HIST1H2BD,CCNB1,HIST1H2AJ
Alcoholism(K)	180	17	0	<1.250E-04	HIST1H2BN,HIST1H2BJ,CREB3L4,HIST1H4A,GNGT1,HIST2H2AB,HIST2H2AC,FOSB,HIST1H2AB,HIST1H2AC,HIST1H2AG,HIST1H2AD,HIST1H2BB,HIST1H2BD,NRAS,HIST1H2AH,HIST1H2AJ
Nucleosome assembly(R)	45	10	0	<1.429E-04	HIST1H2BN,HIST1H2BJ,HIST1H4A,HIST2H2AC,HIST1H2AB,HIST1H2AC,HIST1H2AD,HIST1H2BB,HIST1H2BD,HIST1H2AJ
Senescence-Associated Secretory Phenotype (SASP)(R)	75	13	0	<1.667E-04	HIST1H2BN,HIST1H2BJ,FZR1,HIST1H4A,HIST2H2AC,UBE2C,HIST1H2AB,HIST1H2AC,HIST1H2AD,HIST1H2BB,HIST1H2BD,RPS6KA2,HIST1H2AJ
Meiotic Synapsis(R)	57	12	0	<2.000E-04	HIST1H2BN,HIST1H2BJ,STAG3,HIST1H4A,SMC1A,HIST2H2AC,HIST1H2AB,HIST1H2AC,HIST1H2AD,HIST1H2BB,HIST1H2BD,HIST1H2AJ
Meiotic Recombination(R)	54	12	0	<2.500E-04	HIST1H2BN,HIST1H2BJ,MRE11A,HIST1H4A,MLH1,HIST2H2AC,HIST1H2AB,HIST1H2AC,HIST1H2AD,HIST1H2BB,HIST1H2BD,HIST1H2AJ
Chromatin modifying enzymes(R)	105	16	0	<3.333E-04	MBIP,HIST1H2BN,HIST1H2BJ,ZZZ3,HIST1H4A,TAF9,HIST2H2AB,HIST2H2AC,HIST1H2AB,HIST1H2AC,HIST1H2AG,HIST1H2AD,HIST1H2BB,HIST1H2BD,HIST1H2AH,HIST1H2AJ
Telomere Maintenance(R)	59	13	0	<5.000E-04	HIST1H2BN,HIST1H2BJ,LIG1,HIST1H4A,HIST2H2AC,HIST1H2AB,HIST1H2AC,HIST1H2AD,POLA1,POLA2,HIST1H2BB,HIST1H2BD,HIST1H2AJ
DNA Damage/Telomere Stress Induced Senescence(R)	58	16	0	<1.000E-03	HIST1H2BN,HIST1H2BJ,MRE11A,HIST1H4A,HIST2H2AC,HIST1H1E,HIST1H1D,HIST1H1B,HIST1H1A,HMGA2,HIST1H2AB,HIST1H2AC,HIST1

					H2AD,HIST1H2BB,HIST1H2BD,HIST1H2AJ
Systemic lupus erythematosus(K)	135	13	0	<8.333E-05	HIST1H2BN,HIST1H2BJ,HIST1H4A,HIST2H2AB,HIST2H2AC,HIST1H2AB,HIST1H2AC,HIST1H2AG,HIST1H2AD,HIST1H2BB,HIST1H2BD,HIST1H2AH,HIST1H2AJ
Oxidative Stress Induced Senescence(R)	89	11	0	<9.091E-05	CBX6,HIST1H2BN,HIST1H2BJ,HIST1H4A,HIST2H2AC,HIST1H2AB,HIST1H2AC,HIST1H2AD,HIST1H2BB,HIST1H2BD,HIST1H2AJ
Direct p53 effectors(N)	133	10	0.0001	3.54E-03	EGFR,PIDD,HSPA1A,TAF9,ATF3,PLK3,MLH1,GADD45A,SNAI2,CCNB1
Biosynthesis of amino acids(K)	73	7	0.0002	7.21E-03	ASS1,ASL,PFKL,CTH,PHGDH,PSAT1,CBS
Cysteine and methionine metabolism(K)	34	5	0.0002	8.33E-03	DNMT3B,DNMT3A,TST,CTH,CBS
Cholesterol biosynthesis(R)	19	4	0.0003	8.94E-03	MVD,HMGCS1,FDPS,HSD17B7
g-protein signaling through tubby proteins(B)	10	3	0.0006	1.74E-02	EDN1,GNGT1,GNAQ
Metabolism of amino acids and derivatives(R)	147	9	0.0007	1.87E-02	ASS1,ASL,TST,GLS,CTH,ASNS,PHGDH,PSAT1,CBS
Dissolution of Fibrin Clot(R)	11	3	0.0008	2.14E-02	PLAT,PLAU,SERPINB2
Unfolded Protein Response(R)	74	6	0.0013	3.21E-02	ATF3,TPP1,ASNS,HSPA5,MBTPS2,HSP90B1
Estrogen signaling pathway(K)	100	7	0.0012	3.23E-02	CREB3L4,EGFR,HSPA1A,GNAQ,HSPA8,NRAS,HSP90B1
Apoptotic execution phase(R)	52	5	0.0016	3.70E-02	CLSPN,HIST1H1E,HIST1H1D,HIST1H1B,HIST1H1A
Alanine, aspartate and glutamate metabolism(K)	32	4	0.0019	4.09E-02	ASS1,ASL,GLS,ASNS

(B) BioCarta, (K) KEGG Pathway, (N) NCI - Nature Curated Data, (P) pantherdb, (R) Reactome

Additional file 10 Potential target genes in HN1957 for miRNAs responding to therapy in HNSCC patients (correlation value ≤ -0.5)

miRNA	Gene	Correlation value
miR-106b-5p	ABTB2	-0.71
miR-106b-5p	ADH5	-0.66
miR-106b-5p	ANKFY1	-0.50
miR-106b-5p	APLP2	-0.63
miR-106b-5p	APP	-0.66
miR-106b-5p	BAMBI	-0.85
miR-106b-5p	BRWD1	-0.75
miR-106b-5p	C1orf43	-0.61
miR-106b-5p	CNOT7	-0.63
miR-106b-5p	CWF19L1	-0.72
miR-106b-5p	DDX23	-0.55
miR-106b-5p	DGKD	-0.82
miR-106b-5p	EEF1A1	-0.76
miR-106b-5p	FAM199X	-0.55
miR-106b-5p	FAM91A1	-0.77
miR-106b-5p	FBXO22	-0.54
miR-106b-5p	FBXW2	-0.66
miR-106b-5p	FNBP1	-0.73
miR-106b-5p	GOLT1B	-0.67
miR-106b-5p	GON4L	-0.76
miR-106b-5p	KAT7	-0.77
miR-106b-5p	MAT2A	-0.58
miR-106b-5p	MMADHC	-0.56
miR-106b-5p	PDSS1	-0.61
miR-106b-5p	PPIA	-0.78
miR-106b-5p	PPM1B	-0.64
miR-106b-5p	PTEN	-0.69
miR-106b-5p	PURA	-0.71
miR-106b-5p	RAD23B	-0.64
miR-106b-5p	RHOBTB2	-0.70
miR-106b-5p	RNPS1	-0.82
miR-106b-5p	RPL18A	-0.81
miR-106b-5p	RPP30	-0.79
miR-106b-5p	SHISA2	-0.56
miR-106b-5p	SMEK2	-0.75
miR-106b-5p	SMG7	-0.75
miR-106b-5p	THADA	-0.57

miR-106b-5p	TTPAL	-0.62
miR-106b-5p	UQCRQ	-0.59
miR-106b-5p	VEGFA	-0.68
miR-106b-5p	WDR33	-0.79
miR-106b-5p	YTHDF2	-0.53
miR-106b-5p	ZNF562	-0.72
miR-106b-5p	ZNF587	-0.63
miR-106b-5p	ZNF598	-0.78
miR-106b-5p	ZNF777	-0.66
miR-21-5p	AKT2	-0.58
miR-21-5p	APAF1	-0.59
miR-21-5p	BASP1	-0.64
miR-21-5p	DOCK5	-0.52
miR-21-5p	E2F1	-0.59
miR-21-5p	ISCU	-0.92
miR-21-5p	MARCKS	-0.51
miR-21-5p	MSH6	-0.56
miR-21-5p	NCAPG	-0.81
miR-21-5p	NFIB	-0.66
miR-21-5p	PCBP1	-0.58
miR-21-5p	PDCD4	-0.60
miR-21-5p	PPARA	-0.70
miR-21-5p	RECK	-0.63
miR-21-5p	SMARCA4	-0.54
miR-21-5p	SP1	-0.63
miR-21-5p	TMEM147	-0.56
miR-21-5p	TOPORS	-0.52
miR-425-5p	BAZ2A	-0.59
miR-425-5p	DPYSL2	-0.81
miR-425-5p	FOXK2	-0.67
miR-425-5p	HSP90AA1	-0.81
miR-425-5p	INPP5E	-0.79
miR-425-5p	NADK	-0.67
miR-425-5p	PDZD8	-0.53
miR-425-5p	QKI	-0.57
miR-425-5p	RRM2	-0.75
miR-425-5p	RUFY2	-0.65
miR-425-5p	SMARCD1	-0.57
miR-425-5p	THOP1	-0.67
miR-425-5p	ZNF148	-0.77
miR-93-5p	AP2A2	-0.72

miR-93-5p	APBB2	-0.54
miR-93-5p	APLP2	-0.71
miR-93-5p	ARHGAP32	-0.67
miR-93-5p	ATP5B	-0.57
miR-93-5p	CAP1	-0.73
miR-93-5p	CDC16	-0.78
miR-93-5p	CLN8	-0.61
miR-93-5p	DYRK2	-0.54
miR-93-5p	EEF1A1	-0.88
miR-93-5p	EIF4G2	-0.70
miR-93-5p	ELAC2	-0.52
miR-93-5p	ELAVL1	-0.81
miR-93-5p	EPHA4	-0.67
miR-93-5p	FAM3C	-0.56
miR-93-5p	GAPDH	-0.69
miR-93-5p	H1F0	-0.58
miR-93-5p	HK1	-0.69
miR-93-5p	HPS1	-0.73
miR-93-5p	IBA57	-0.76
miR-93-5p	IGF2	-0.76
miR-93-5p	IPO5	-0.88
miR-93-5p	JUN	-0.79
miR-93-5p	KAT2B	-0.57
miR-93-5p	LATS2	-0.83
miR-93-5p	LOXL1	-0.81
miR-93-5p	MAP3K13	-0.62
miR-93-5p	MED21	-0.64
miR-93-5p	NOB1	-0.75
miR-93-5p	NPEPPS	-0.57
miR-93-5p	NPM1	-0.66
miR-93-5p	NUP205	-0.74
miR-93-5p	PI4KA	-0.64
miR-93-5p	PPAN	-0.64
miR-93-5p	PPTC7	-0.77
miR-93-5p	PTEN	-0.68
miR-93-5p	PURA	-0.74
miR-93-5p	RAB8B	-0.61
miR-93-5p	RBM23	-0.53
miR-93-5p	RFC3	-0.77
miR-93-5p	RPL30	-0.61
miR-93-5p	SAMD4B	-0.67

miR-93-5p	SH3BP4	-0.62
miR-93-5p	SMG7	-0.69
miR-93-5p	SPATA2	-0.70
miR-93-5p	TAF8	-0.78
miR-93-5p	TRAK1	-0.59
miR-93-5p	TRIM8	-0.64
miR-93-5p	UBAP2L	-0.61
miR-93-5p	UBN1	-0.57
miR-93-5p	UPF1	-0.57
miR-93-5p	VAT1	-0.55
miR-93-5p	VEGFA	-0.53
miR-93-5p	WAC	-0.60
miR-93-5p	YWHAQ	-0.69
miR-93-5p	ZIC2	-0.53
miR-93-5p	ZNFX1	-0.68

Additional file 11 Potential target genes in HN2092 for miRNAs responding to therapy in HNSCC patients (correlation value ≤ -0.5)

miRNA	Gene	Correlation value
miR-106b-5p	BRWD1	-0.60
miR-106b-5p	C9orf40	-0.59
miR-106b-5p	CCND2	-0.53
miR-106b-5p	INSIG1	-0.54
miR-106b-5p	ITCH	-0.56
miR-106b-5p	MSH6	-0.50
miR-106b-5p	PLEKHM1	-0.73
miR-106b-5p	PSMA3	-0.52
miR-106b-5p	RBL2	-0.59
miR-106b-5p	RBM12B	-0.68
miR-106b-5p	RPL7	-0.58
miR-106b-5p	SLC9A1	-0.51
miR-106b-5p	STX12	-0.55
miR-106b-5p	THADA	-0.51
miR-106b-5p	UGP2	-0.62
miR-106b-5p	ZBTB7B	-0.54
miR-106b-5p	ZFYVE16	-0.63
miR-21-5p	LRRFIP1	-0.53
miR-21-5p	PPARA	-0.51
miR-425-5p	NPNT	-0.53
miR-93-5p	AP2A2	-0.87
miR-93-5p	ARL9	-0.54
miR-93-5p	ATP5B	-0.62
miR-93-5p	BAG2	-0.51
miR-93-5p	BIRC5	-0.85
miR-93-5p	CBX3	-0.66
miR-93-5p	CCDC88C	-0.84
miR-93-5p	CCT8	-0.79
miR-93-5p	EIF4G2	-0.74
miR-93-5p	FAM3C	-0.81
miR-93-5p	FAM57A	-0.67
miR-93-5p	GAPDH	-0.81
miR-93-5p	HK1	-0.66
miR-93-5p	HPS1	-0.62
miR-93-5p	IBA57	-0.90
miR-93-5p	IGF2	-0.55
miR-93-5p	IPO5	-0.87

miR-93-5p	JUN	-0.79

Additional file 12 Primer sequences for *TP53* and *EGFR* sequencing

Gene (region)	PCR Primer 5' → 3'	Sequencing Primer 5' → 3'
TP53 (exons 3-10)	ATGGAGGAGCCGCAGTCAG TCAGTCTGAGTCAGGCCCTTCT	ATGGAGGAGCCGCAGTCAG TCAGTCTGAGTCAGGCCCTTCT
EGFR (exons 2-16)	ATGCGACCCTCCGGGAC CACCACCAGCAGCAAGAGG	ATGCGACCCTCCGGGAC CACCACCAGCAGCAAGAGG
EGFR (exons 9-27)	CCGACAGCTATGAGATGGAGGA TCATGCTCCAATAAATTCACTGCT	CCGACAGCTATGAGATGGAGGA CCTCTTGCTGCTGGTGGTG TCATGCTCCAATAAATTCACTGCT
EGFR (exons 9-14)	CCTCTTGCTGCTGGTGGTG ATCGATGGTACATATGGGTGGC	CCTCTTGCTGCTGGTGGTG ATCGATGGTACATATGGGTGGC